Chapter III

Results and Discussion

Section (A)

Effect of Inhibitor on Corrosion of Carbon Steel

In this section, the effect of increasing concentrations of N-3-Hydroxyl-2-Naphthoyl Hydrazone derivatives on the corrosion behavior of carbon steel in 0.5M sulfuric acid solution and also in presence of potassium iodide, bromide and thiocyanate was studied. It is generally accepted that the organic compounds inhibit the corrosion process by adsorbing at the metal / solution interface, the modes of adsorption are depends on:

i) Effect of molecular chemical structure on corrosion inhibition

ii) Chemical composition of the solution.

iii) Nature of the metal surface, and

iv) Electrochemical potential at the interface, one or a combination of more of the three principal types of adsorption: π bond, electrostatic and /or chemisorptions [(93)]. In addition, it is believed that the formation of a solid organic molecule complex with the metal atom has received considerable attention [(94)].

when designing inhibitors, all of the theories are in common agreement that adsorption phenomena involves either:-

1) Proton acceptor (cathodic site absorbers), material in this group accepts the hydrogen ions or proton and migrates to the cathode .

2) Electron acceptor (anodic site absorbers), inhibitor functions due to their ability to accept electrons.

3) Adsorb at anodic and cathodic sites.

It has been generally accepted that group contributions vary considerably from molecule to molecule. Utilization of these concepts permits the systematic construction of an increasing efficiency of organic molecule.

3.1- Effect of Inhibitor Concentrations

The inhibition behavior of N-3-Hydroxyl-2-Naphthoyl Hydrazone derivatives for carbon steel corrosion in 0.5M sulfuric acid solutions was studied using weight loss method. This can be quantified by using the simple relation (2.1) $\Delta W = (W_1 - W_2) / A$

The degree of dissolution, of course , depends on the exposed the metal and the time of exposure; hence the amount of corrosion is given with respect to area and time. The resulting quantity, corrosion rate, is thus a fundamental measurement in corrosion science. Corrosion rates can be evaluated by measuring either the concentration of the dissolved metal in solution by chemical analysis or by measuring weight of specimen before and after exposure and applying equation (2.1). The later is most common method. The weight- loss method is usually preferred because the quantity measured is directly related to the extent of corrosion and does not rely on any assumptions about reactions occurring during corrosion.

Figures (3.1-3.4) show the weight loss-time curves for carbon steel in 0.5M H_2SO_4 in absence and presence of different concentrations of the selected organic compounds. As shown from these figures, by increasing the concentration of these compounds, the weight loss of carbon steel samples are decreased. This means that the presence of these compounds retards the corrosion of carbon steel in 0.5M H_2SO_4 or in other words, these compounds act as an inhibitor.

The linear variation of weight loss with time in uninhibited and inhibited 0.5M H_2SO_4 indicates the absence of insoluble surface films during corrosion. In the absence of any surface films, the inhibitors are first adsorbed onto the metal surface and thereafter impede corrosion either by merely blocking the reaction sites (anodic

and cathodic) or by altering the mechanism of the anodic and cathodic partial processes.

The inhibition efficiency (%IE) of the selected organic compounds were determined by using the equation:

$$\%IE = (\Delta W - \Delta W') / \Delta W \times 100 \qquad (3.1)$$

where, ΔW and $\Delta W'$ are the corrosion rates of carbon steel in the absence and presence of the selected organic compounds, respectively, at given time period and temperature.

Weight loss of carbon steel in mg cm^{-2} of the surface area was determined at various time intervals in absence and presence of N-3-Hydroxyl-2-Naphthoyl Hydrazone derivatives. The obtained weight loss-time curves are represented in Figs. (3.1-3.4). The inhibition efficiency was found to be dependent on the inhibitor concentration, nature of substituents and their positions in phenyl ring.

The curves obtained in the presence of inhibitors fall significantly below that of free acid. In all cases, the increase in the inhibitor concentration was accompanied by a decrease in weight loss and an increase in the percentage inhibition efficiency. These results lead to the conclusion that, the compounds under investigation are efficient as inhibitors for carbon steel dissolution in sulfuric acid solution.

In order to get a comparative view, the variation of the inhibition efficiencies of the fourth inhibitors with their molar concentrations at 303K were calculated according to equation (3.1); values obtained are summarized in Table (3.1).Inspection of these results showed that, at the same inhibitor concentration, the order inhibition efficiencies is decreased as follow:

$$1 > 2 > 3 > 4$$

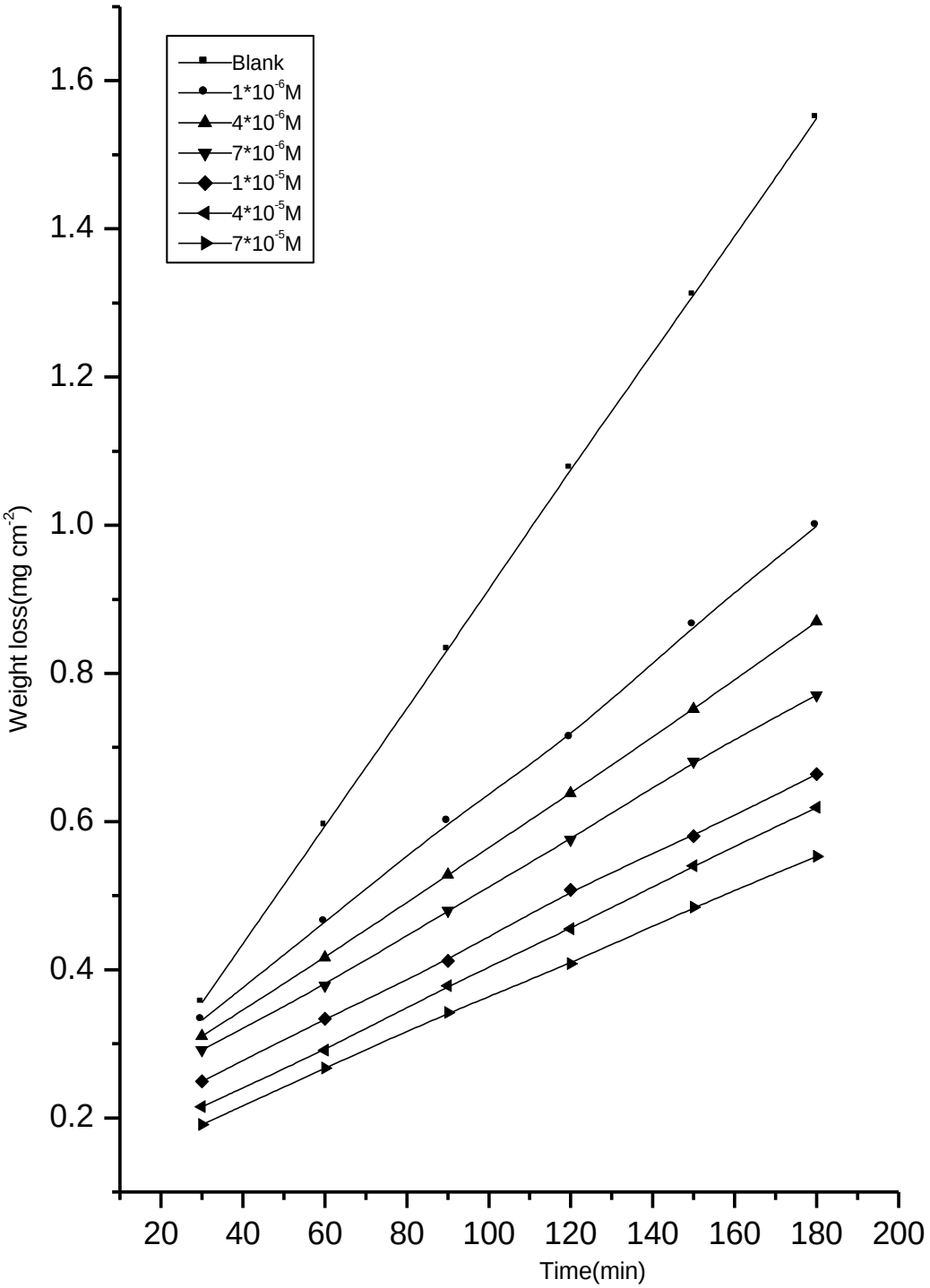

Fig(3.1) weight loss-time curves for carbon steel dissolution in 0.5M H_2SO_4 in absence and presence of different concentrations of compound(1) at 303 K

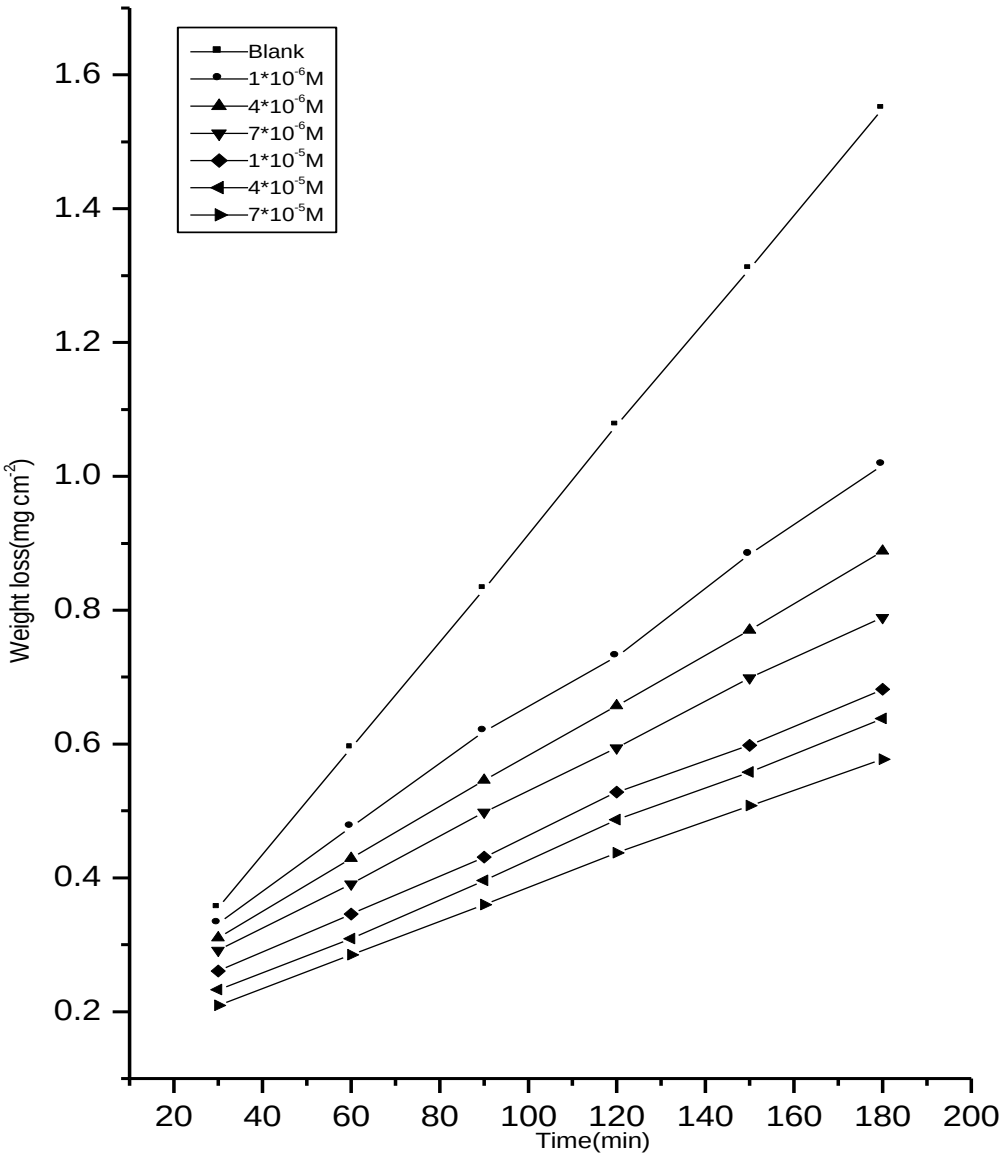

Fig(3.2) weight loss-time curves for carbon steel dissolution in 0.5M H_2SO_4 in absence and presence of different concentrations of compound(2) at 303 K

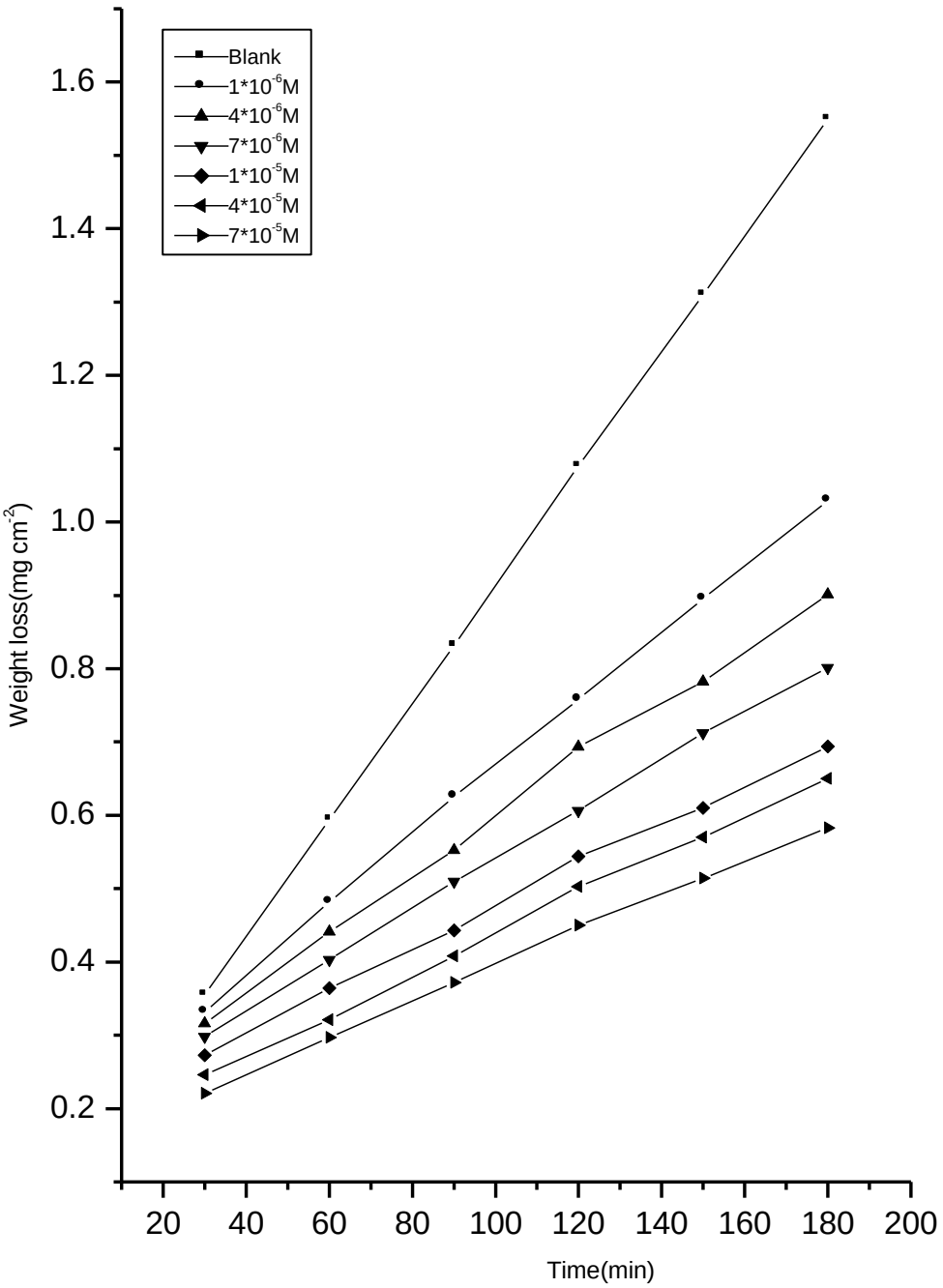

Fig(3.3) weight loss-time curves for carbon steel dissolution in 0.5M H_2SO_4 in absence and presence of different concentrations of compound(3) at 303 K

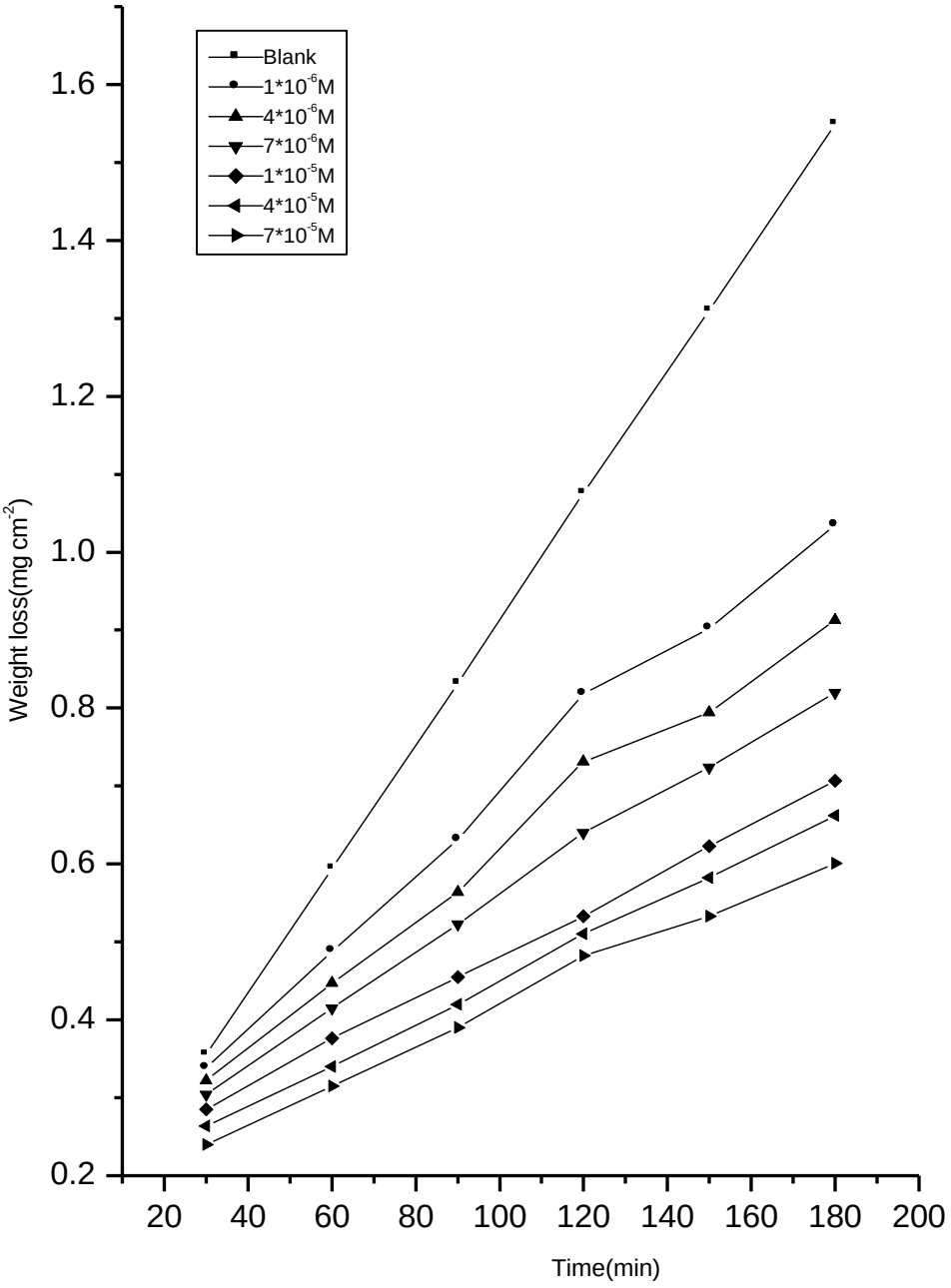

Fig(3.4) weight loss-time curves for carbon steel dissolution in 0.5M H_2SO_4 in absence and presence of different concentrations of compound(4) at 303 K

Table (3.1): Percentage inhibition efficiency values (%IE) from weight loss method of carbon steel dissolution in 0.5M H_2SO_4 for different concentrations of N-3-Hydroxyl-2-Naphthoyl Hydrazone derivatives at 303K.

Concentration, M	Percentage inhibition efficiency (% IE)			
	Compounds			
	1	2	3	4
$1X10^{-6}$	33.71	32.06	29.60	23.98
$4X10^{-6}$	40.67	38.95	35.60	32.06
$7X10^{-6}$	46.46	44.77	43.64	40.52
$1X10^{-5}$	52.79	50.94	49.46	46.38
$4X10^{-5}$	57.73	54.75	53.25	52.60
$7X10^{-5}$	62.08	59.41	58.18	55.20

3.2-Adsorption Isotherms

Organic molecules inhibit the corrosion process by the adsorption on metal surface. Theoretically, the adsorption process can be regarded as a single substitutional process in which an inhibitor molecule (Inh.) in the aqueous phase substitutes an "x" number of water molecules adsorbed on the metal surface [95] vis,

$$Inh._{(aq.)} + xH_2O_{(sur)} \longrightarrow Inh._{(sur.)} + xH_2O_{(aq.)} \qquad (3.2)$$

where x is known as the size ratio and simply equals the number of adsorbed water molecules replaced by a single inhibitor molecule. The adsorption depends on the structure of the inhibitor, the type of the metal and the nature of its surface, the nature of the corrosion medium and its pH value, the temperature, and the electrochemical potential of the metal-solution interface. Also, the adsorption provides information about the interaction among the adsorbed molecules themselves as well as their interaction with the metal surface. Actually an adsorbed molecule may make the surface more difficult or less difficult for another molecule to become attached to a neighboring site and multilayer adsorption may take place. There may be more or less than one inhibitor molecule per surface site. Finally, various surface sites could have varying degrees of activation. For these reasons a number of mathematical adsorption isotherm expressions have been developed to take into consideration some of non-ideal effects .

Adsorption isotherm equations are generally of the form [96]:

$$f(\theta,x)\exp(-a,\theta) = KC \qquad (3.3)$$

Where f (θ, x) is the configurational factor that depends essentially on the physical model and assumptions underlying the derivation of the isotherm, (a) is a molecular interaction parameter depending upon molecular interactions in the adsorption layer and the degree of heterogeneity of the surface; it is a measure of steepness of adsorption isotherm; the more positive the value of (a) the steeper the adsorption isotherm, θ is the degree of surface coverage, C is the inhibitor concentration in the

bulk of solution; K is the equilibrium constant of the adsorption process, which is related to the standard free energy of adsorption ($\Delta G°_{ads.}$) by:

$$K = 1/55.5 \exp (-\Delta G°_{ads.} / RT) \quad (3.4)$$

Where R is the universal gas constant and T is the absolute temperature.

A number of mathematical relationships for the adsorption isotherms have been suggested to fit the experiment data of the present work. The Frumkin's adsorption isotherm [97] is given by the following equation:

$$K C = \theta / 1 - \theta \exp (-2 a \theta) \quad (3.5)$$

Where K is the equilibrium constant of the adsorption reaction, C is the inhibitor concentration in the bulk of the solution, and θ is the surface coverage. The surface coverage, i.e., the fraction of the surface covered by the inhibitor molecules, θ was calculated before.

Plots of θ vs. log C (Frumkin adsorption plots) for adsorption of the used inhibitors on the surface of C-steel in 0.5M H_2SO_4 acid solutions at 303 K are shown in Fig. (3.5). The data gave S-shape indicating that Frumkin's isotherm is valid for these systems.

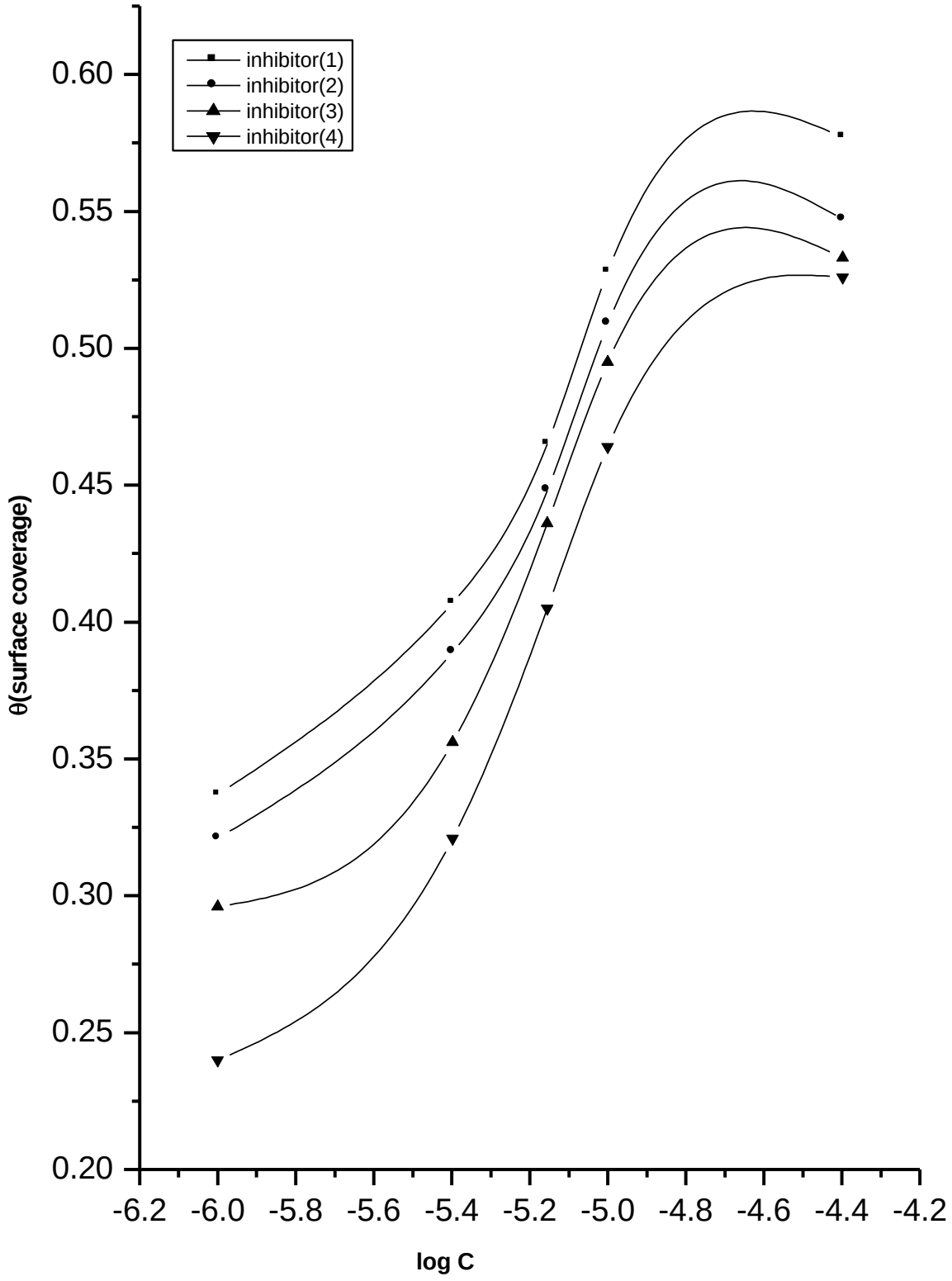

Fig.(3.5): θ -log C curves for C-steel dissolution in 0.5M H_2SO_4 in presence of all inhibitors from weight loss measurements at 303K .

3.3- Synergistic Effect

The effect of I^-,SCN^- and Br^- ions on the corrosion-inhibition of carbon steel in 0.5 M H_2SO_4 solution in presence and in absence of the N-3-Hydroxyl-2-Naphthoyl Hydrazone derivatives was studied by the weight loss method. Figs.(3.6-3.17) represent the weight loss-time curves for carbon steel dissolution in 0.5 M H_2SO_4 in presence of 10^{-2}M of I^-, SCN^-, Br^- and also in presence of different concentrations of N-3-Hydroxyl-2-Naphthoyl Hydrazone compounds. The values of inhibition efficiency (% IE) for various concentrations of inhibitors in the presence of specific concentrations of these anions are given in Tables (3.2-3.4)

It is observed that %IE of the inhibitors increases on addition of these different anions due to synergistic effects [98]. The strong chemisorption of these anions on the metal surface is responsible for the synergistic effect of these ions in combination with cation of the inhibitor. The cation is then adsorbed by coulombic attraction on the metal surface where these anions are already adsorbed by chemisorption. Stabilization of these adsorbed anions with cations leads to greater surface coverage and therefore greater inhibition.

The synergistic inhibition effect was evaluated using a parameter, S_θ, obtained from the surface coverage values (θ) of the anion, cation and both. Aramaki and Hackerman [99] calculated the synergism parameter S_θ using the following equation.

$$S_\theta = 1-\theta_{1+2}/1-\theta'_{1+2} \qquad (3.6)$$

where:

$\theta_{1+2} = (\theta_1 + \theta_2) - (\theta_1\theta_2)$;

θ_1 = surface coverage by anion;

θ_2 = surface coverage by cation;

θ'_{1+2} = measured surface coverage by both the anion and cation.

We calculate synergism parameters from the above equation . The plot of the synergism parameter (S_θ) against various concentrations of N-3-Hydroxyl-2-

Naphthoyl Hydrazone derivatives are given in Figs (3.18-3.20) and the corresponding values are shown in Tables (3.5-3.7). As can be seen from this Table, values of S_θ are nearly equal to unity, which suggests that the enhanced inhibition efficiencies caused by the addition of these anions to N-3-Hydroxyl-2-Naphthoyl Hydrazone derivatives is due mainly to the synergistic effect. lt is known that KI would be considered as one of the effective anions for synergistic action within the investigated salts. The net increment of inhibition efficiency shows a synergistic effect of KBr, KI, KSCN with N-3-Hydroxyl-2-Naphthoyl Hydrazone derivatives .The synergistic effect depends on the type and concentration of anions. The adsorption ability on the carbon steel surfaces was in the order KI> KSCN> KBr [100]. This order parallel to the covalent radii of these anions.

$$I^- > SCN^- > Br^-$$

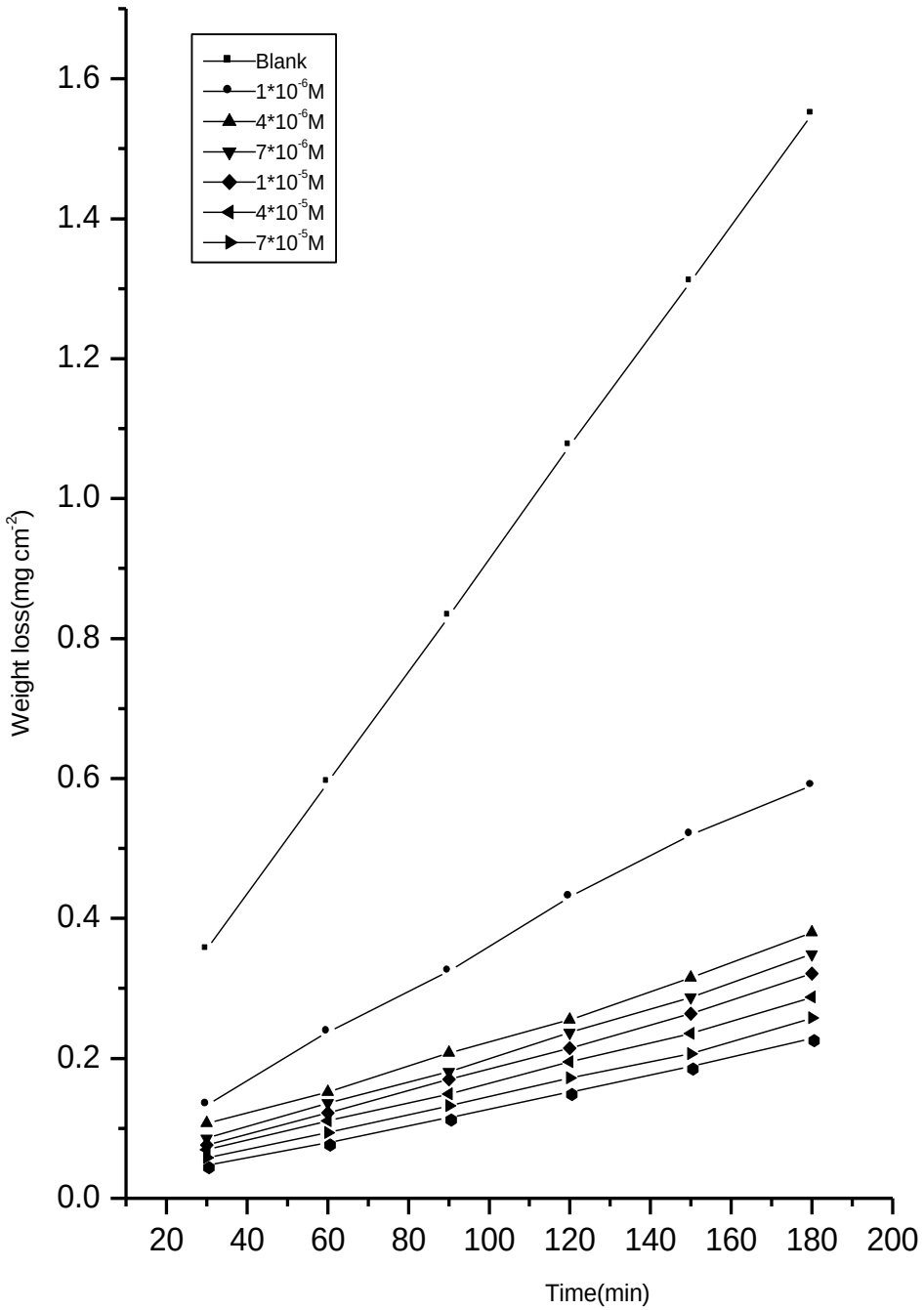

Fig(3.6) weight loss-time curves for carbon steel dissolution in 0.5M H_2SO_4 in absence and presence of10^{-2}M KI and different concentrations of compound(1) at 303 K

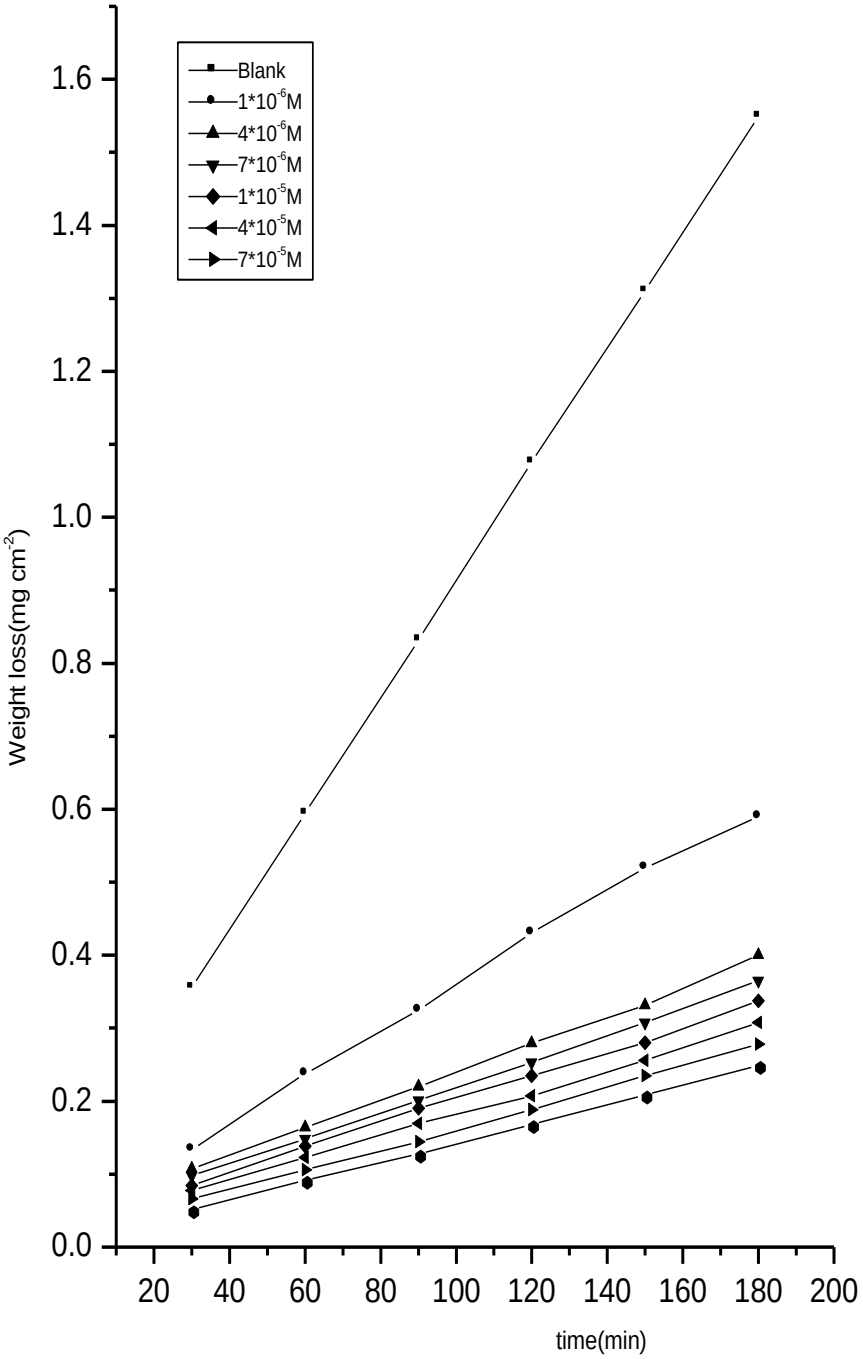

Fig(3.7) weight loss-time curves for carbon steel dissolution in 0.5M H_2SO_4 in absence and presence of10^{-2}M KI and different concentrations of compound(2) at 303 K

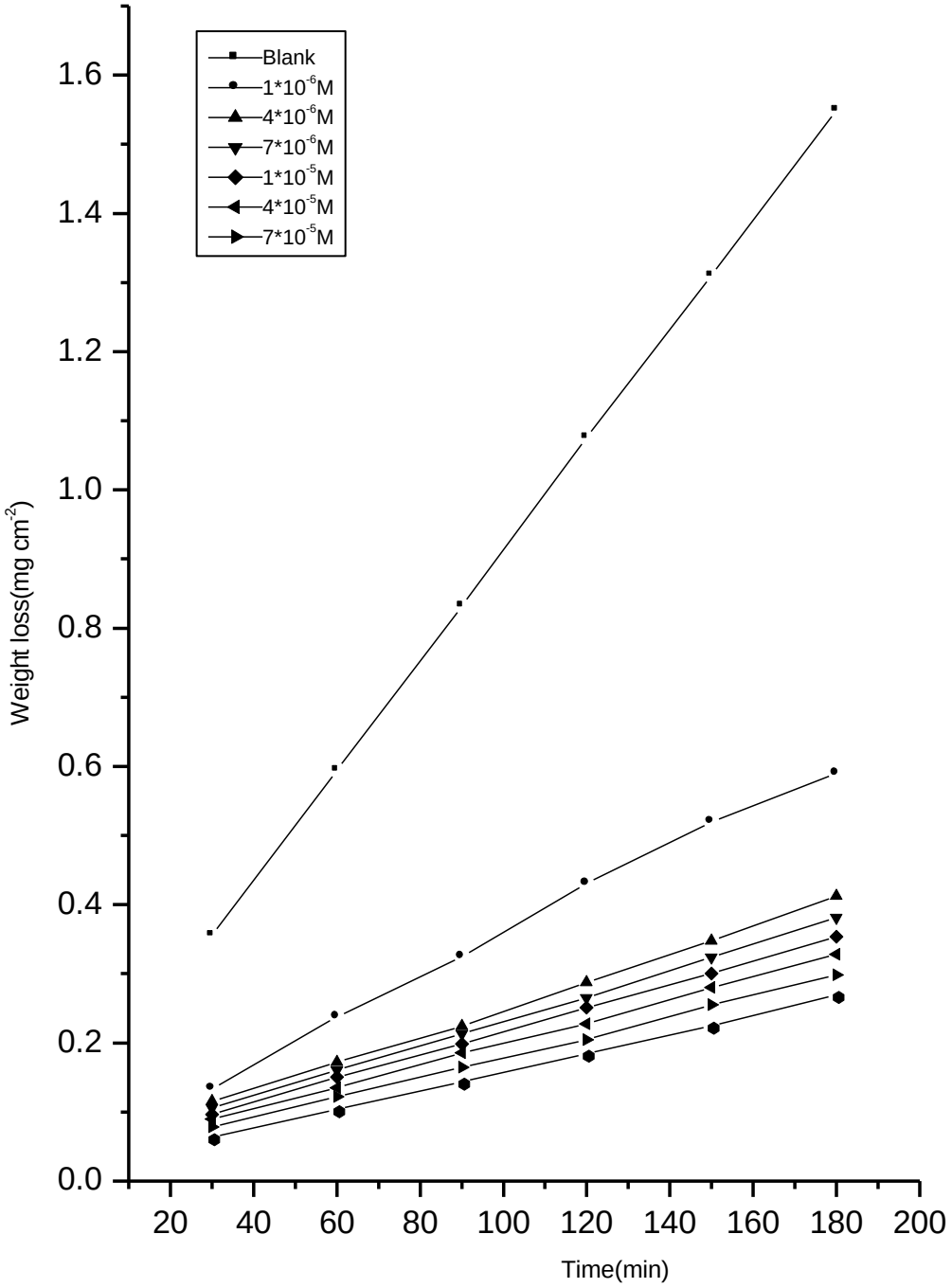

Fig(3.8) weight loss-time curves for carbon steel dissolution in 0.5M H_2SO_4 in absence and presence of10^{-2}M KI and different concentrations of compound(3) at 303 K

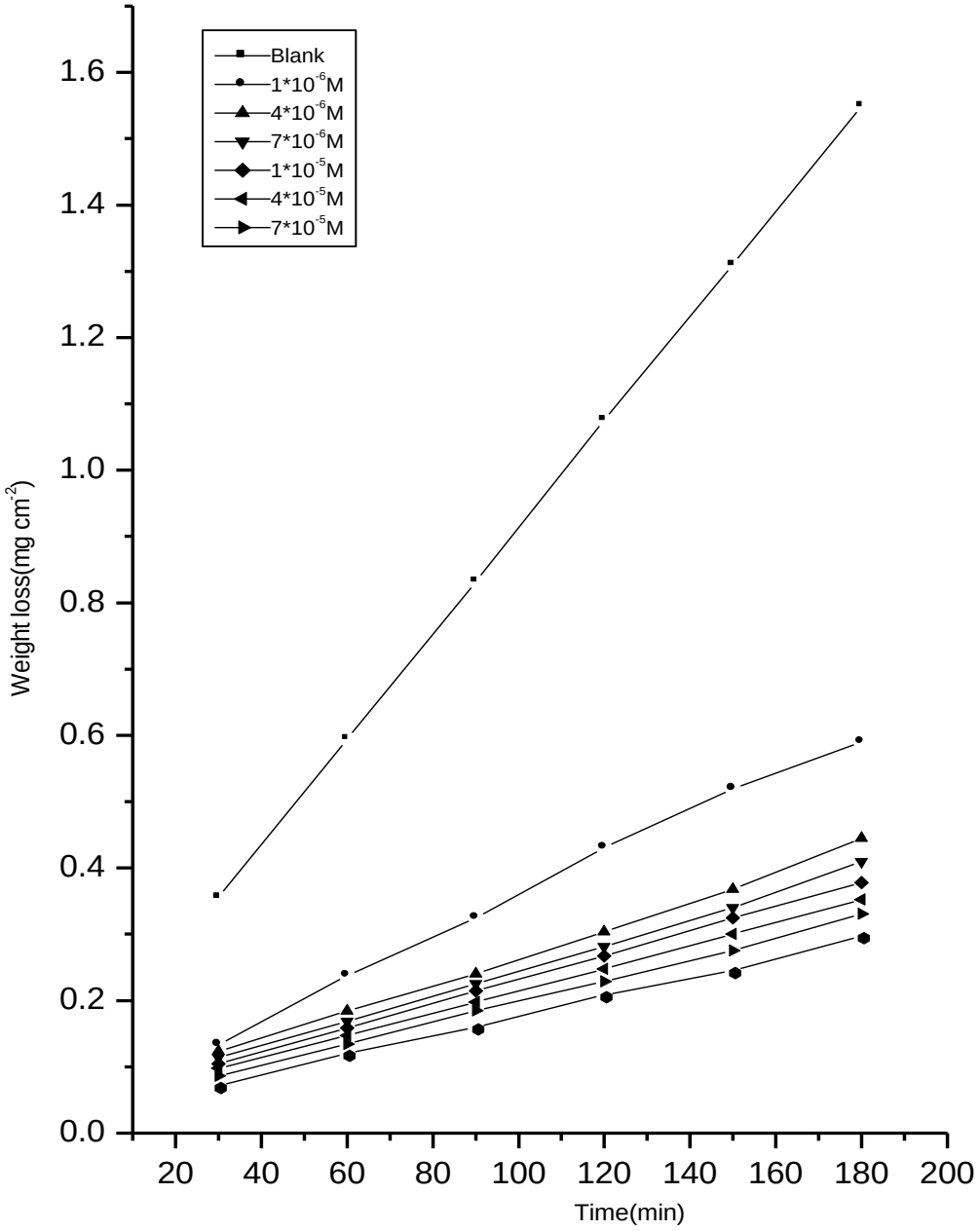

Fig(3.9) weight loss-time curves for carbon steel dissolution in 0.5M H_2SO_4 in absence and presence of 10^{-2}M KI and different concentrations of compound(4) at 303 K

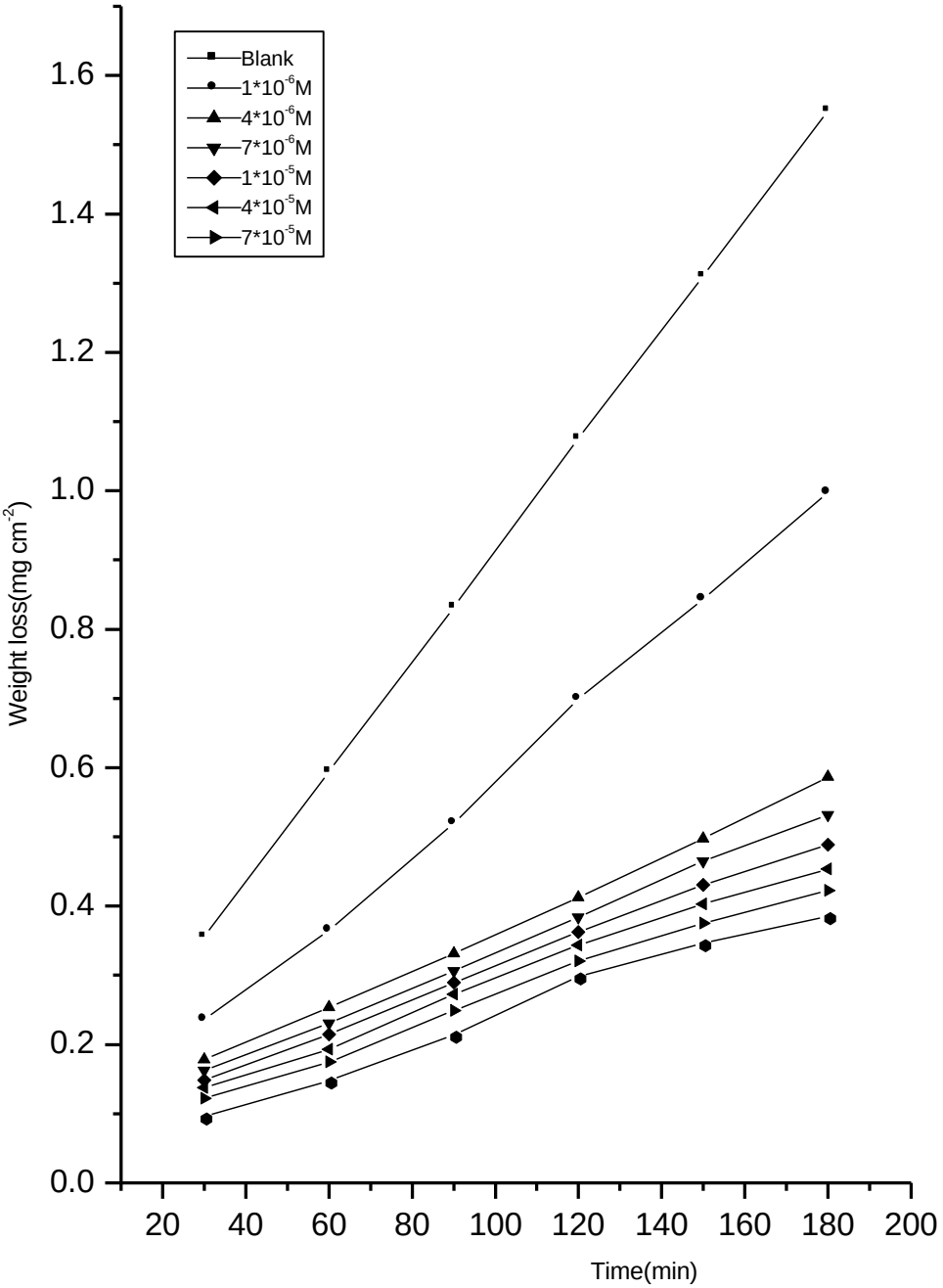

Fig(3.10) weight loss-time curves for carbon steel dissolution in 0.5M H_2SO_4 in absence and presence of10^{-2}M KSCN and different concentrations of compound(1) at 303 K

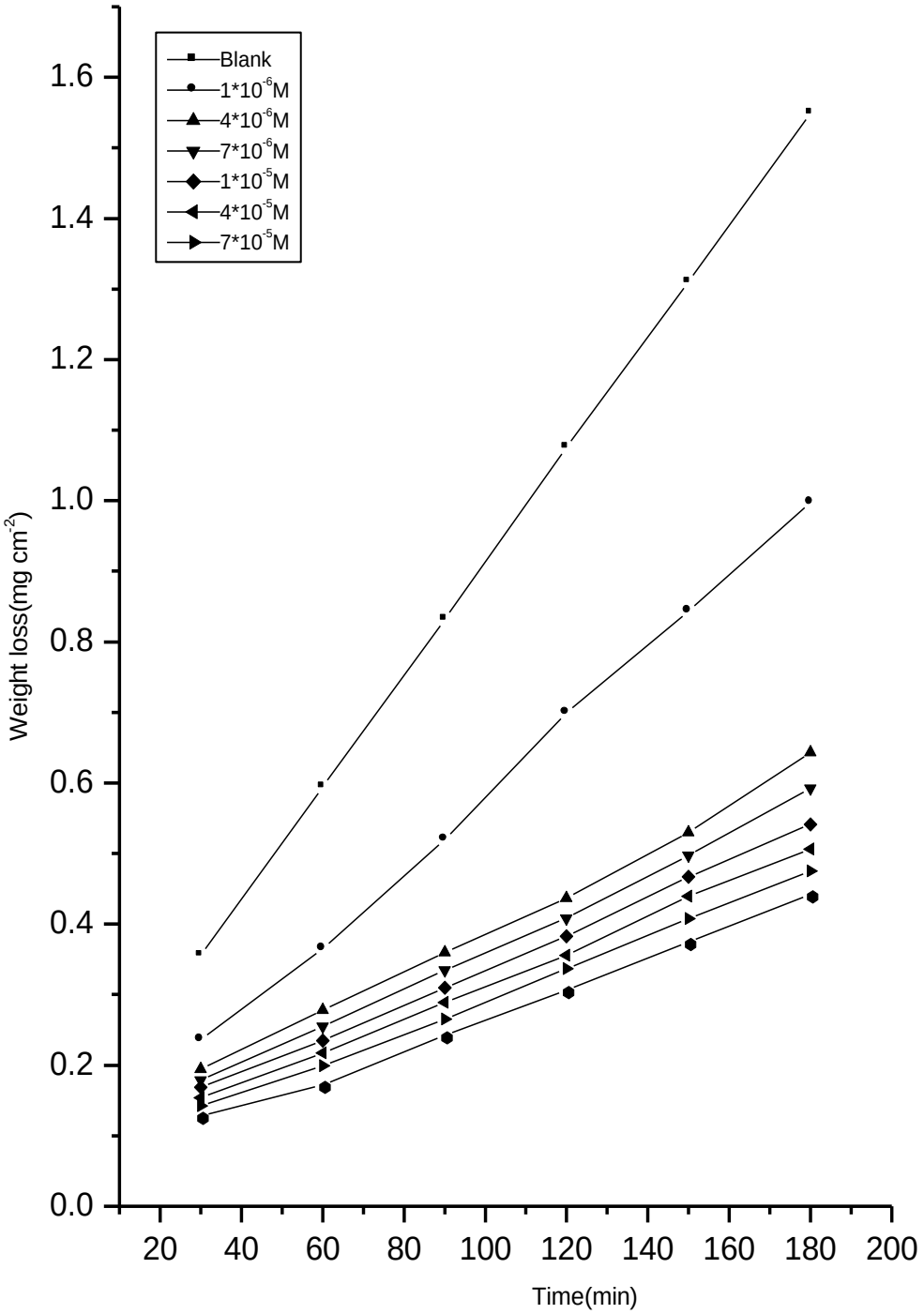

Fig(3.11) weight loss-time curves for carbon steel dissolution in 0.5M H_2SO_4 in absence and presence of 10^{-2}M KSCN and different concentrations of compound(2) at 303 K

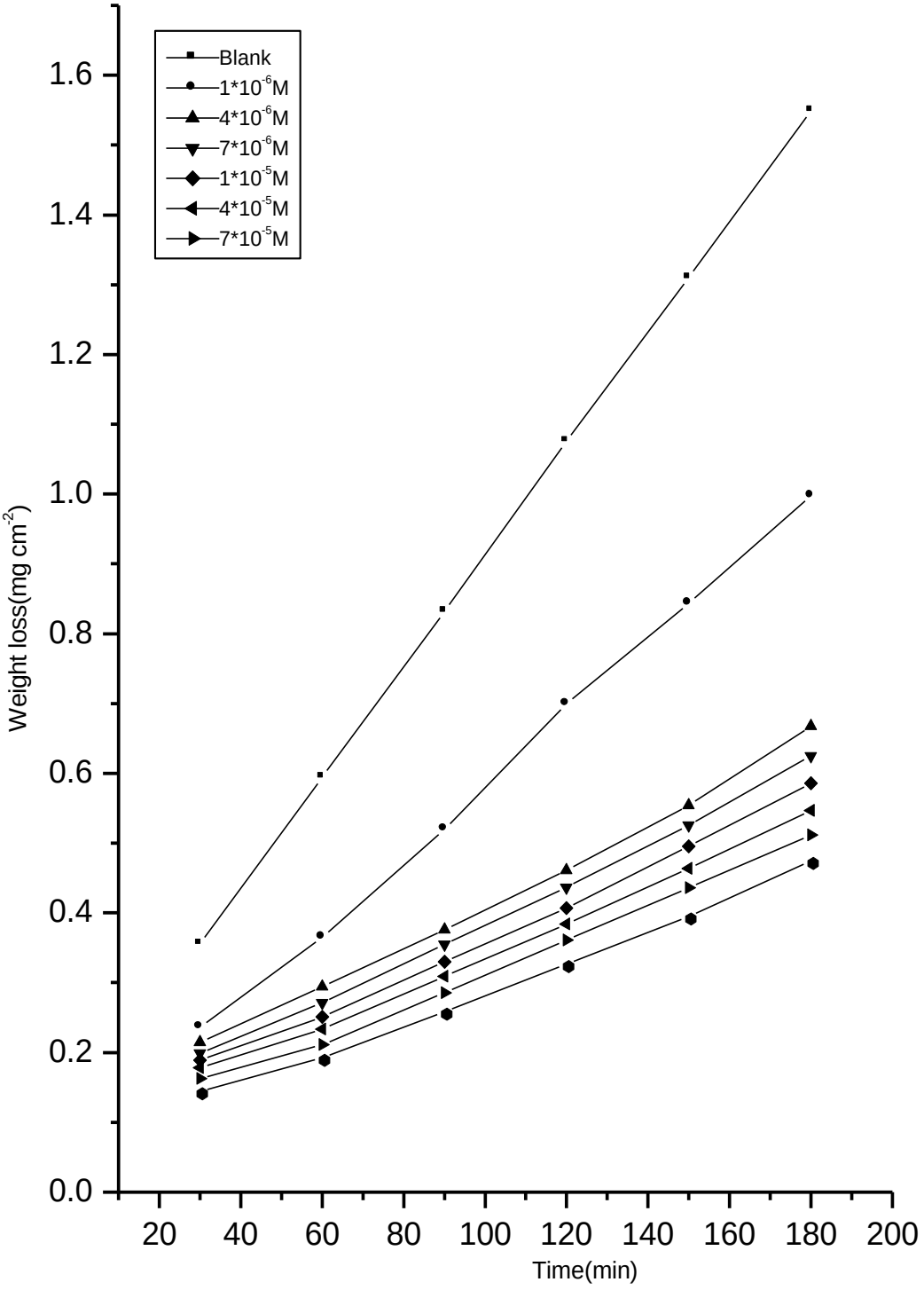

Fig(3.12) weight loss-time curves for carbon steel dissolution in 0.5M H_2SO_4 in absence and presence of 10^{-2}M KSCN and different concentrations of compound(3) at 303 K

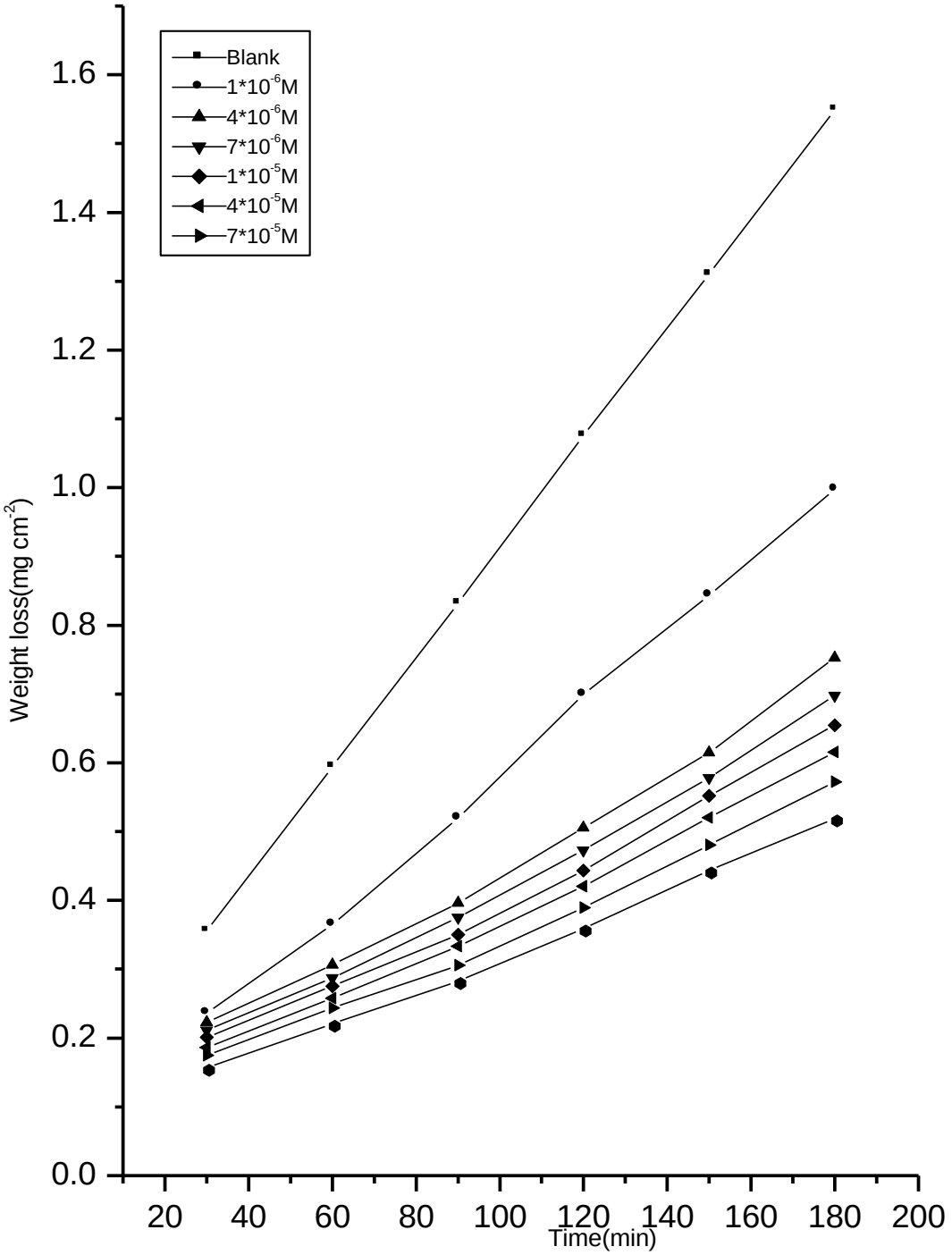

Fig(3.13) weight loss-time curves for carbon steel dissolution in 0.5M H_2SO_4 in absence and presence of 10^{-2}M KSCN and different concentrations of compound(4) at 303 K

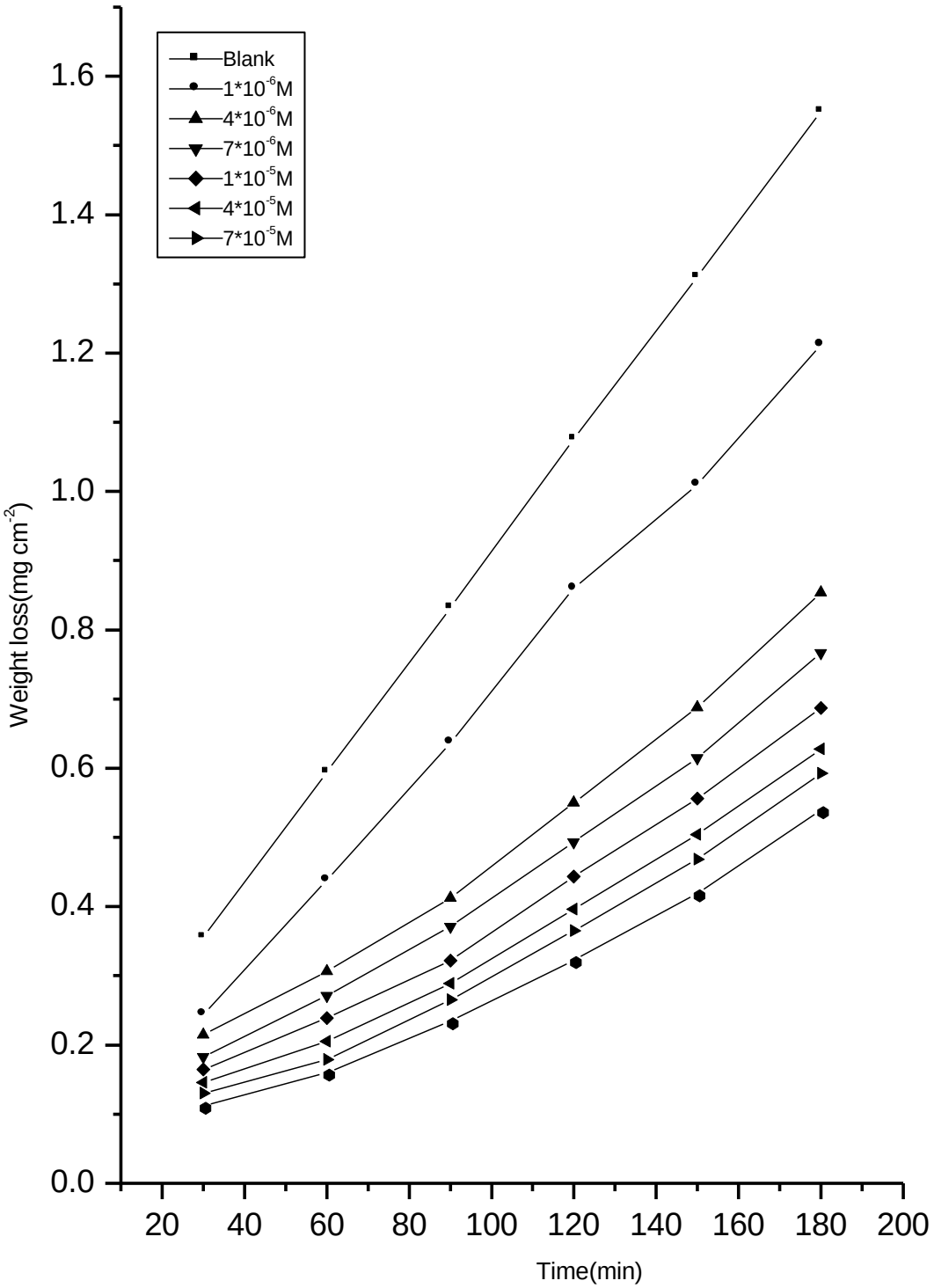

Fig(3.14) weight loss-time curves for carbon steel dissolution in 0.5M H_2SO_4 in absence and presence of 10^{-2}M KBr and different concentrations of compound(1) at 303 K

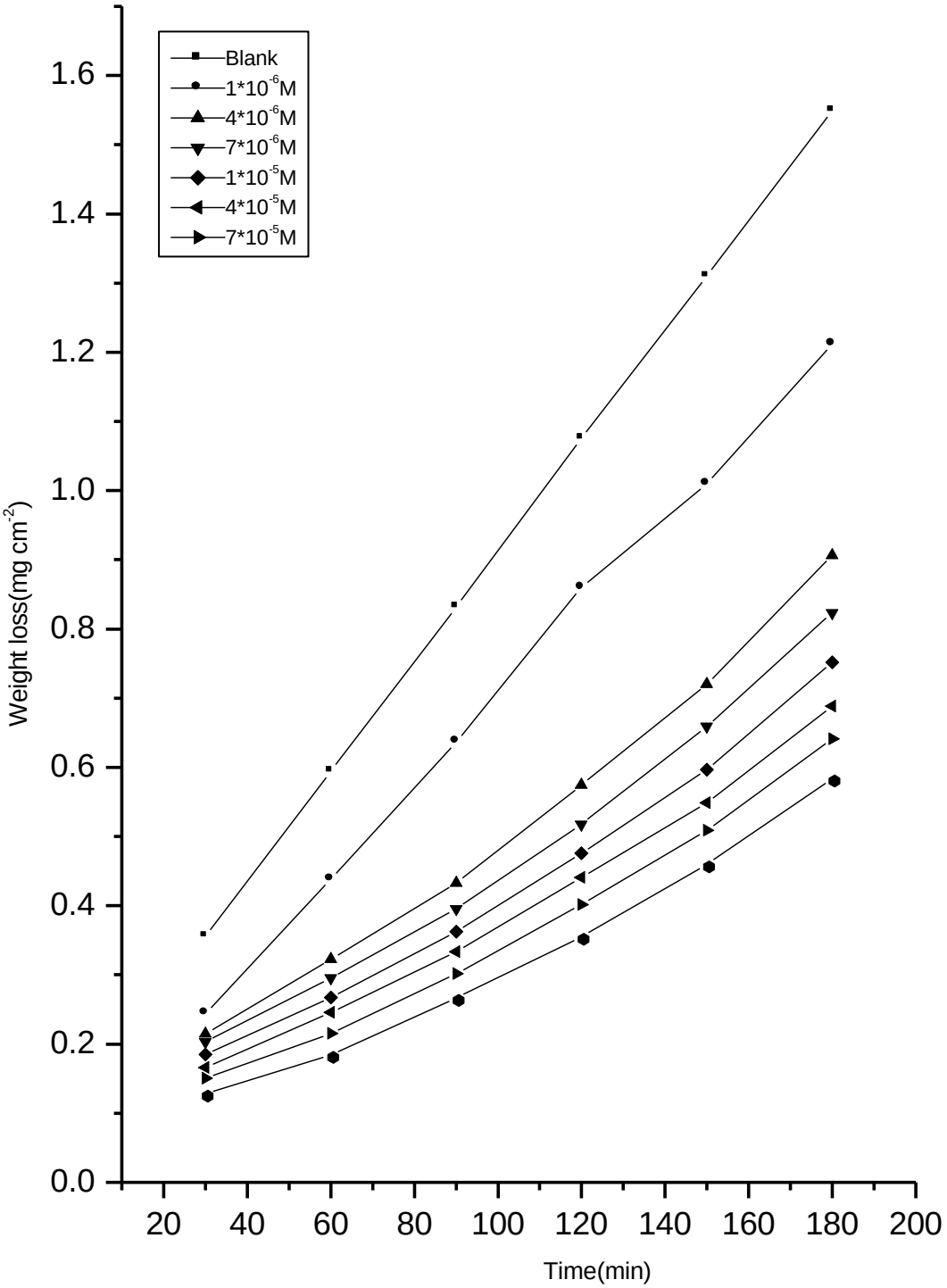

Fig(3.15) weight loss-time curves for carbon steel dissolution in 0.5M H_2SO_4 in absence and presence of 10^{-2}M KBr and different concentrations of compound(2) at 303 K

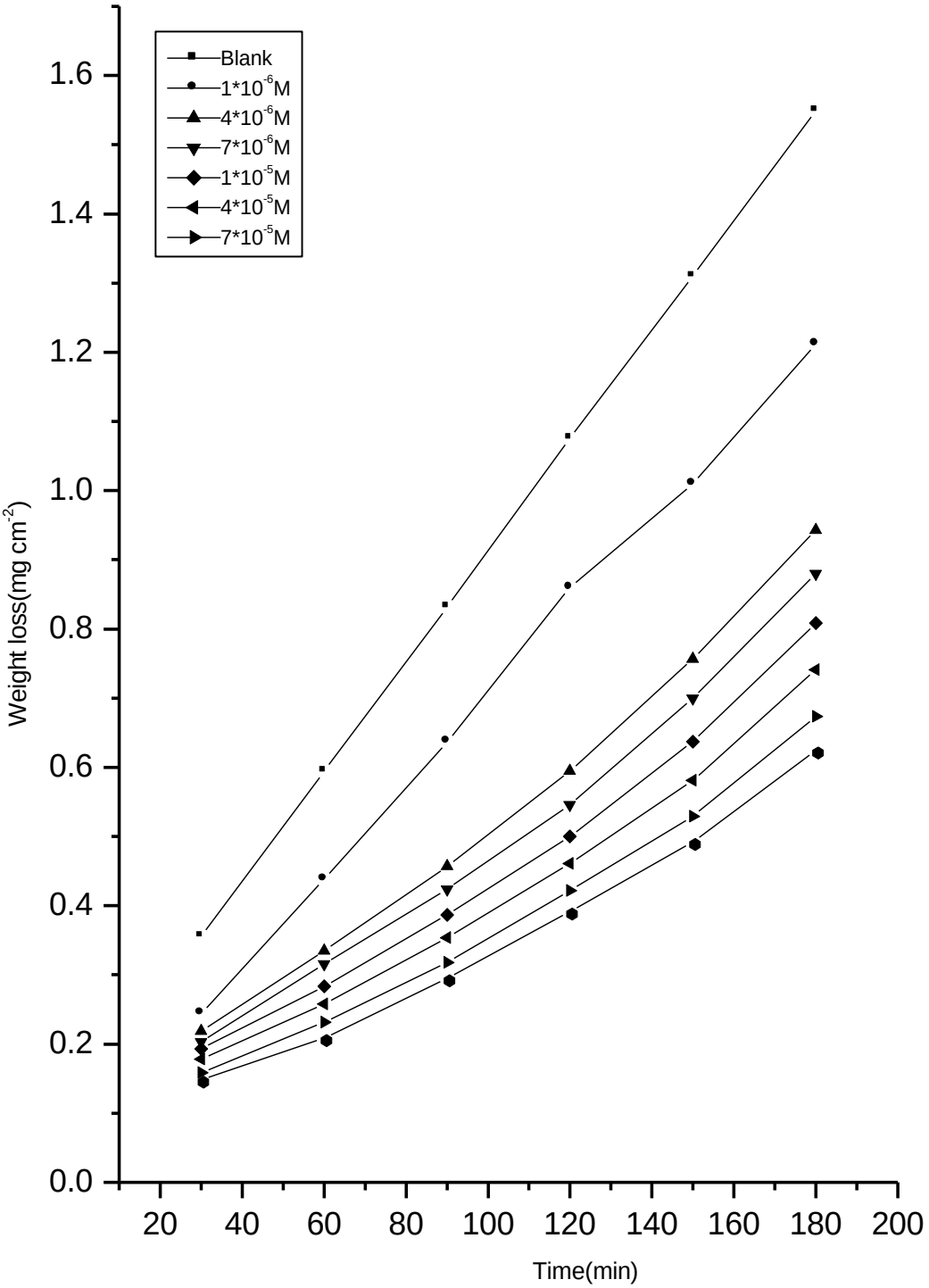

Fig(3.16) weight loss-time curves for carbon steel dissolution in 0.5M H_2SO_4 in absence and presence of 10^{-2}M KBr and different concentrations of compound(3) at 303 K

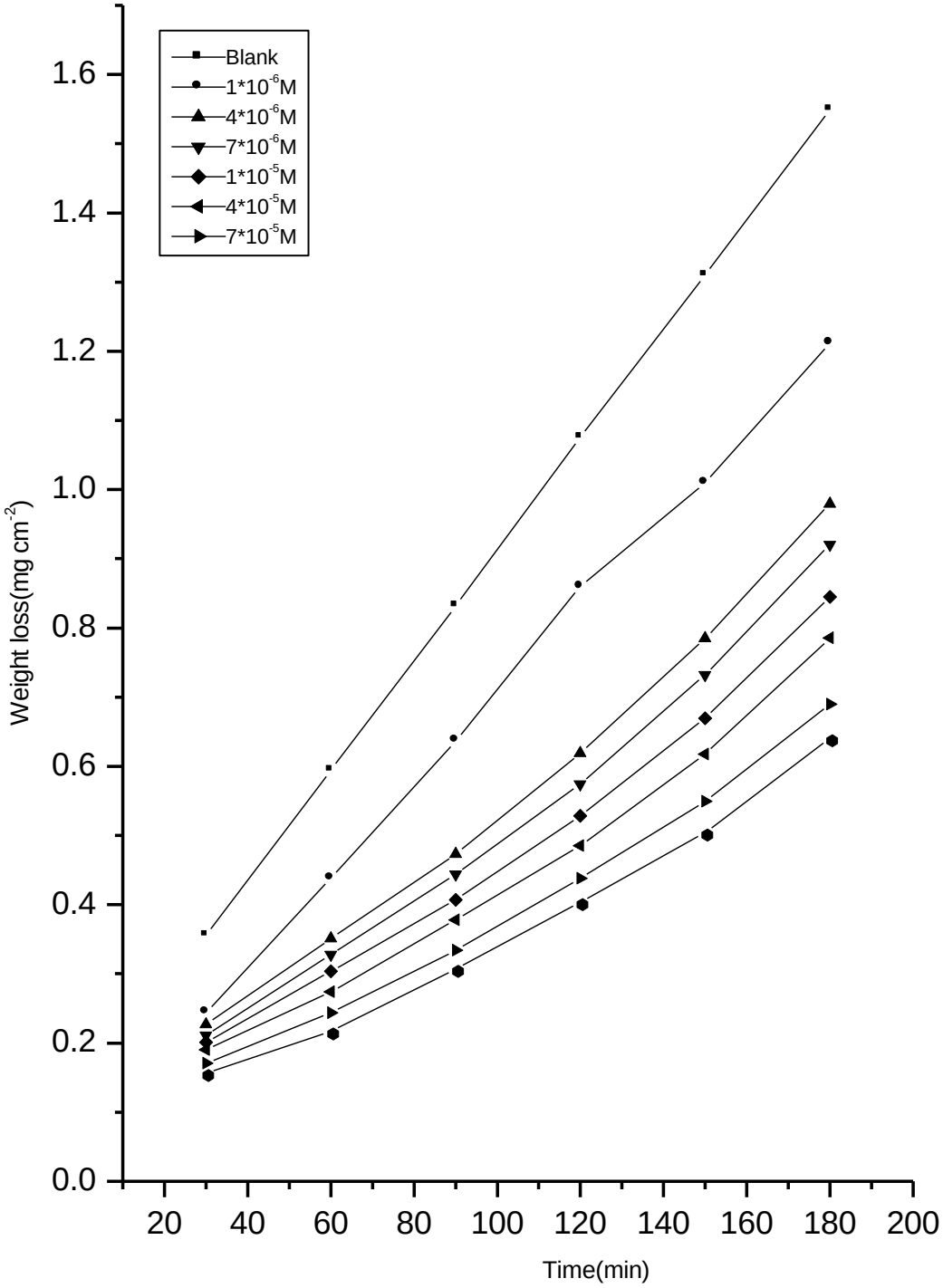

Fig(3.17) weight loss-time curves for carbon steel dissolution in 0.5M H_2SO_4 in absence and presence of 10^{-2}M KBr and different concentrations of compound(4) at 303 K

Table(3.2) Percentage inhibition efficiency values (% IE) of carbon steel dissolution in 0.5M H_2SO_4 in presence of $1x10^{-2}$M KI at different concentrations of N-3-Hydroxyl-2-Naphthoyl Hydrazone derivatives at 303K.

Concentration, M	Percentage inhibition efficiency (% IE) compounds			
	1	2	3	4
$1X10^{-6}$	76.2	74	73.2	71.7
$4X10^{-6}$	77.9	76.4	75.3	73.8
$7X10^{-6}$	80	78.1	76.6	75.1
$1X10^{-5}$	81.8	80.7	78.8	76.9
$4X10^{-5}$	84	82.5	80.9	78.7
$7X10^{-5}$	85.8	84.3	82.8	80.6

Table(3.3) Percentage inhibition efficiency values (% IE) of carbon steel dissolution in 0.5M H_2SO_4 in presence of $1x10^{-2}$M KSCN at different concentrations of N-3-Hydroxyl-2-Naphthoyl Hydrazone derivatives at 303K.

Concentration, M	Percentage inhibition efficiency (% IE)			
	compounds			
	1	2	3	4
$1X10^{-6}$	61.6	59.4	56.7	53
$4X10^{-6}$	64.3	62	59.7	56
$7X10^{-6}$	66.3	64.4	61.8	58.7
$1X10^{-5}$	68	66.9	64.3	60.9
$4X10^{-5}$	70	68.7	66.4	63.8
$7X10^{-5}$	72.2	71.5	69.2	66.6

Table(3.4) Percentage inhibition efficiency values (% IE) of carbon steel dissolution in 0.5M H_2SO_4 in presence of $1x10^{-2}$M KBr at different concentrations of N-3-Hydroxyl-2-Naphthoyl Hydrazone derivatives at 303K.

Concentration, M	Percentage inhibition efficiency (% IE)			
	compounds			
	1	2	3	4
$1X10^{-6}$	48.8	46.6	44.7	42.4
$4X10^{-6}$	54.1	51.8	49.2	46.6
$7X10^{-6}$	58.7	55.7	53.5	50.3
$1X10^{-5}$	63.1	59	57.2	54.9
$4X10^{-5}$	66	62.6	60	59.2
$7X10^{-5}$	70	67	63.6	62.5

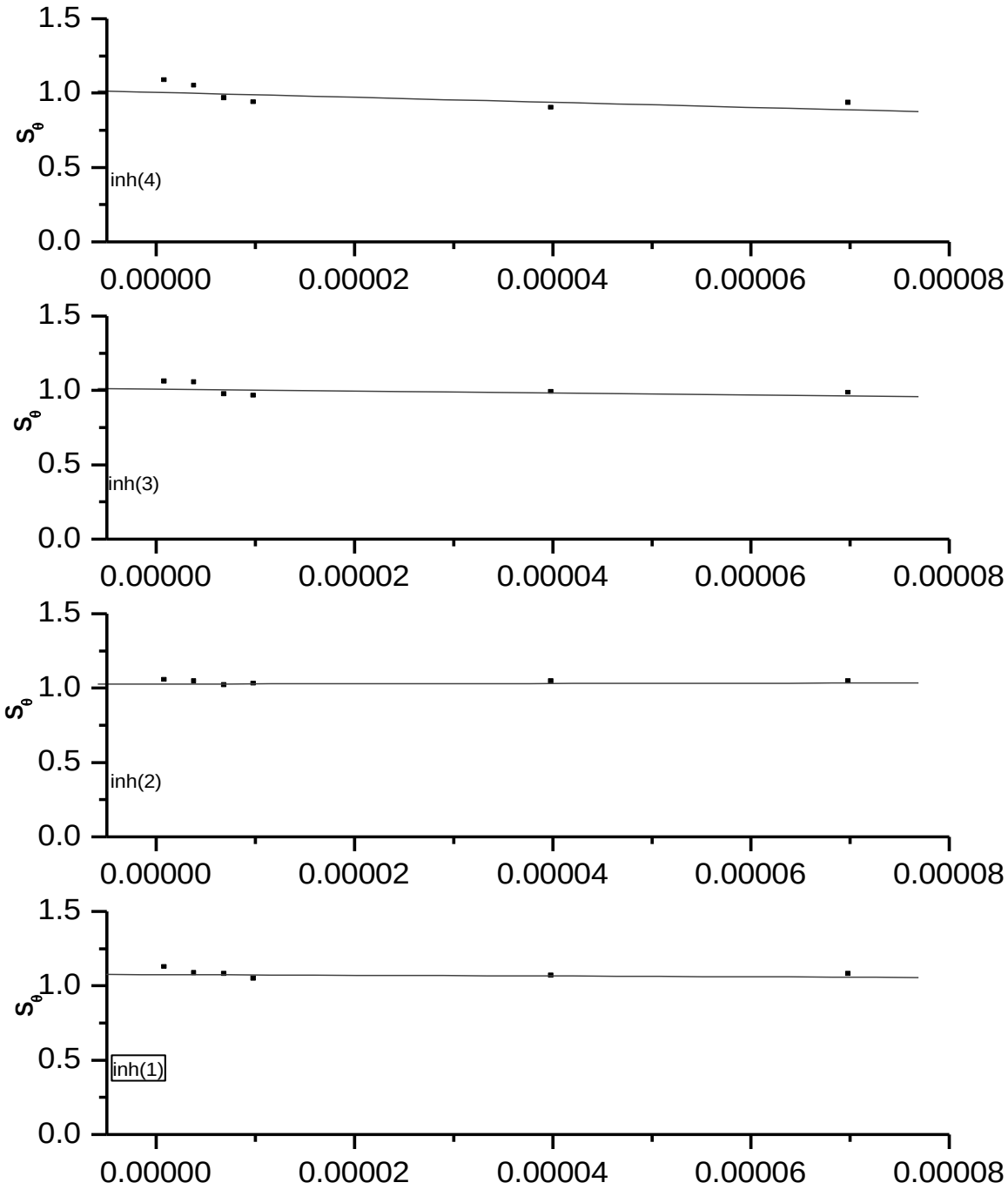

Fig.(3.18): Plot of synergism parameter (S_θ) versus the concentration of all inhibitors, in presence of 1X10^{-2} M, KI at 303K.

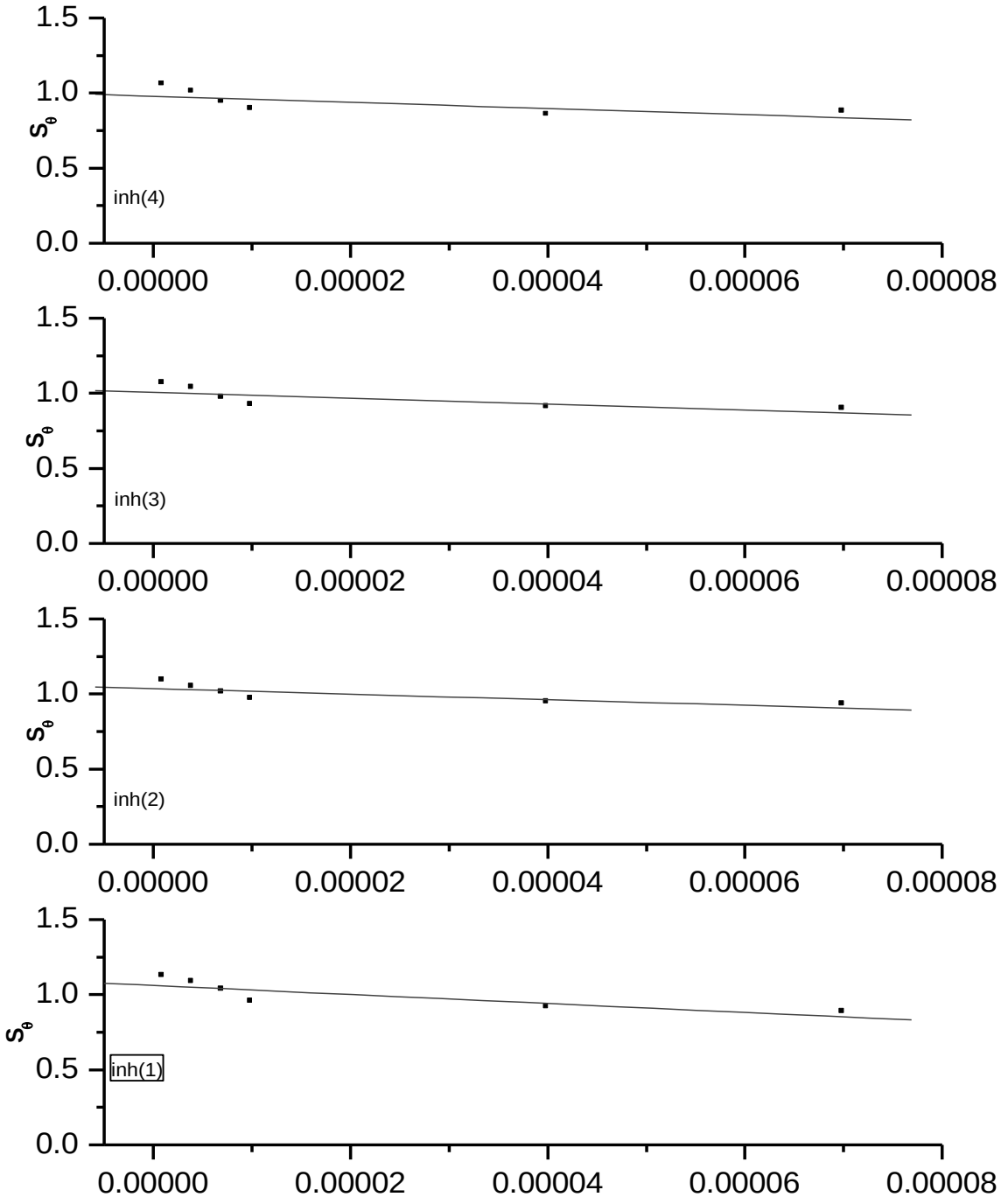

Fig.(3.19): Plot of synergism parameter (S_θ) versus the concentration of all inhibitors, in presence of 1X10^{-2} M, KSCN at 303K.

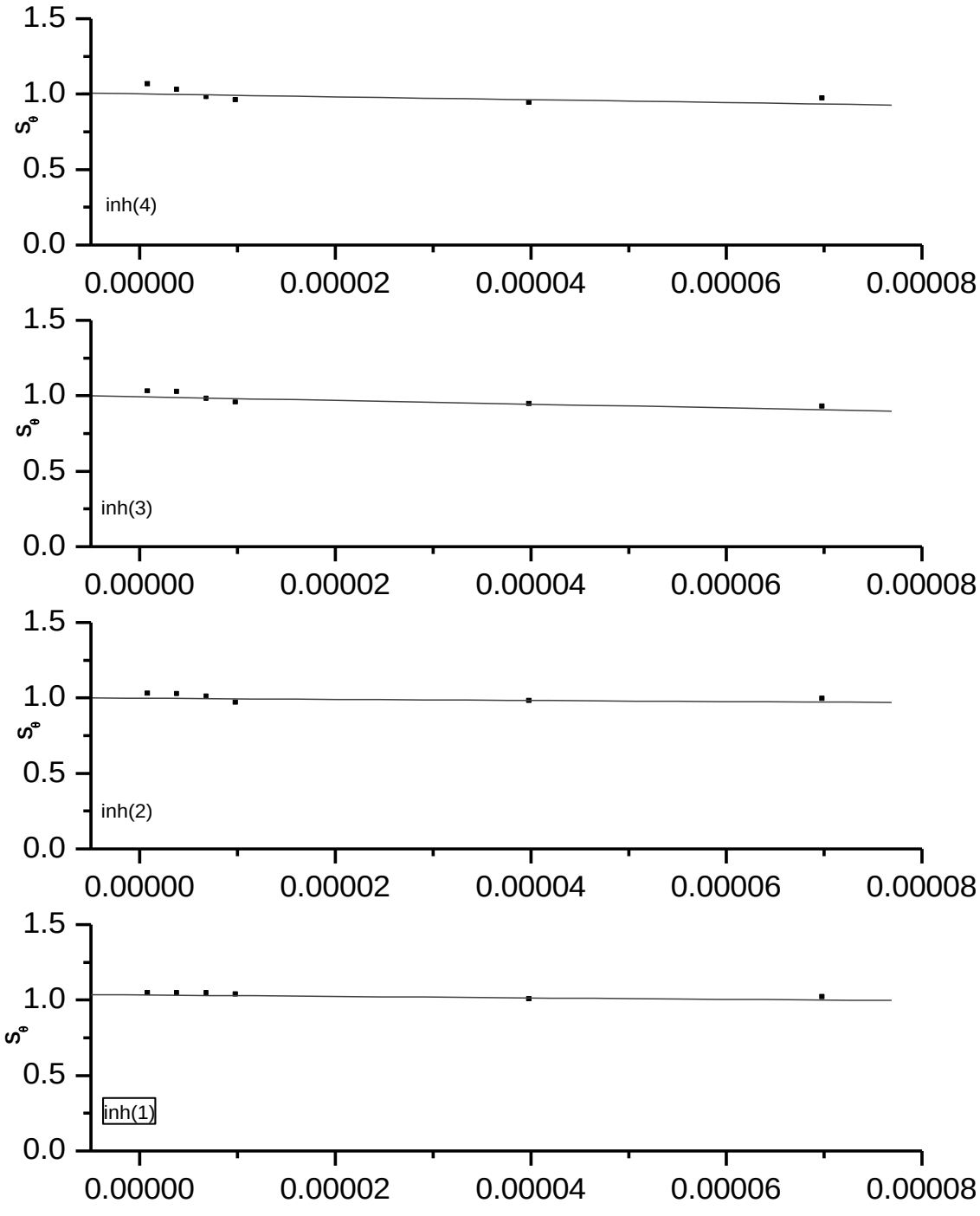

Fig.(3.20): Plot of synergism parameter (S_θ) versus the concentration of all inhibitors, in presence of 1X10^{-2} M, KBr at 303K.

Table(3.5) Synergistic parameter ($S_{\square}$ for different concentrations of inhibitors and in presence of 1 $X10^{-2}$M of KI

Concentration M	S_θ			
	1	2	3	4
1X10-6	1.11	1.04	1.05	1.07
$4X10^{-6}$	1.07	1.04	1.04	1.04
$7X10^{-6}$	1.07	1.01	0.96	0.96
$1X10^{-5}$	1.04	1.01	0.95	0.93
$4X10^{-5}$	1.06	1.04	0.98	0.89
$7X10^{-5}$	1.07	1.03	0.97	0.92

Table(3.6) Synergistic Parameter ($S_\theta$for different concentrations of inhibitors and in presence of 1 $X10^{-2}$M of KSCN

Concentration M	S_θ			
	1	2	3	4
1X10-6	1.12	1.09	1.06	1.05
$4X10^{-6}$	1.08	1.05	1.03	1.00
$7X10^{-6}$	1.03	1.01	0.96	0.93
$1X10^{-5}$	0.95	0.96	0.91	0.89
$4X10^{-5}$	0.91	0.94	0.90	0.85
$7X10^{-5}$	0.88	0.92	0.89	0.87

Table(3.7) Synergistic Parameter (S_θ for different concentrations of inhibitors and in presence of 1 $X10^{-2}$M of KBr

Concentration M	S_θ			
	1	2	3	4
1X10-6	1.04	1.02	1.02	1.06
$4X10^{-6}$	1.03	1.01	1.01	1.02
$7X10^{-6}$	1.04	0.99	0.97	0.97
$1X10^{-5}$	1.03	0.95	0.94	0.95
$4X10^{-5}$	0.99	0.97	0.93	0.92
$7X10^{-5}$	1.01	0.98	0.92	0.96

3.4- Effect of Temperatures.

The study of the effect of temperature on the inhibition efficiency of different inhibitors is important in the elucidation of the mechanism and the kinetics of their action and ultimately the proper selection of these inhibitors for specific practical situations. Accordingly the effect of temperature on the corrosion medium on the reaction of carbon steel in pure acids was reported by many authors [101,79].

In this part, the effect of temperatures on both corrosion and corrosion inhibition of carbon steel was investigated by weight loss measurement.

Weight loss-time curves in absence and presence of different concentrations of compounds (1-4) at different temperatures ranging from 308 to 323K are shown graphically in Figures (3.21-3.36). From these figures, one can conclude that, by increasing the temperature the weight loss increases for the same concentration. This means that, the adsorption of N-3-Hydroxyl-2-Naphthoyl Hydrazone derivatives on the metal surface is physically.

The results of Tables (3.8– 3.11) show that, the percentage efficiency decreases in presence of low concentrations of the inhibitors, and inhibition with increasing the temperature. This behavior can explained on the basis that the increase of the temperature leads to desorption of the adsorbed molecules of the inhibitors from the metal surface. Also the order of inhibition efficiency decreased as follow:

$$1 > 2 > 3 > 4$$

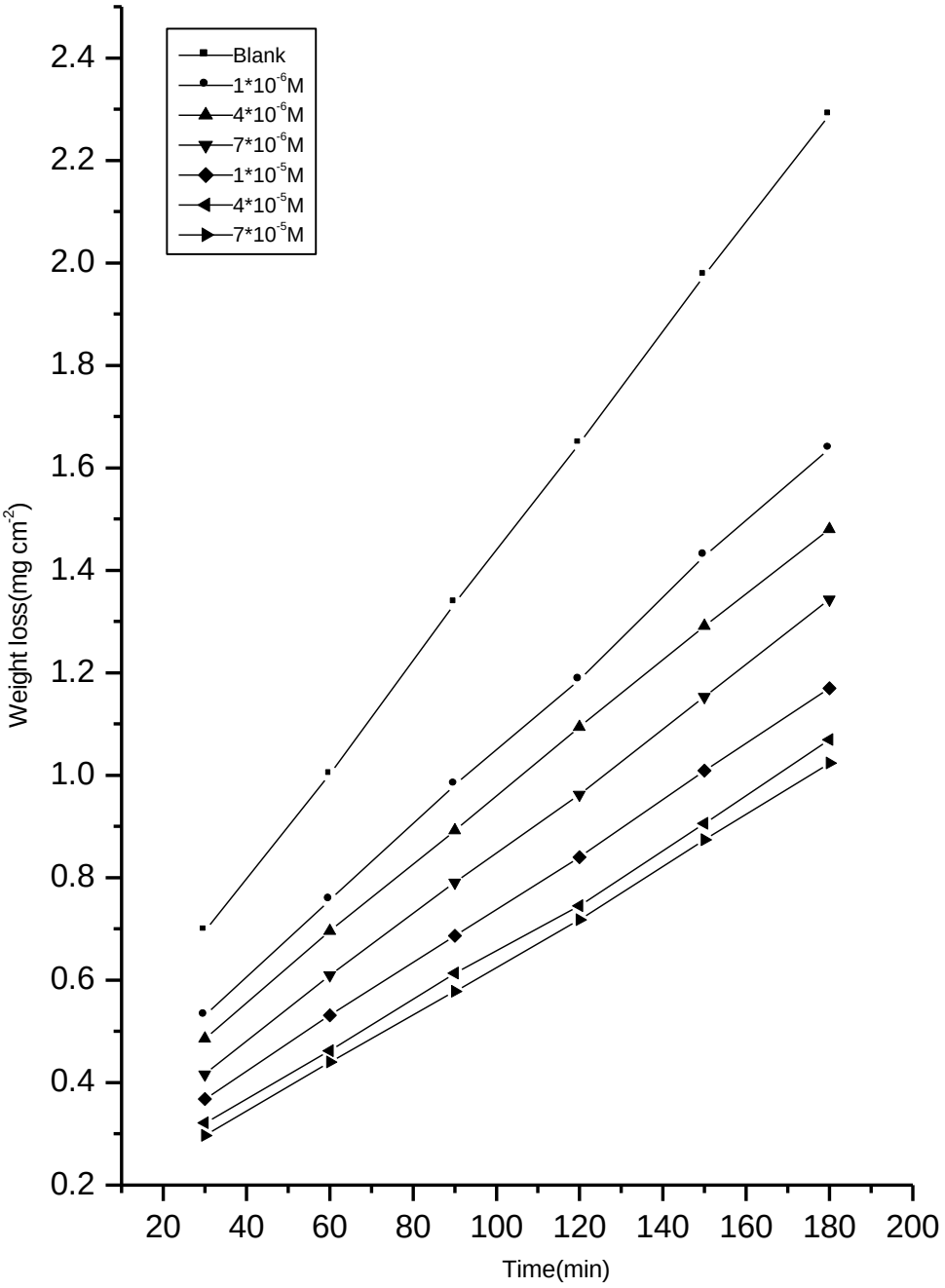

Fig(3.21) weight loss-time curves for carbon steel dissolution in 0.5M H_2SO_4 in absence and presence of different concentrations of compound(1) at 308 K

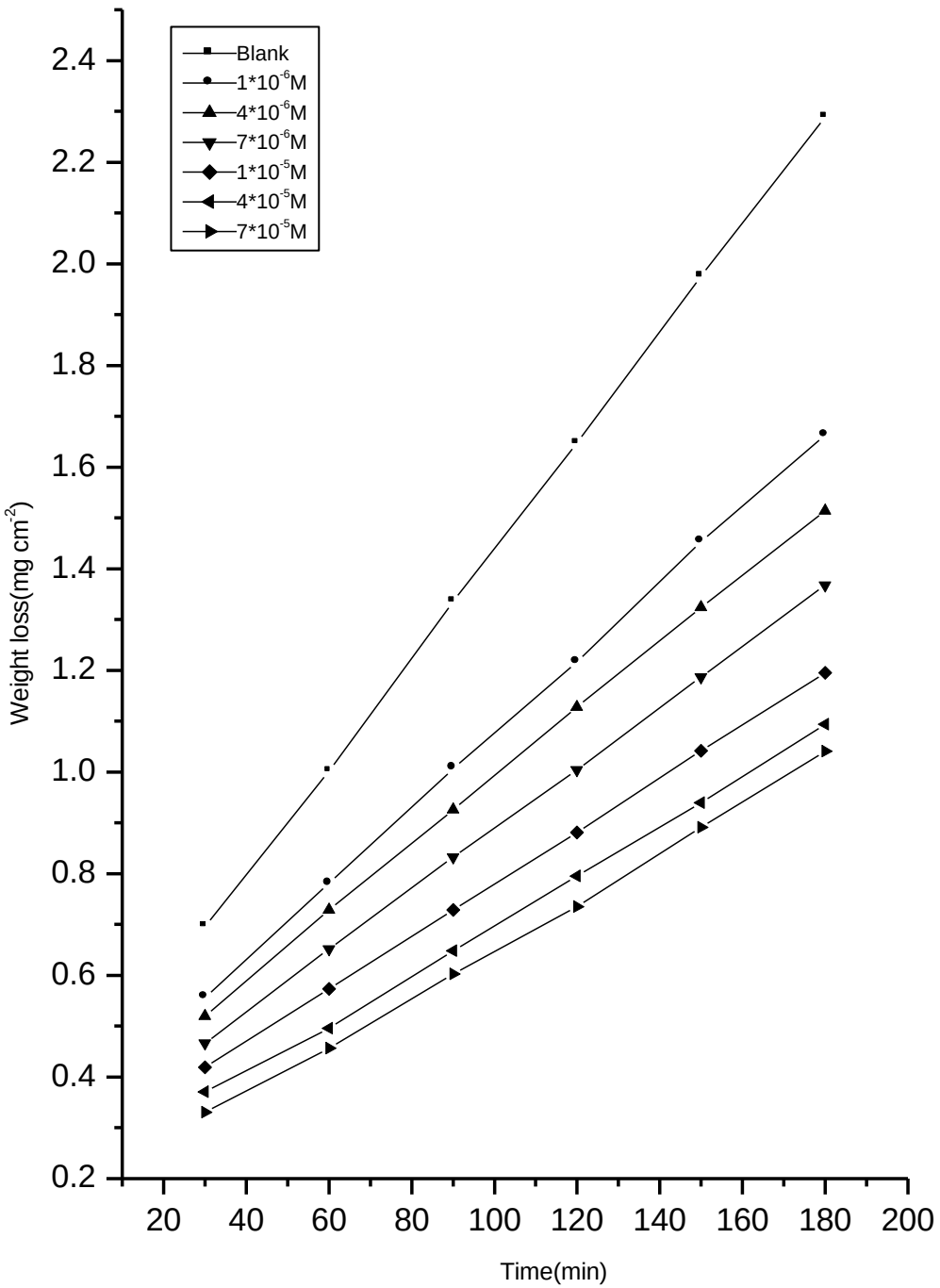

Fig(3.22) weight loss-time curves for carbon steel dissolution in 0.5M H_2SO_4 in absence and presence of different concentrations of compound(2) at 308 K

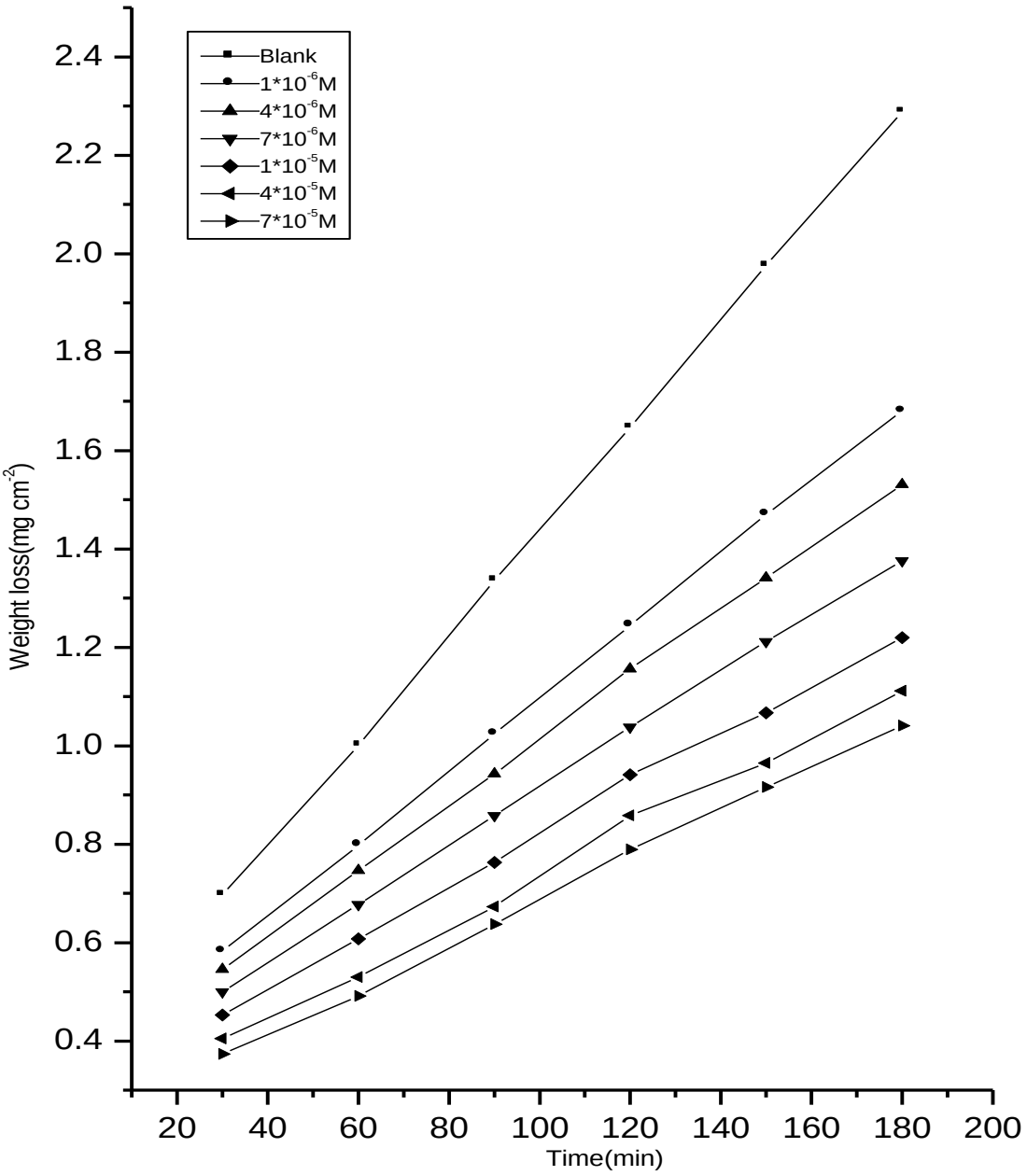

Fig(3.23) weight loss-time curves for carbon steel dissolution in 0.5M H_2SO_4 in absence and presence of different concentrations of compound(3) at 308 K

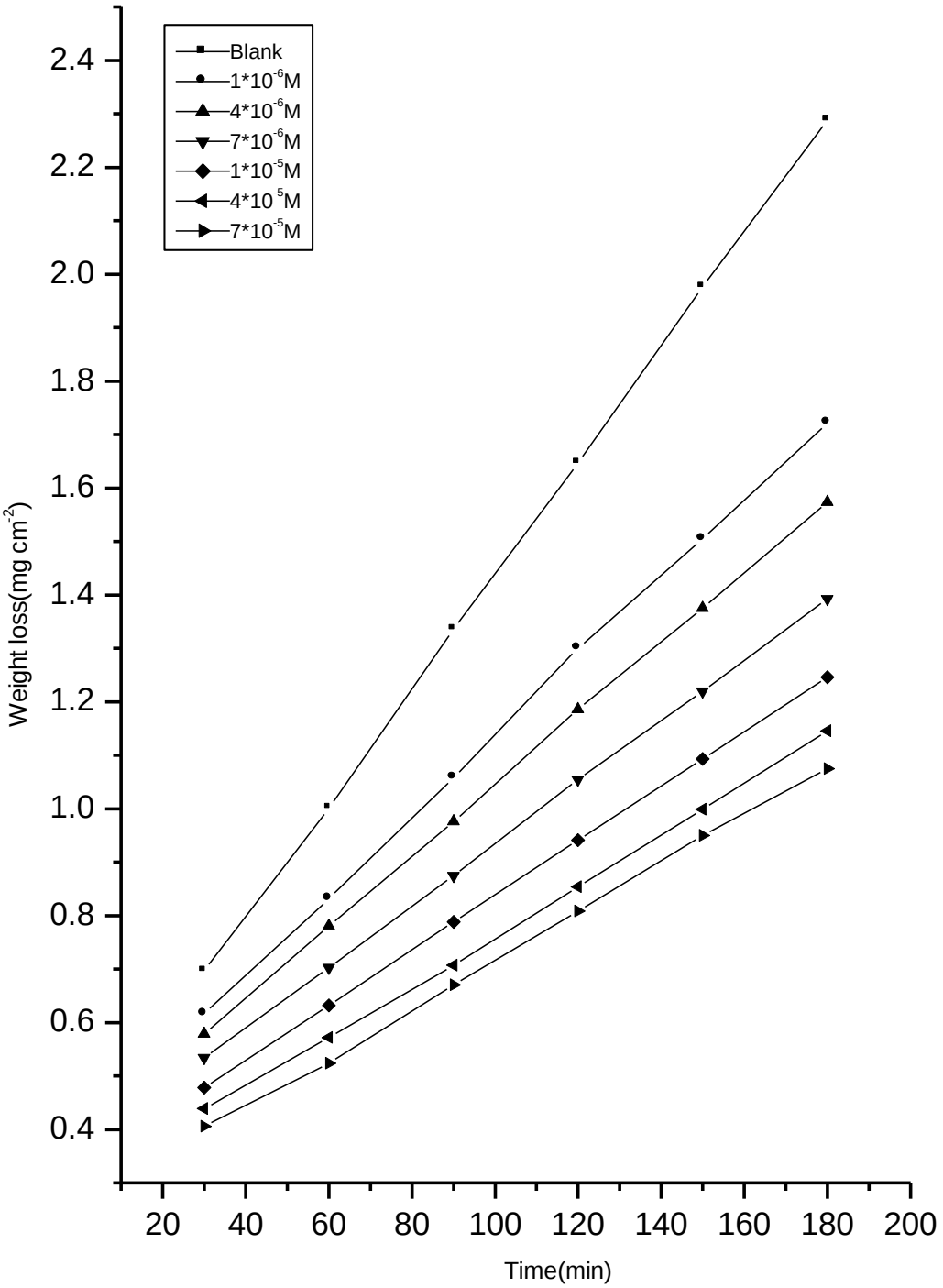

Fig(3.24) weight loss-time curves for carbon steel dissolution in 0.5M H_2SO_4 in absence and presence of different concentrations of compound(4) at 308 K

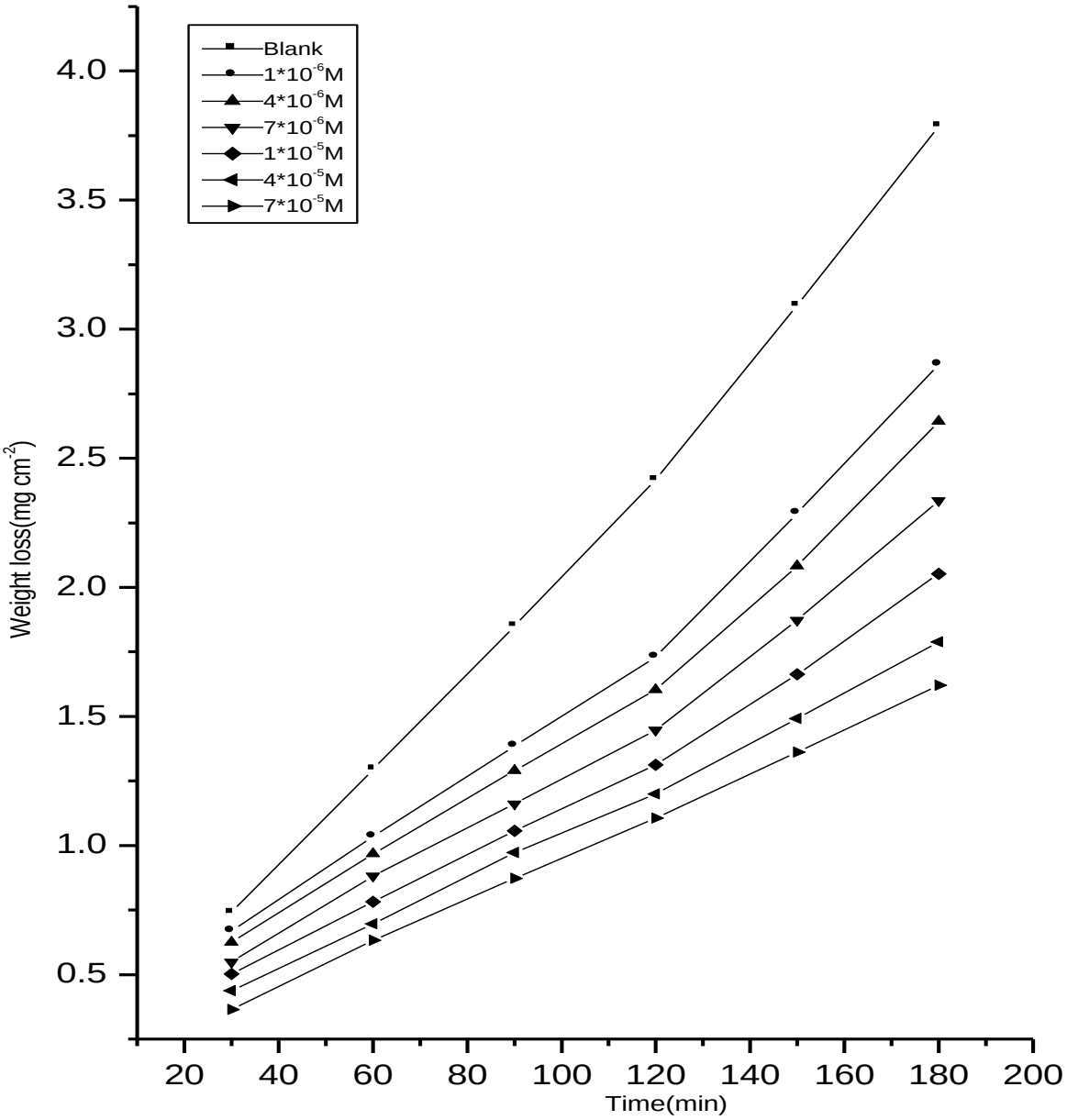

Fig(3.25) weight loss-time curves for carbon steel dissolution in 0.5M H_2SO_4 in absence and presence of different concentrations of compound(1) at 313 K

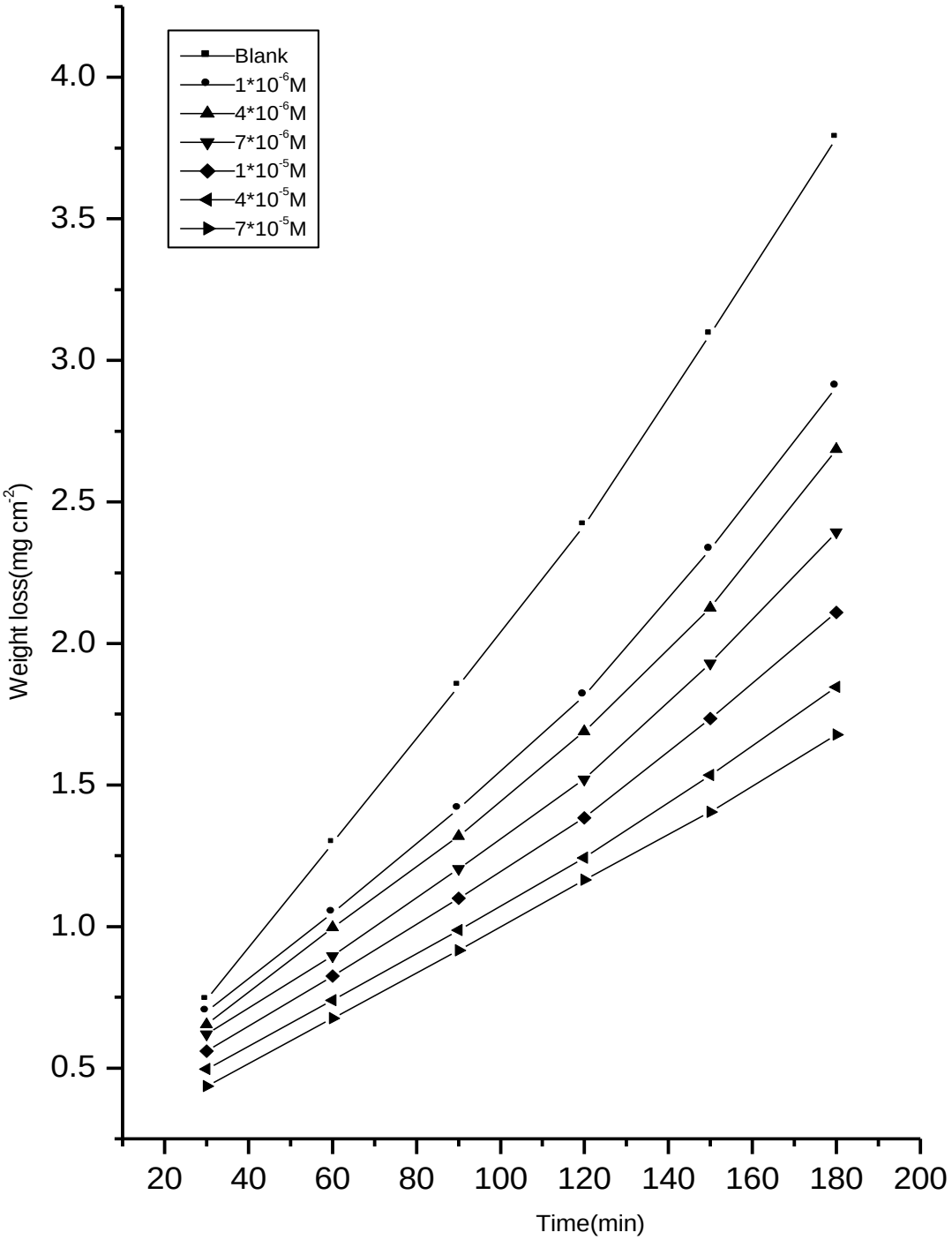

Fig(3.26) weight loss-time curves for carbon steel dissolution in 0.5M H_2SO_4 in absence and presence of different concentrations of compound(2) at 313 K

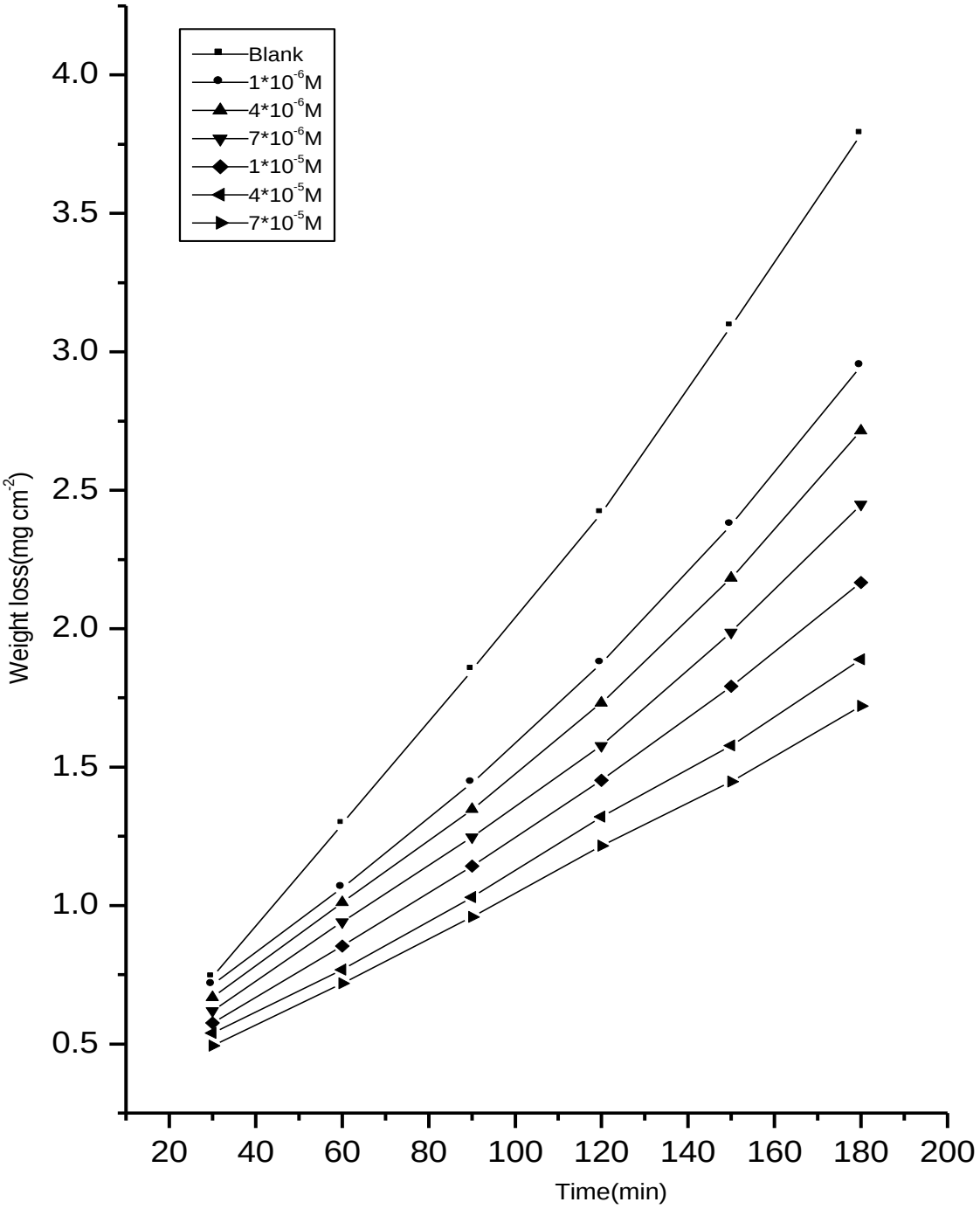

Fig(3.27) weight loss-time curves for carbon steel dissolution in 0.5M H_2SO_4 in absence and presence of different concentrations of compound(3) at 313 K

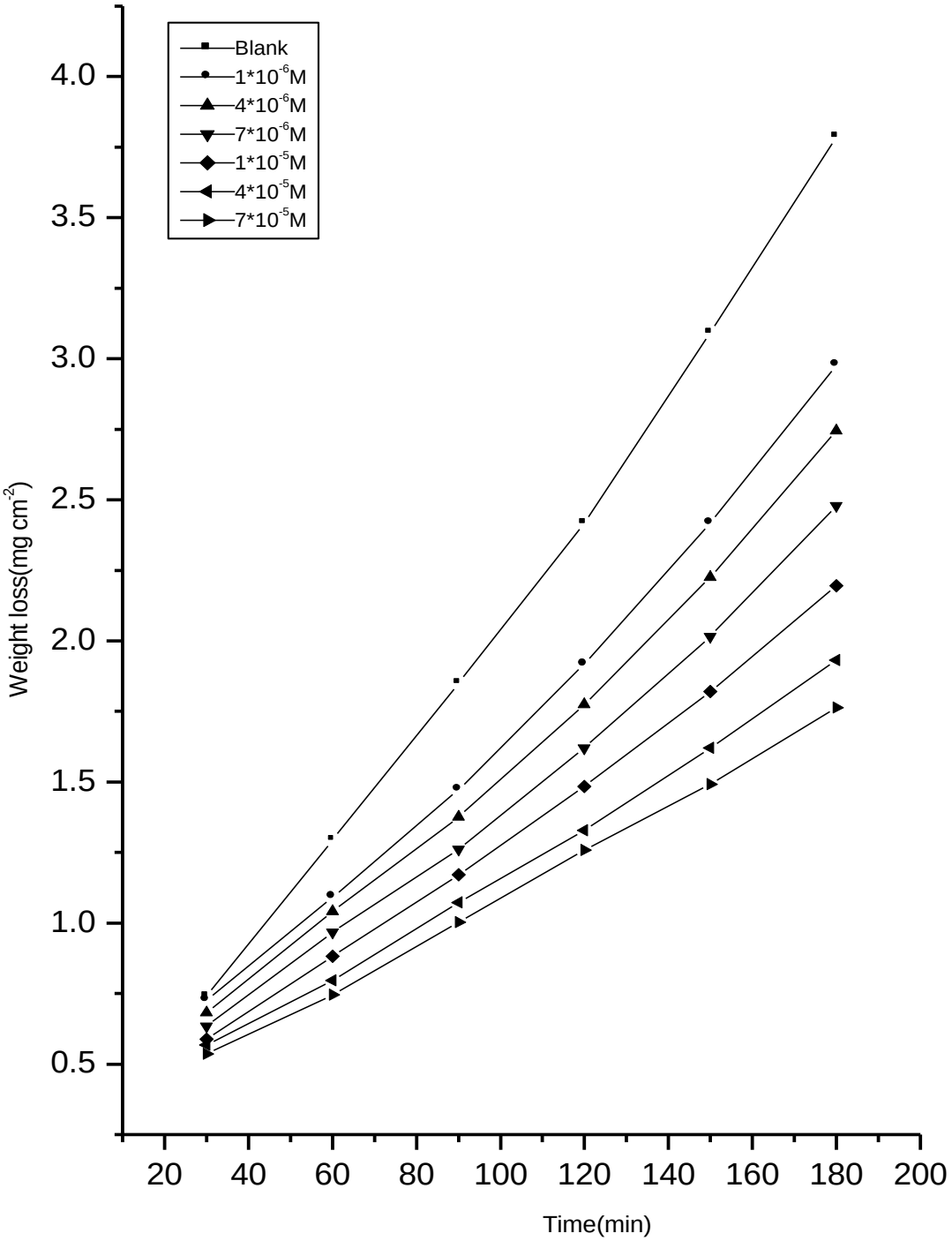

Fig(3.28) weight loss-time curves for carbon steel dissolution in 0.5M H_2SO_4 in absence and presence of different concentrations of compound(4) at 313 K

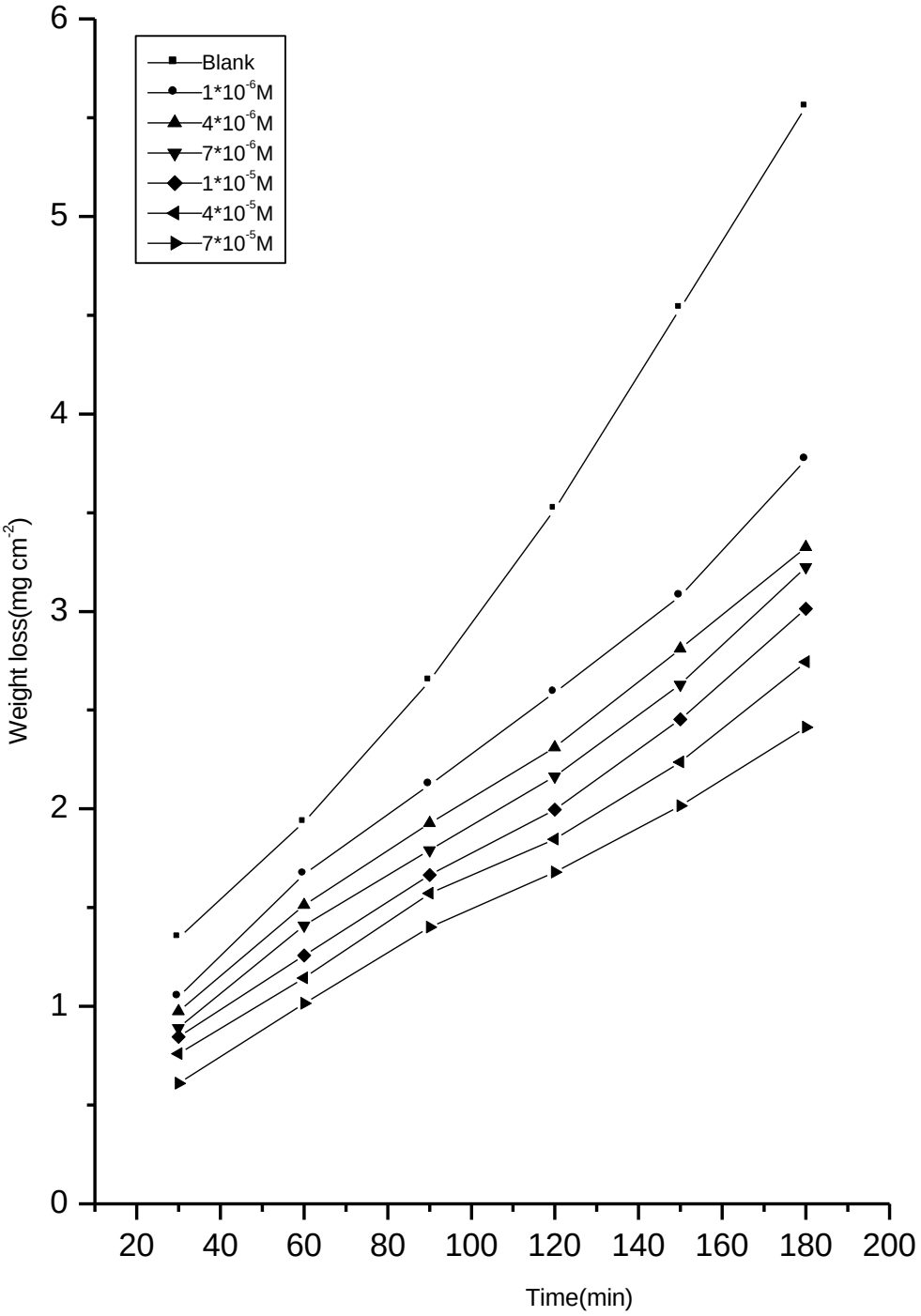

Fig(3.29) weight loss-time curves for carbon steel dissolution in 0.5M H_2SO_4 in absence and presence of different concentrations of compound(1) at 318 K

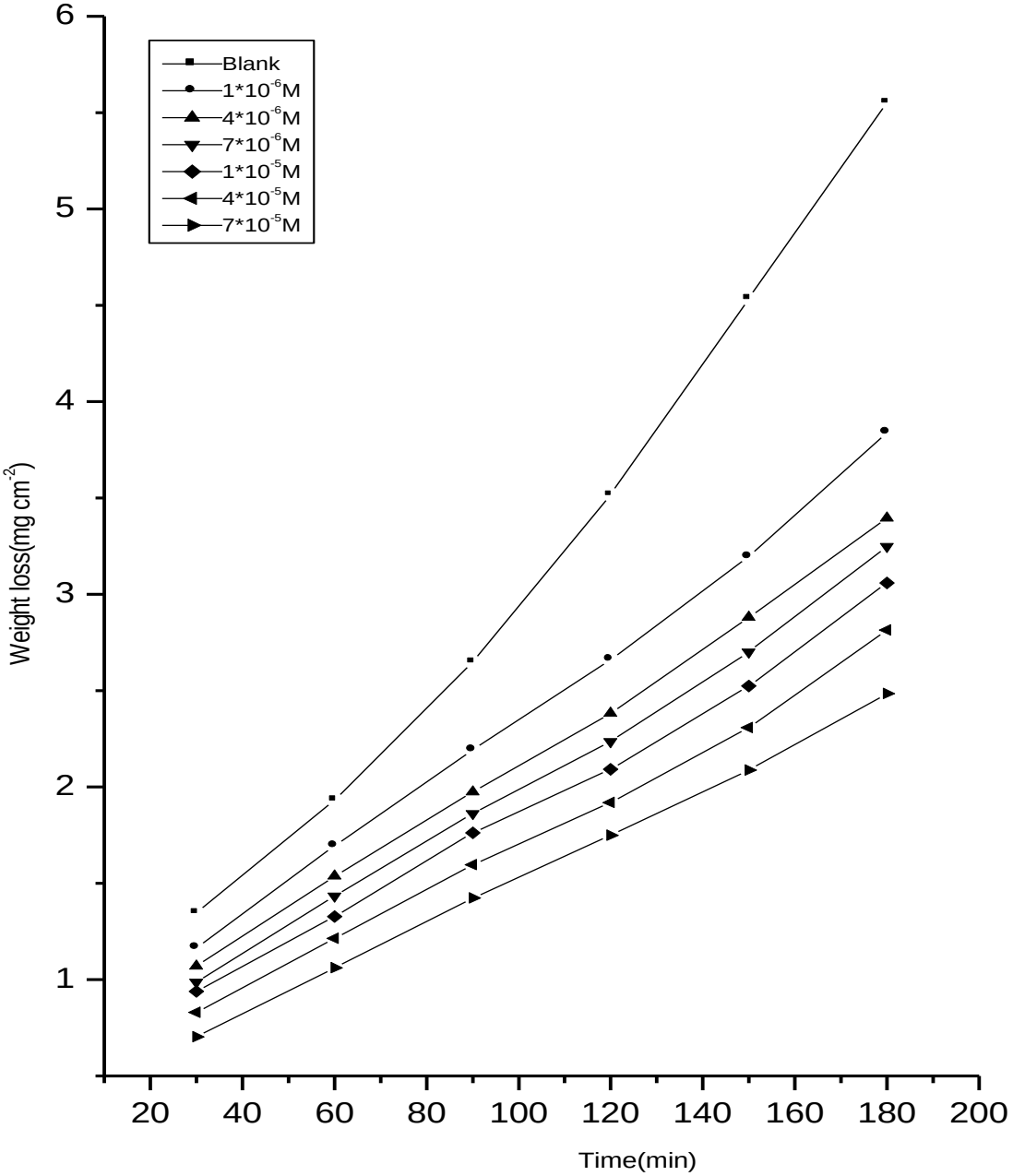

Fig(3.30) weight loss-time curves for carbon steel dissolution in 0.5M H_2SO_4 in absence and presence of different concentrations of compound(2) at 318 K

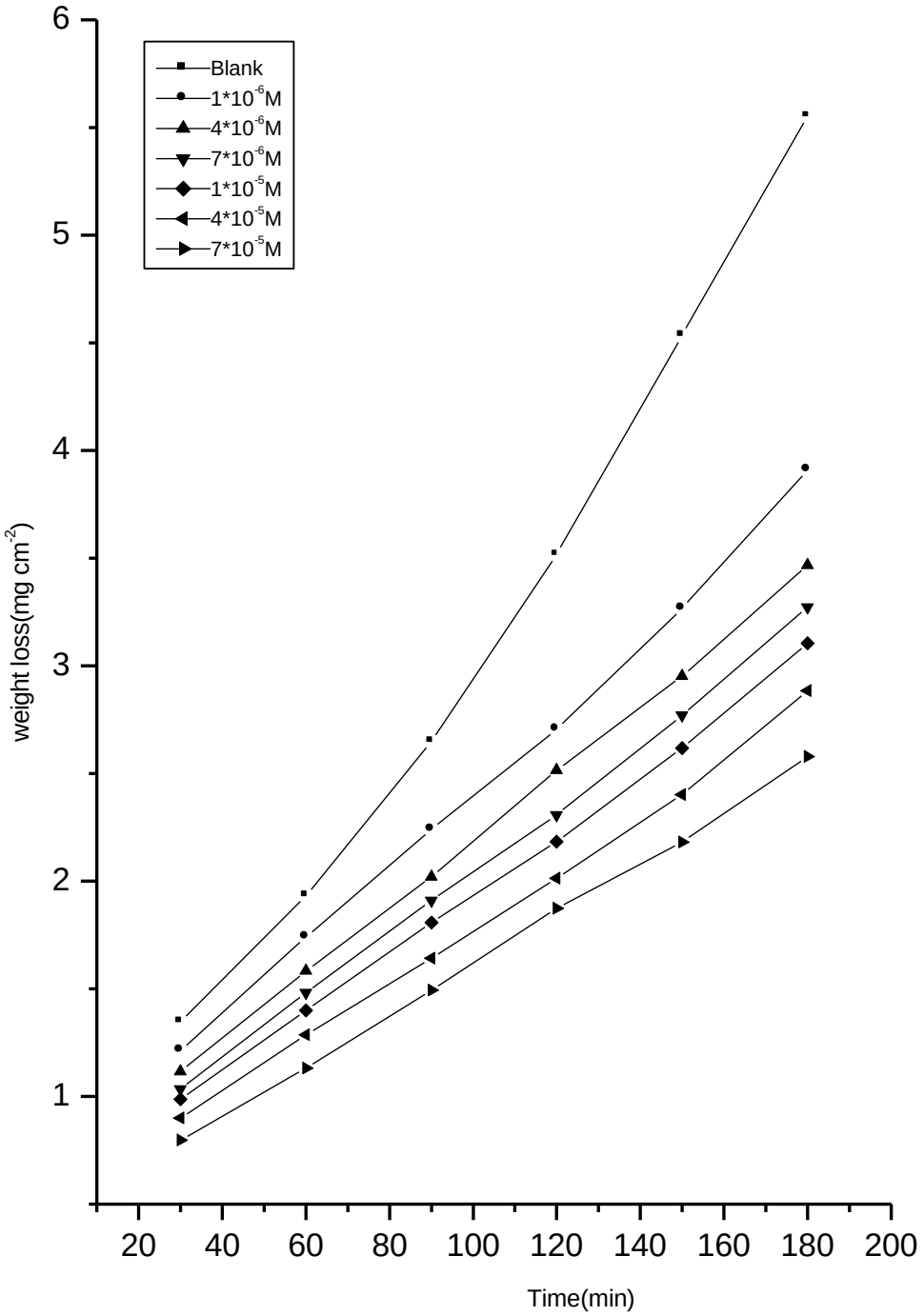

Fig(3.31) weight loss-time curves for carbon steel dissolution in 0.5M H_2SO_4 in absence and presence of different concentrations of compound(3) at 318 K

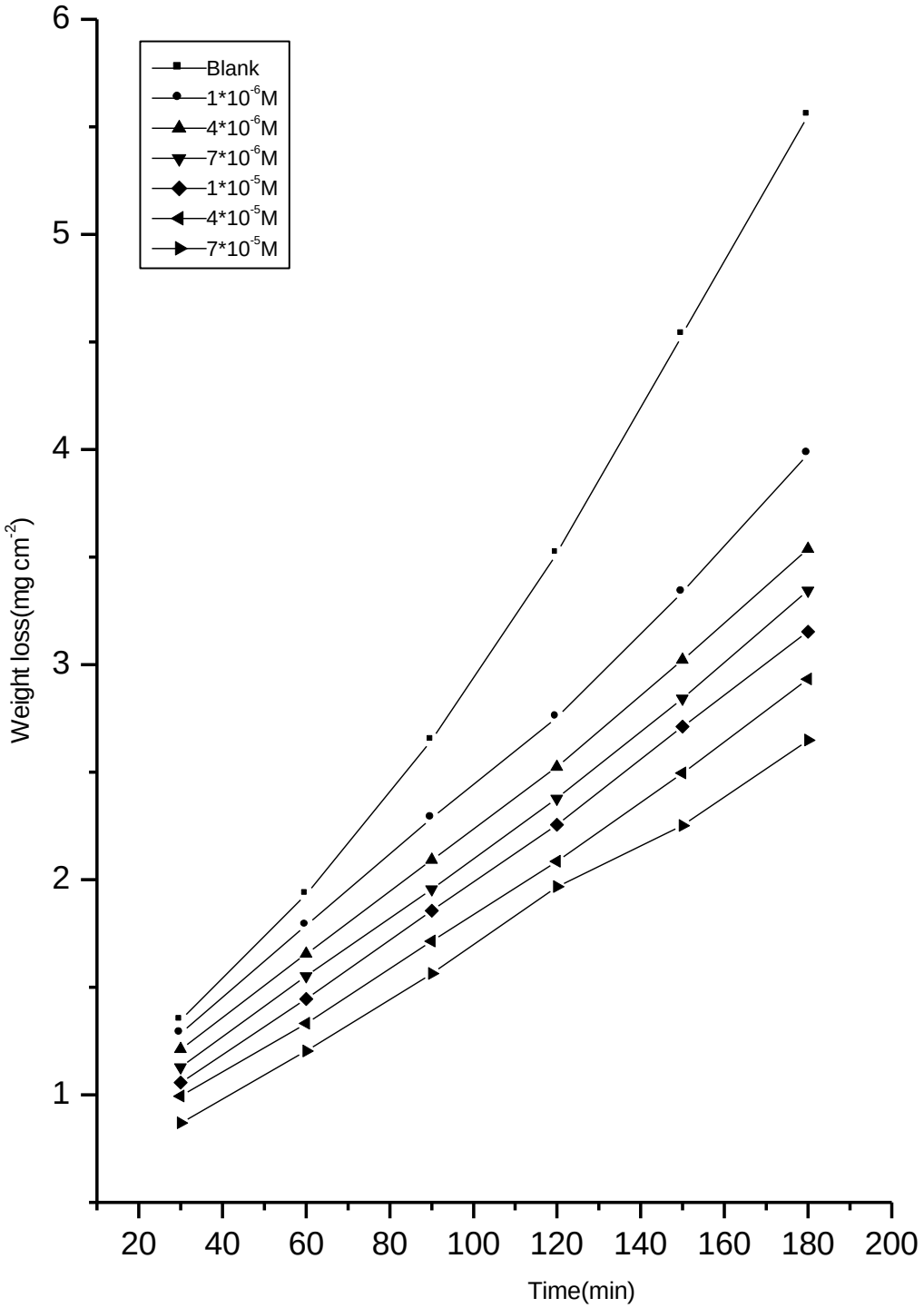

Fig(3.32) weight loss-time curves for carbon steel dissolution in 0.5M H_2SO_4 in absence and presence of different concentrations of compound(4) at 318 K

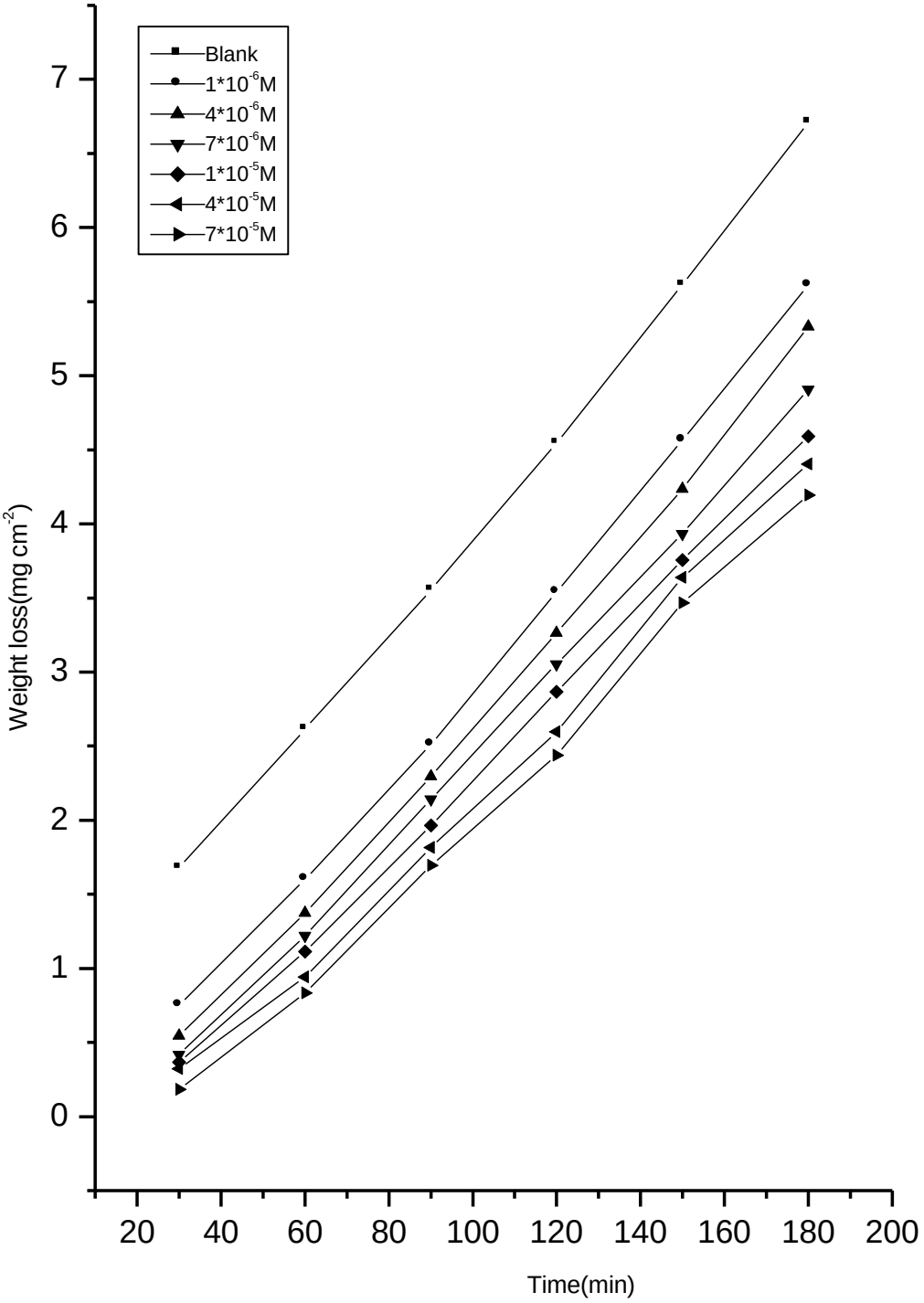

Fig(3.33) weight loss-time curves for carbon steel dissolution in 0.5M H_2SO_4 in absence and presence of different concentrations of compound(1) at 323 K

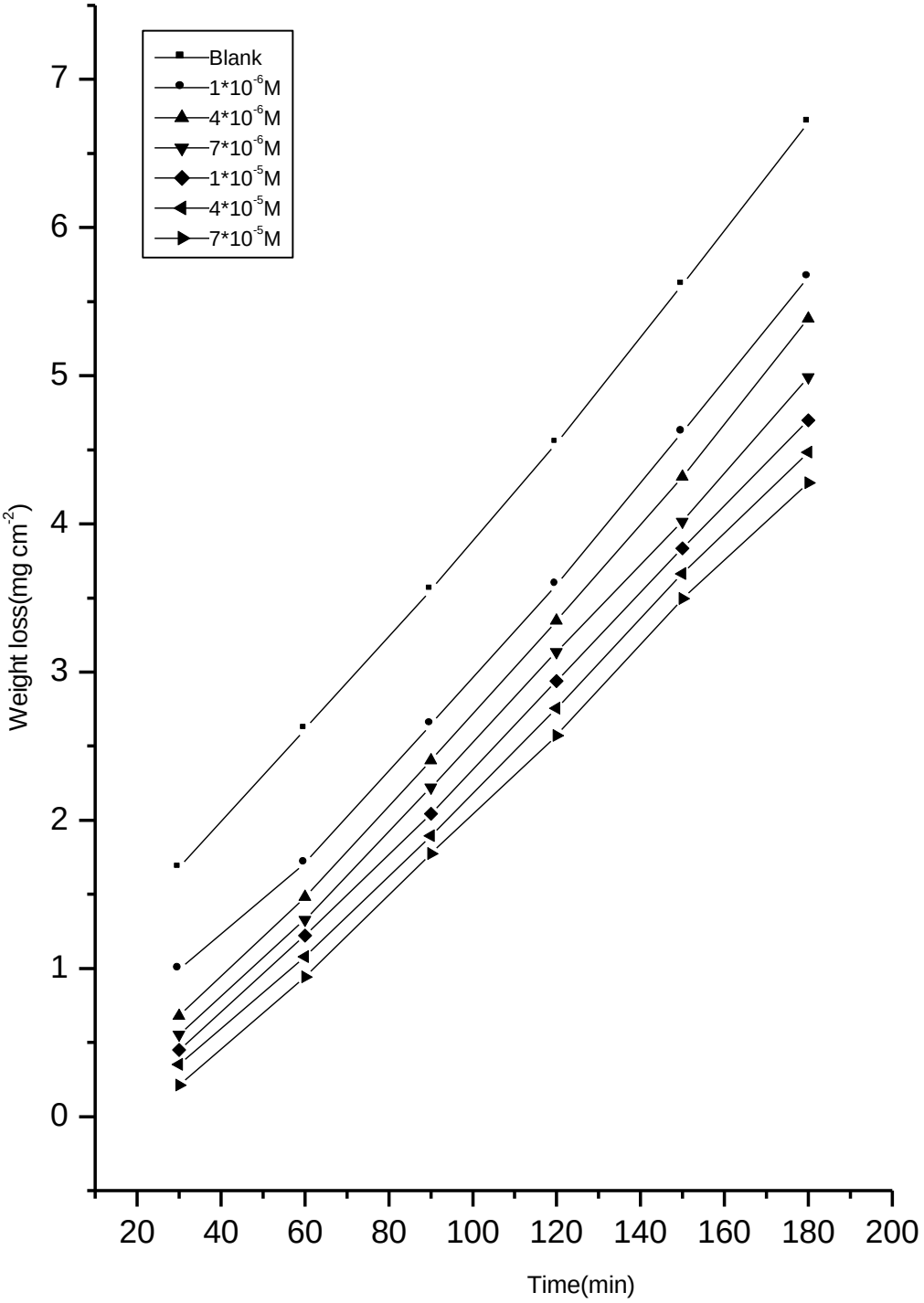

Fig(3.34) weight loss-time curves for carbon steel dissolution in 0.5M H_2SO_4 in absence and presence of different concentrations of compound(2) at 323 K

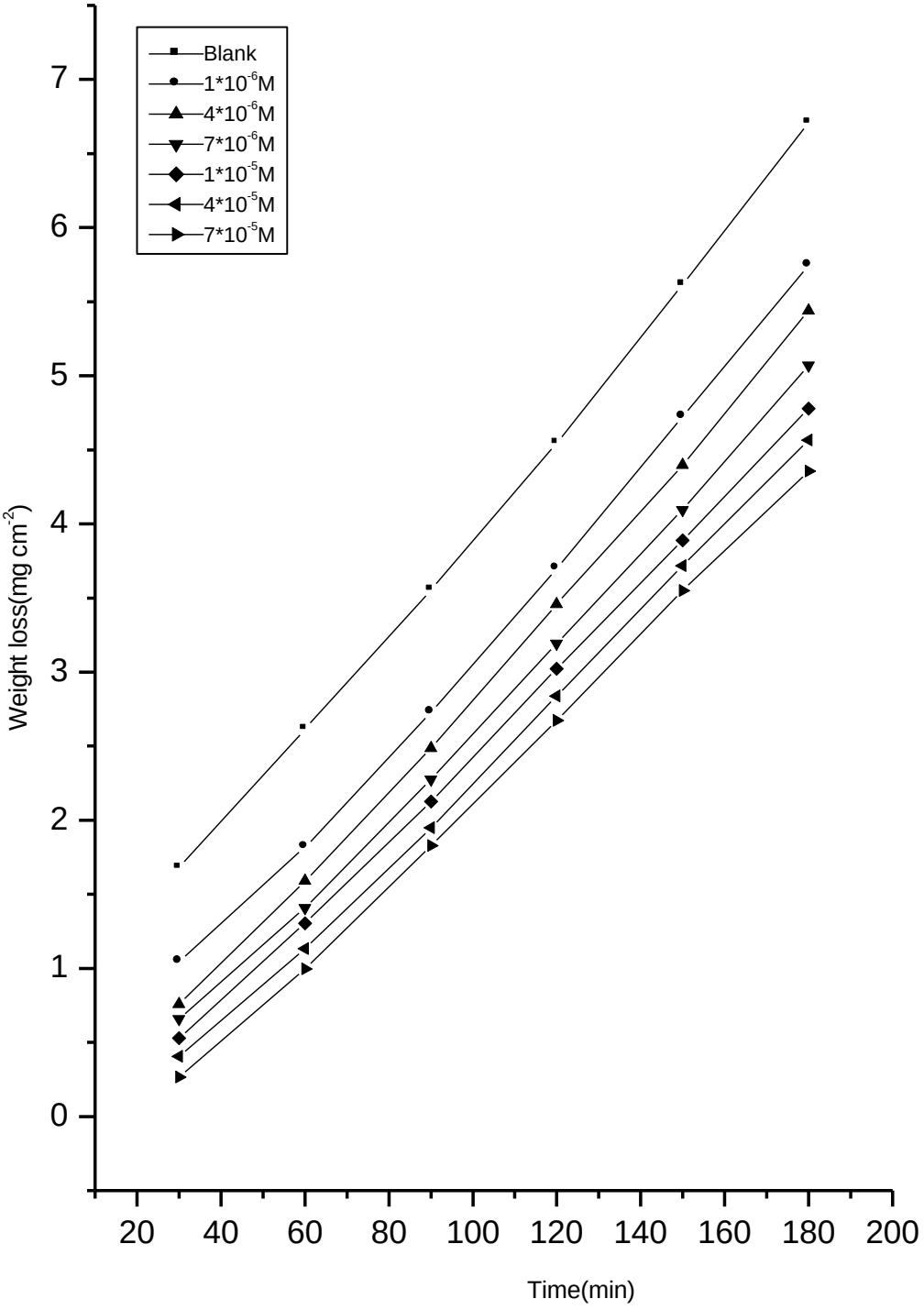

Fig(3.35) weight loss-time curves for carbon steel dissolution in 0.5M H_2SO_4 in absence and presence of different concentrations of compound(3) at 323 K

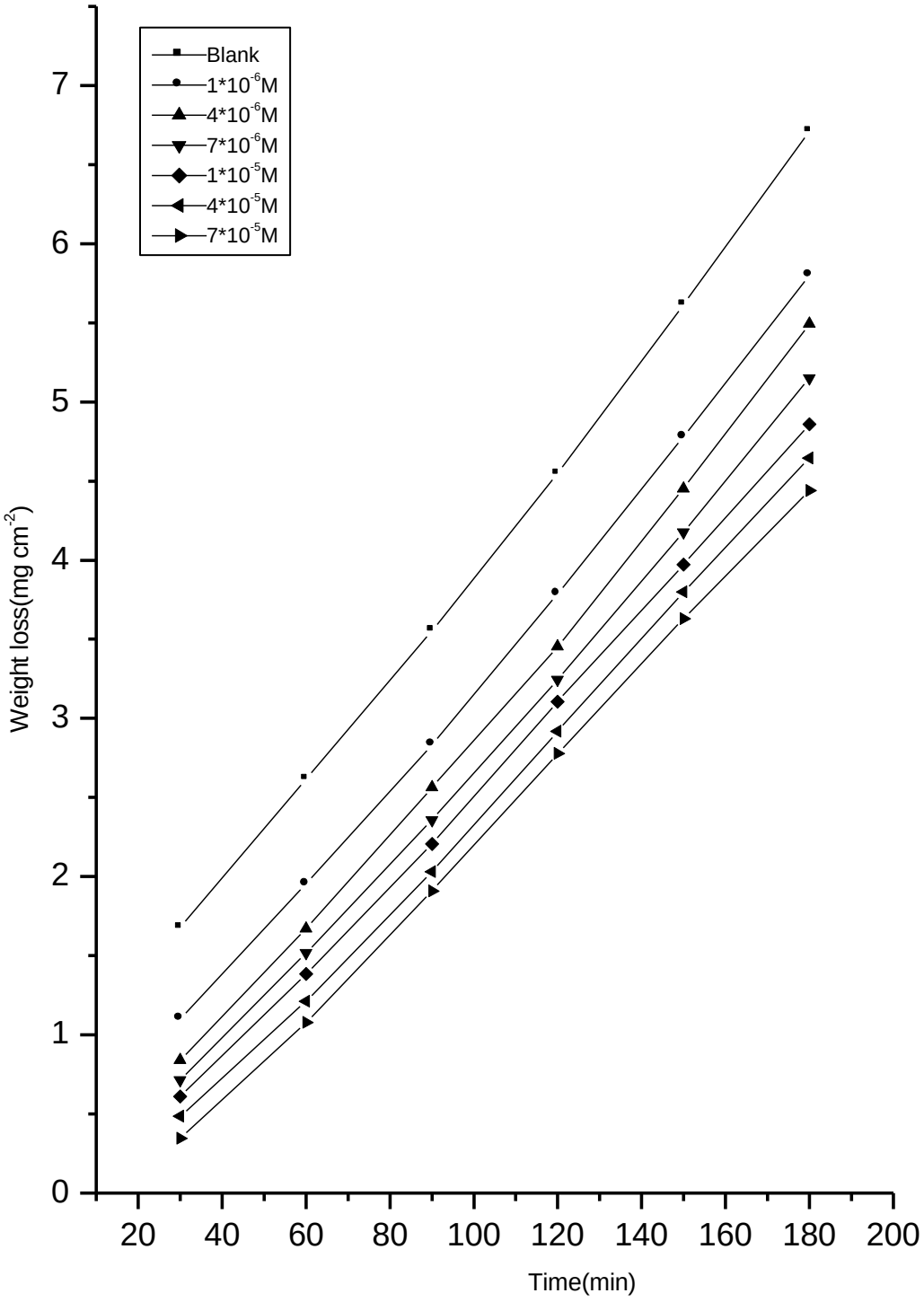

Fig(3.36) weight loss-time curves for carbon steel dissolution in 0.5M H_2SO_4 in absence and presence of different concentrations of compound(4) at 323 K

Table (3.8): % inhibition efficiency values (%IE) from weight loss method of carbon steel dissolution in 0.5M H_2SO_4 at different concentrations of compounds at 308K.

Concentration, M	Percentage inhibition efficiency (% IE)			
Compounds	1	2	3	4
$1X10^{-6}$	27.99	26.15	24.45	21.09
$4X10^{-6}$	33.58	31.52	29.84	27.99
$7X10^{-6}$	41.58	39.02	36.98	35.95
$1X10^{-5}$	48.99	46.51	42.87	42.86
$4X10^{-5}$	54.77	51.73	47.91	48.14
$7X10^{-5}$	56.41	55.38	52.12	50.94

Table (3.9): % inhibition efficiency values (%IE) from weight loss method of carbon steel dissolution in 0.5M H_2SO_4 at different concentrations of compounds at 313K.

Concentration, M	Percentage inhibition efficiency (% IE)			
Compounds	1	2	3	4
$1X10^{-6}$	28.43	24.92	22.43	20.65
$4X10^{-6}$	33.69	30.13	28.35	26.58
$7X10^{-6}$	40.10	37.14	34.77	32.99
$1X10^{-5}$	45.68	42.75	39.93	38.62
$4X10^{-5}$	50.40	48.62	45.35	45.06
$7X10^{-5}$	54.25	51.82	49.72	47.97

Table. (10): Percentage inhibition efficiency values (%IE) from weight loss method of carbon steel dissolution in 0.5M H_2SO_4 for different concentrations of compounds at 318K.

Concentration, M	Percentage inhibition efficiency (% IE)			
Compounds	1	2	3	4
$1X10^{-6}$	26.40	24.36	23.10	21.68
$4X10^{-6}$	34.33	32.25	28.51	28.23
$7X10^{-6}$	38.48	36.42	34.41	32.43
$1X10^{-5}$	43.26	40.56	37.94	35.90
$4X10^{-5}$	47.52	45.45	42.75	40.73
$7X10^{-5}$	52.24	50.28	46.74	44.06

Table (3.11): Percentage inhibition efficiency values (%IE) from weight loss method of carbon steel dissolution in 0.5M H_2SO_4 for different concentrations of compounds at 323K.

Concentration, M	Percentage inhibition efficiency (% IE)			
Compounds	1	2	3	4
$1X10^{-6}$	22.11	21.03	18.63	16.72
$4X10^{-6}$	28.20	26.39	23.96	24.04
$7X10^{-6}$	32.84	31.03	29.78	28.62
$1X10^{-5}$	36.98	35.35	33.54	31.68
$4X10^{-5}$	42.92	39.40	37.55	35.81
$7X10^{-5}$	46.35	43.44	41.18	38.89

3.5- Activation Parameters of Inhibition Process

The apparent activation energy (E_a^*) of the corrosion of carbon steel in 0.5M H_2SO_4 solution in the absence and presence of the selected organic compounds at different temperatures were calculated from the Arrhenius equation:

$$k = A \exp(-E_a^* / RT) \quad (3.7)$$

and the logarithmic form:

$$\log k = \log A - E_a^*/2.303RT \quad (3.8)$$

where k is the corrosion rate, A is the Arrhenuis constant, R is the gas constant and T is the absolute temperature. Arrhenius plots of log k vs. 1/T at different concentrations of compounds (1-4) were shown graphically in Figs (3.37-3.40). From the slopes of the plots, the respective activation energies were calculated and given in Table (3.12).

Some authors have reported values of ($E_a^* < 80$ kj mol^{-1}) as an indicator of physical adsorption , while values of ($E_a^* > 80$ kj mol^{-1}) are related to chemical adsorption [102-104]. Also , the values of activation energy (E_a^*) increases in the same order of increasing inhibition efficiency of the inhibitors. It is also indicated that the whole process is controlled by surface reaction since the energy of activation of the corrosion process is over 20 $kJmol^{-1}$ [105].

As obvious from these Figures, the increase of temperature activates the corrosion reaction and consequently, the rate of corrosion increases.

The activation energy, E_a^*, calculated from the slopes of Figs (3.37-3.40) $E_a^*/2.303R$, is equal to 60.52 $kJmol^{-1}$ for carbon steel in 0.5M H_2SO_4. Atya [106], found that the activation energy is 47.5 $kJmol^{-1}$ for low carbon steel in pH 4-6, Gomma [107], found it to be 51.832 $kJmol^{-1}$for steel (0.05%C) in 0.5M H_2SO_4 solution. Fouda [108], found it to be 63.56 $kJmol^{-1}$ for carbon steel in 2M HCl solution, on the other hand, Muthur [109], found that the activation energy of iron in 0.6M HCl is equal to 61.15 $kJmol^{-1}$ and in 0.4M H_2SO_4 is equal to 64.1 $kJmol^{-1}$.

Generally, one can say that the nature and concentration of the electrolyte and the type of metal affect greatly the activation energy for the corrosion process.

Enthalpy and entropy of activation (ΔH^*, ΔS^*) were calculated from transition state theory [110] using the following equation:

$$k = (RT/Nh)\exp(\Delta S^*/R)\exp(-\Delta H^*/RT) \qquad (3.9)$$

Where, h is Plank's constant, N is Avogadro's number, R is the universal gas constant, ΔH^* is the enthalpy of activation and ΔS^* is the entropy of activation. A plot of k/T vs 1/T (equation 3.9), also gave straight lines as shown in Figures (3.41-3.44) for C-steel dissolution in 0.5M H_2SO_4 at different concentrations of N-3-Hydroxyl-2-Naphthoyl Hydrazone inhibitors (1-4). The slopes of these lines equal $-\Delta H^*/2.303R$ and the intercept equal to $\log R/Nh + (\Delta S^*/2.303R)$ from which the value of ΔH^* and ΔS^* were calculated and givenin Tables (3.13-3.14). The order of the inhibition efficiency of the investigated compounds as gathered from the increase in E_a^* and ΔH^* and the decrease in ΔS^* values remains unchanged and follows the order:

$$1 > 2 > 3 > 4$$

From the results of Tables (3.12-3.14), it is clear that the presence of tested compounds increased the activation energy values and consequently decreased the corrosion rate of the carbon steel. Also, activation energy increased by increasing the concentration of the inhibitors, suggesting that the adsorbed organic matter produces aphysical barrier film , retards charge transfer , leading to reduction in corrosion rate[111,112]. The positive signs of ΔH^* reflect the endothermic nature of the steel dissolution process in 0.5 M H_2SO_4[113,114]. Large and negative values of ΔS^* imply that the activated complex in the rate-determining step represents an association rather than dissociation step, this reflects the formation of an ordered stable layer of inhibitor on the steel surface i.e increasing inhibitor concentration

causes an increase in ordering on going from reactants to the activated complex[115, 116].

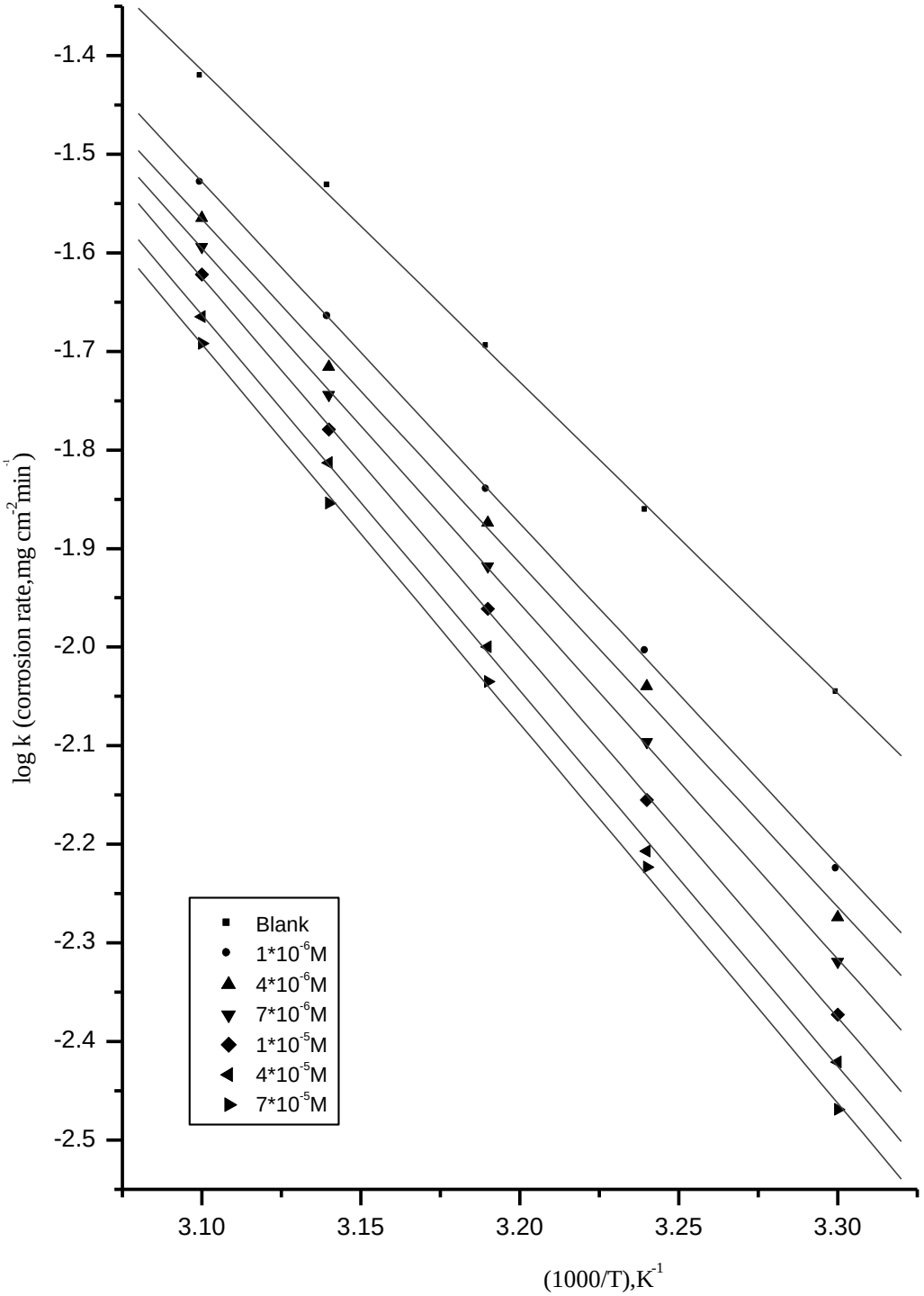

Fig(3.37) log corrosion rate vs.1/T curves for carbon steel dissolution in 0.5 M H_2SO_4 in absence and presence of different concentrations of compound(1)

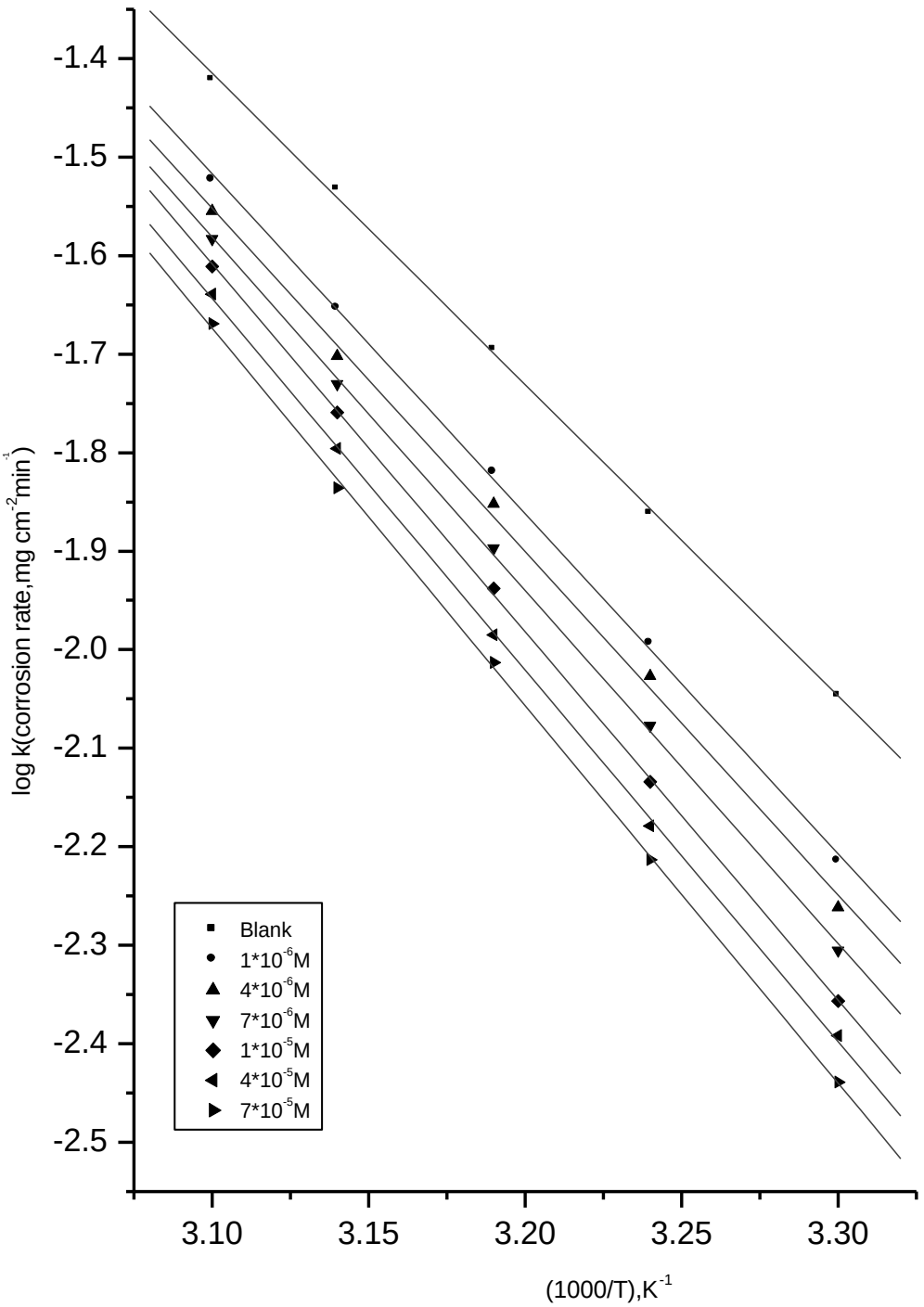

Fig(3.38) log corrosion rate vs.1/T curves for carbon steel dissolution in 0.5 M H_2SO_4 in absence and presence of different concentrations of compound(2)

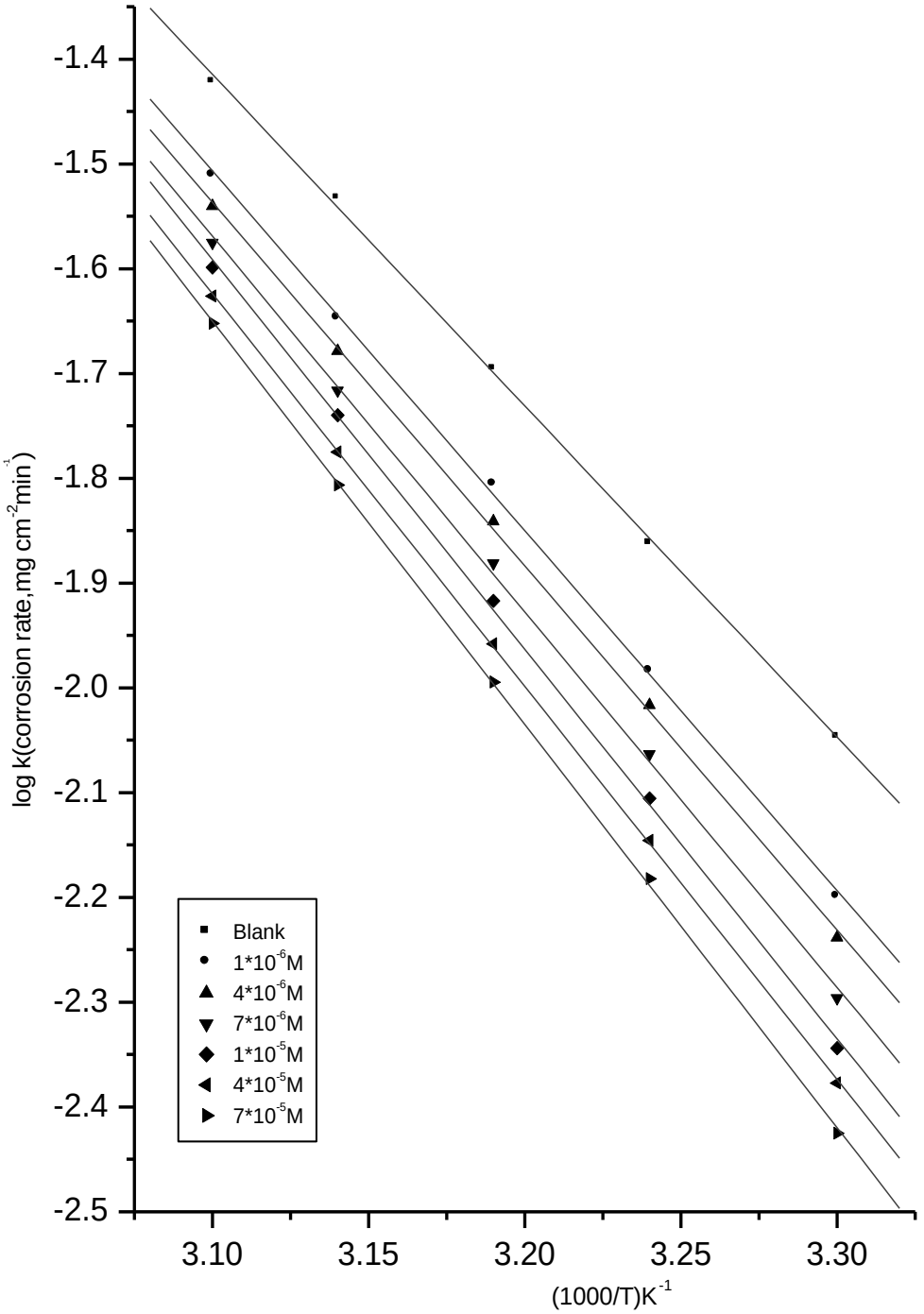

Fig(3.39) log corrosion rate vs.1/T curves for carbon steel dissolution in 0.5 M H_2SO_4 in absence and presence of different concentrations of compound(3)

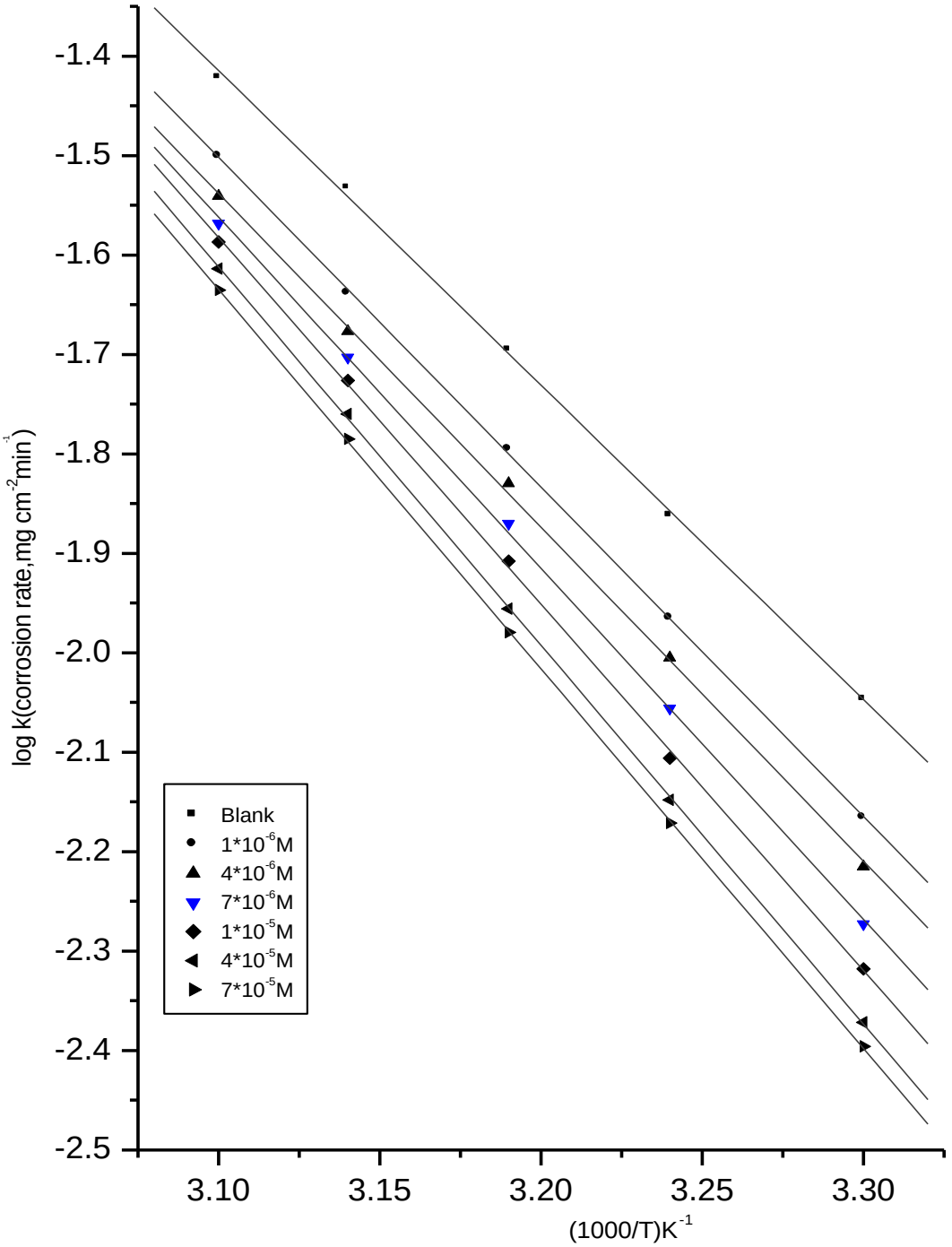

Fig(3.40) log corrosion rate vs.1/T curves for carbon steel dissolution in 0.5 M H_2SO_4 in absence and presence of different concentrations of compound(4)

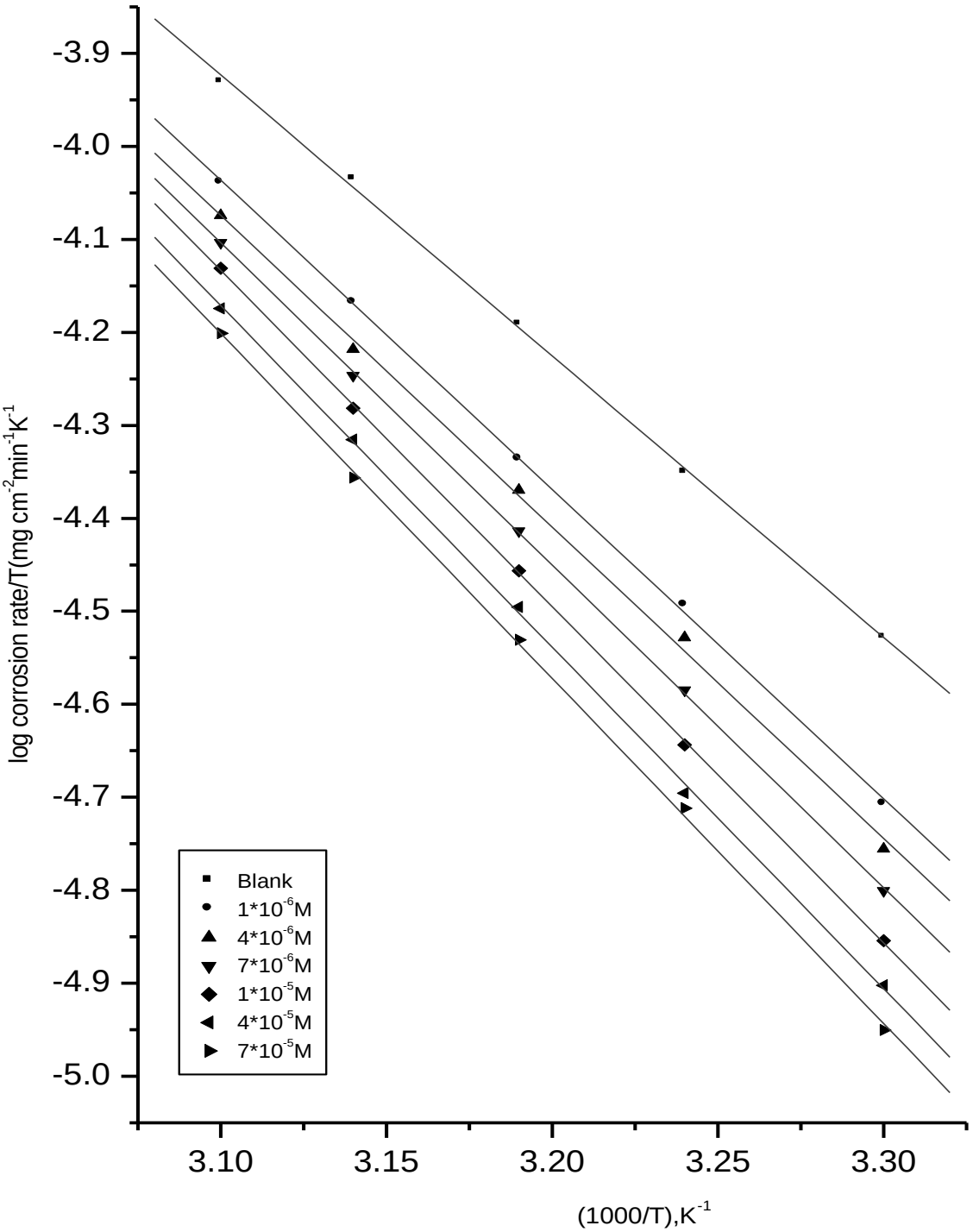

Fig(3.41) log(corrosion rate/T)-(1/T)curves for carbon steel dissolution in 0.5M H_2SO_4
In absence and presence of different concentrations of compoun(1)

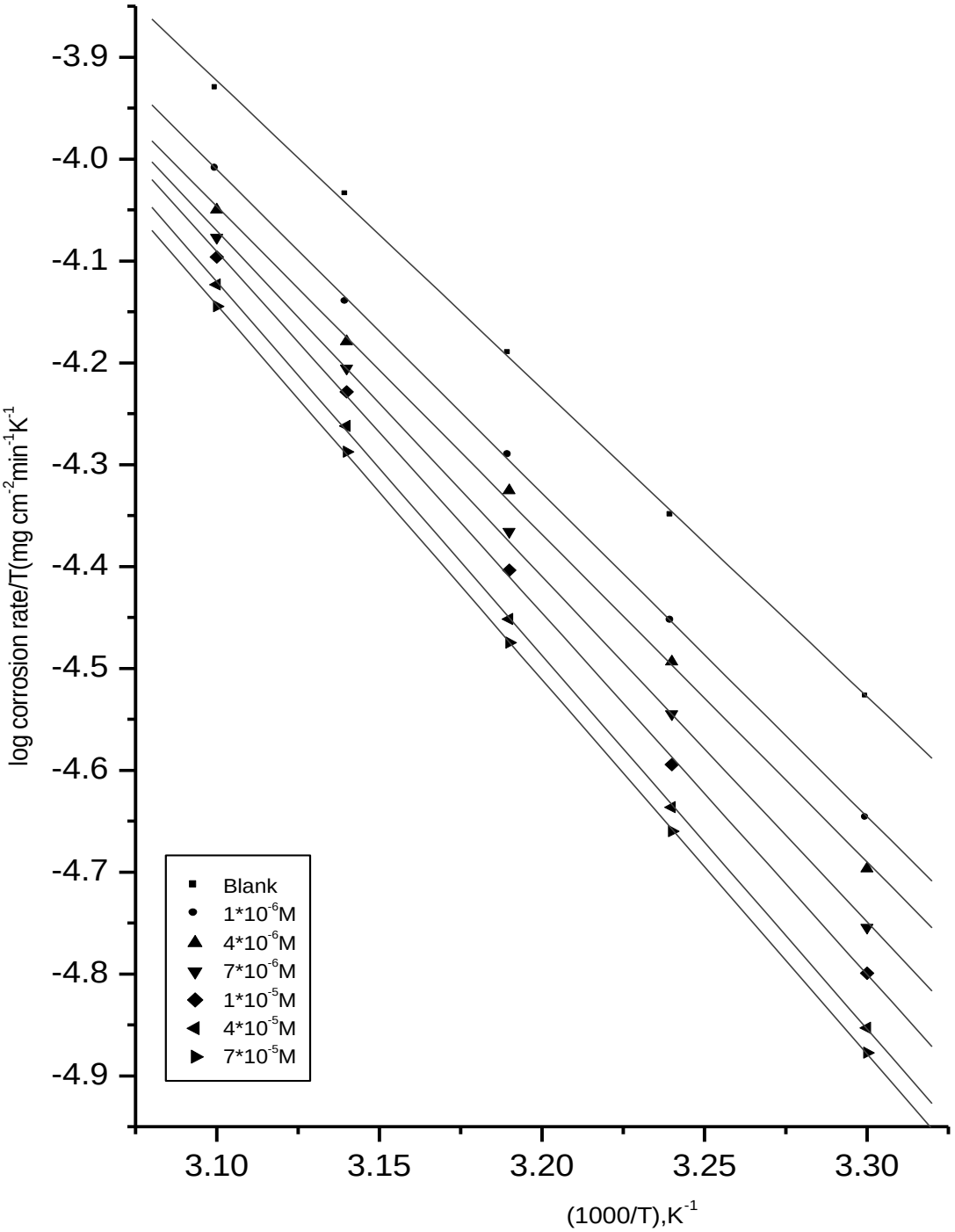

Fig(3.42) log(corrosion rate/T)-(1/T)curves for carbon steel dissolution in 0.5M H_2SO_4
In absence and presence of different concentrations of compoun(2)

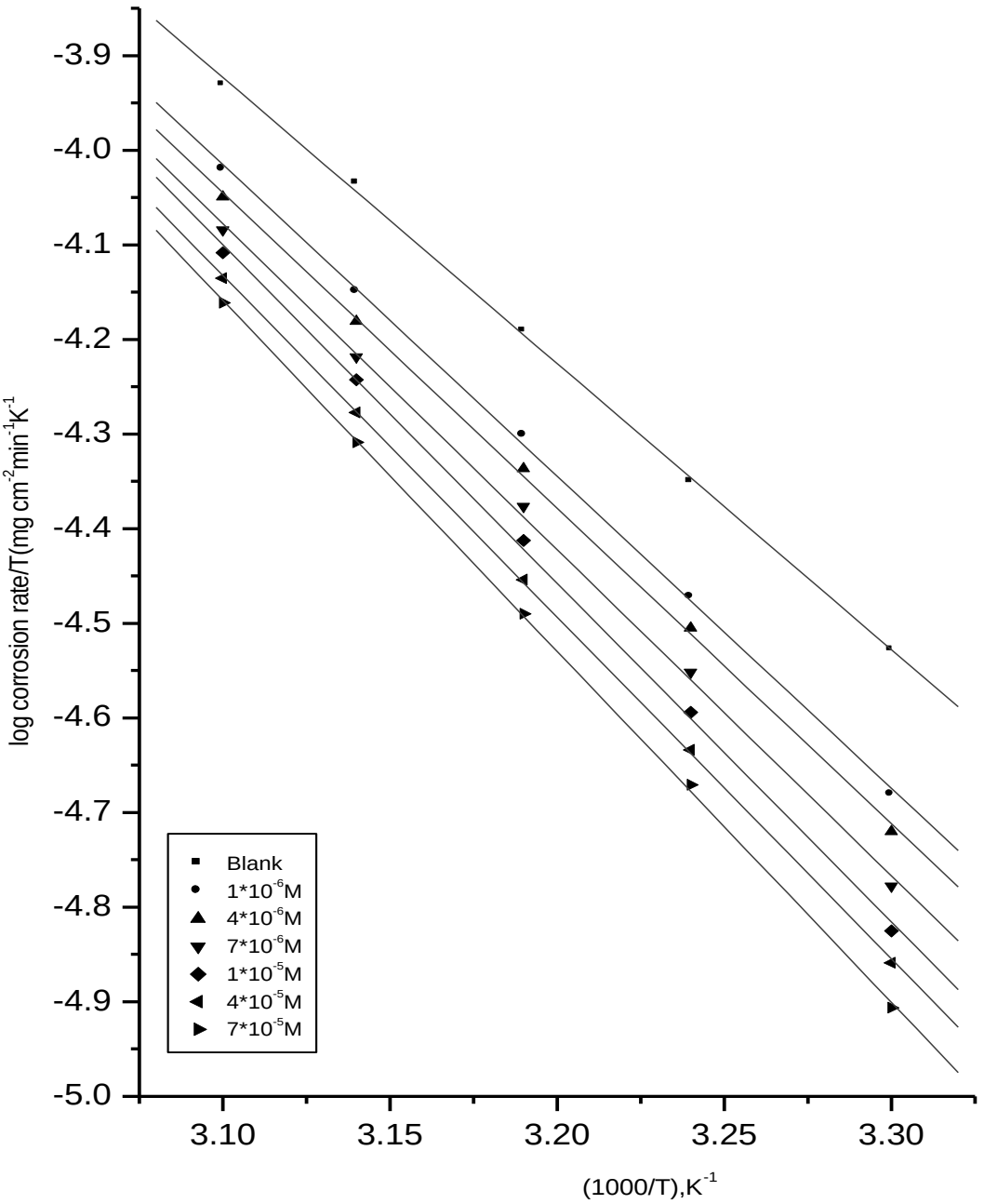

Fig(3.43) log(corrosion rate/T)-(1/T)curves for carbon steel dissolution in 0.5M H_2SO_4
In absence and presence of different concentrations of compoun(3)

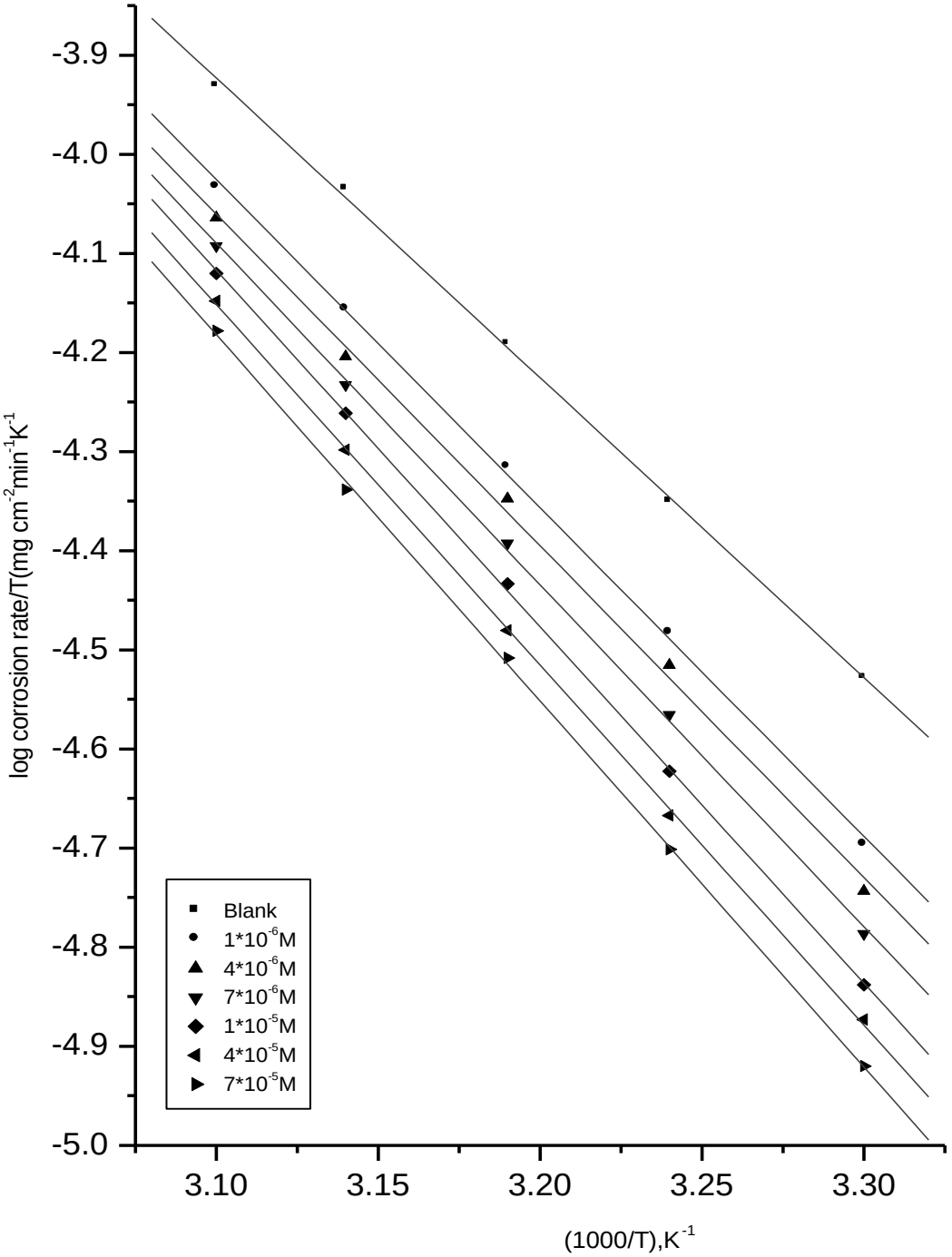

Fig(3.44) log(corrosion rate/T)-(1/T)curves for carbon steel dissolution in 0.5K H_2SO_4
In absence and presence of different concentrations of compoun(4)

Table (3.12): Effect of concentrations of investigated compounds on activation energy of carbon steel dissolution in 0.5M H_2SO_4.

Concentration M	Activation energy, E_a^*, kJ mol^{-1}			
	Compound (1)	Compound (2)	Compound (3)	Compound (4)
$1x10^{-6}$	66.33	66.07	65.73	63.44
$4x10^{-6}$	66.78	66.71	66.47	64.26
$7x10^{-6}$	68.92	68.64	68.62	67.56
$1x10^{-5}$	71.85	71.49	71.15	70.54
$4x10^{-5}$	72.97	72.21	71.77	72.87
$7x10^{-5}$	73.68	73.34	73.60	73.00

E_a^* for 0.5M H_2SO_4 = 60.52 kJ mol^{-1}.

Table (3.13): Effect of concentrations of investigated compounds on activation enthalpy of carbon steel dissolution in 0.5M H_2SO_4.

Concentration M	Activation enthalpy, ΔH^*, kJ mol^{-1}			
	Compound (1)	Compound (2)	Compound (3)	Compound (4)
$1x10^{-6}$	63.66	63.39	63.06	60.77
$4x10^{-6}$	64.11	64.04	63.80	61.59
$7x10^{-6}$	66.34	65.97	65.95	64.89
$1x10^{-5}$	69.17	68.81	68.47	67.87
$4x10^{-5}$	70.29	69.54	69.09	70.19
$7x10^{-5}$	71.00	70.67	70.97	70.35

ΔH^* for 0.5M H_2SO_4 =57.84 kJ mol^{-1}.

Table (3.14): Effect of concentrations of investigated compounds on activation entropy of carbon steel dissolution in 0.5M H_2SO_4.

Concentration M	Activation entropy, $-\Delta S^*$, J mol^{-1} K^{-1}			
	Compound (1)	Compound (2)	Compound (3)	Compound (4)
$1x10^{-6}$	77.40	78.02	78.85	85.86
$4x10^{-6}$	76.74	67.68	77.12	84.01
$7x10^{-6}$	70.38	71.26	71.09	74.23
$1x10^{-5}$	62.16	62.97	63.68	65.38
$4x10^{-5}$	59.42	61.38	62.39	58.75
$7x10^{-5}$	57.79	58.46	57.07	58.70

$-\Delta S^*$ for 0.5M H_2SO_4 = 93.25J mol^{-1} K^{-1}.

Section (B)

Studying the Corrosion Inhibition of Carbon Steel in Sulfuric Acid by Some N-3-Hydroxyl-2-Naphthoyl Hydrazone Derivatives Using Electrochemical Technique

Electrochemical techniques are based on current and potential measurements. According to the choice of the technique, accurate and confidential data, concerning the corrosion process, can be obtained.

3.6- Galvanostatic Polarization Measurements

Galvanostatic polarization curves of carbon steel electrode in 0.5M H_2SO_4 in the absence and presence of N-3-Hydroxyl-2-Naphthoyl Hydrazone derivatives at 303K are illustrated in Figs.(3.45-3.49) respectively. Inspection of these figures revealed that, there is a transition region at the beginning of cathodic or anodic polarization known as pre-Tafel region. This region starts from the corrosion potential and extends to the beginning of Tafel region. It is characterized by simultaneous occurrence of cathodic hydrogen evolution reaction and anodic dissolution of carbon steel. The hydrogen evolution leads to cover a fraction (θ_H) of electrode surface by the adsorbed hydrogen atoms $(MH)_{ads}$ and the anodic reaction causes a coverage of a fraction (θ_{OH}) of the same electrode by the adsorbed $OH^{\ddot{o}}$ groups $(MOH)_{ads}$. These two reactions in competion and hence give rise to mixed kinetics. Mc Cafferty et al [117] and others [118,119] considered that, at the corrosion potential almost the whole electrode surface is covered by $(MH)_{ads}$ and consequently the coverage fraction (θ_H)is closed to unity at cathodic potentials and decrease when anodic polarization is increased. At the end of transition region there is a metal dissolution, in case of anodic polarization, and the current becomes purely cathodic due to the hydrogen evolution reaction. The extrapolation of anodic and /or cathodic Tafel lines of charge transfer controlled corrosion reaction gives the corrosion current density, $I_{corr.}$, at the corrosion potential, $E_{corr.}$. this method is based

on the electrochemical theory of corrosion process developed by Wagner and Traud [120]. Corrosion rates are determined through polarization curves. Polarization curves are produced through the application of a current to the metal surface. If the potential of the metal surface is polarized by the current in a positive signs it is referred to as being anodically polarized; a negative signs signifies that is cathodically polarized. The degree of polarization is a measure of how the rates of the anodic and cathodic reactions are hindered by various environmental and surface process factors. The environmental factors (the concentrations of metal ions, dissolved oxygen in the solution, etc.) are referred to as the concentration polarization. The surface process factors (film formation, adsorption, etc.) are referred to as the activation polarization. The polarization curve is a graph of the variation of the potential as a function of the current, which allows the effects of the concentration and activation processes on the rate at which the anodic or cathodic reactions can give or receive electrons to be determined. This allows for a rate determination for the reactions that are involved in the corrosion process.

The polarization curve shown in Fig. (3.45) shows the polarization curves for both anodic and cathodic reactions. The potential, E, is plotted as a function of the logarithm of $I_{corr.}$. The corrosion potential, $E_{corr.}$, is determined by the intersection of the extrapolation of the linear portions of the anodic and cathodic polarization curves. The value of the current at the intersection is the rate of corrosion expressed in current density, $I_{corr.}$.

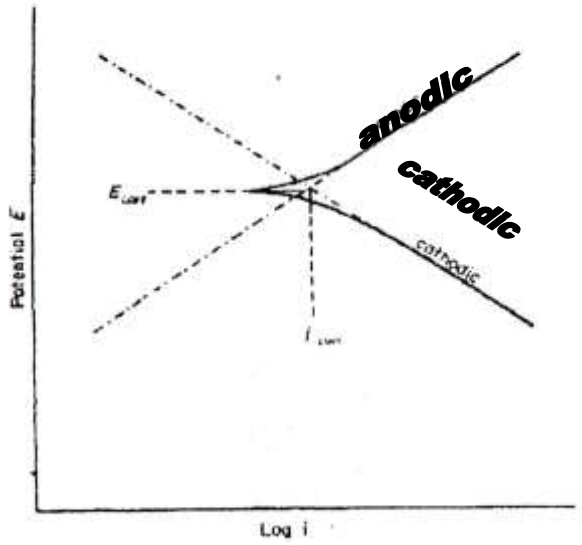

Fig.(3.45): General polarization curves for a material with both anodic and cathodic polarization curves.

The degree of surface coverage (θ) by the adsorbed molecules was calculated from equation (3.10) using galvanostatic polarization measurements, from which inhibition efficiencies, %IE was calculated using equation (3.11).

$$\theta = 1-(I_{inh}./ I_{corr}.) \quad (3.10)$$

where $i_{corr.}$ and $i_{inh.}$ are the corrosion current densities in absence and presence of the inhibitor, respectively.

$$\%IE = \theta \times 100 \quad (3.11)$$

Tables (3.15-3.18) shows the effect of inhibitors concentrations on the corrosion parameters such as, corrosion potential $E_{corr.}$, corrosion current density $I_{corr.}$, anodic and cathodic Tafel slopes (β_a & β_c), surface coverage (θ) and percentage inhibition efficiency values (%IE).

Anodic and cathodic polarization was carried out galvanostatically in unstirred 0.5M H_2SO_4 in presence and absence of various concentrations of the inhibitors (1-4) at 303K. At all current densities, during polarization, the overpotentials were slightly shifted with time and then attained steady values. This steady overpotentials values were used for the construction of anodic and cathodic Tafel plot. The results are

represented in Figures. (3.46 -3.49). The numerical values of the variation of the corrosion current density ($I_{corr.}$), the corrosion potential ($E_{corr.}$), Tafel slope (βa and βc), degree of surface coverage (θ) and the inhibition efficiency (%IE) with the concentrations of different N-3-Hydroxyl-2-Naphthoyl Hydrazone derivatives are given in tables (3.15 -3.18).

An inspection of these tables it is obvious that:

1- The cathodic and anodic curves obtained exhibit Tafel-type behavior. Addition of N-3-Hydroxyl-2-Naphthoyl Hydrazone derivatives increased both the cathodic and anodic overvoltages and caused mainly parallel displacement to the more negative and positive values, respectively. i.e. the presence of N-3-Hydroxyl-2-Naphthoyl Hydrazone derivatives in solution inhibits both the hydrogen evolution and the anodic dissolution processes.

2- The corrosion potential ($E_{corr.}$) shifted to more negative values while the corrosion current density ($I_{corr.}$)decrease with increasing the inhibitor concentration indicates the inhibiting effect of these compounds for dissolution of carbon steel in 0.5M sulphuric acid solution.

3- The results also show that the slopes of the anodic and the cathodic Tafel lines (βa and βc) were slightly changed on increasing the concentration of tested compounds. The N-3-Hydroxyl-2-Naphthoyl Hydrazone derivatives are mixed

type inhibitors, but the cathode is more polarized than the anode when an external current was applied. It is interest to note that, the values of inhibition efficiencies obtained from weight loss and polarization measurements gave the same order of inhibition efficiency of the tested compounds but yielded different absolute values probably due to the varied experimental conditions.

4- The orders of inhibition efficiency of all selective additives at different concentrations as given by polarization measurements are listed in Table (3.19). The order of investigated compounds remains unchanged; it is as follow:

$$1 > 2 > 3 > 4$$

Our measured free corrosion potential was found to be -535 mV for carbon steel in 0.5M H_2SO_4. Wang [121] found that the free corrosion potential for low carbon steel in 3M H_3PO_4 is -537 mV, El-Awady [122] found it to be -498 mV, for mild steel in 0.1M H_2SO_4, Ibrahim [123] and Venkatarman [124] found the same value of free corrosion potential (-550 mV) for mild steel in 0.1 and 0.5M H_2SO_4, respectively, -590 mV for Delta steel in 0.5M HCl [125], and -443 mV for iron in 3M HCl [126]. From these results, one can conclude that, the free corrosion potential depends on both the composition of the electrode and the electrolyte (type and concentration) used.

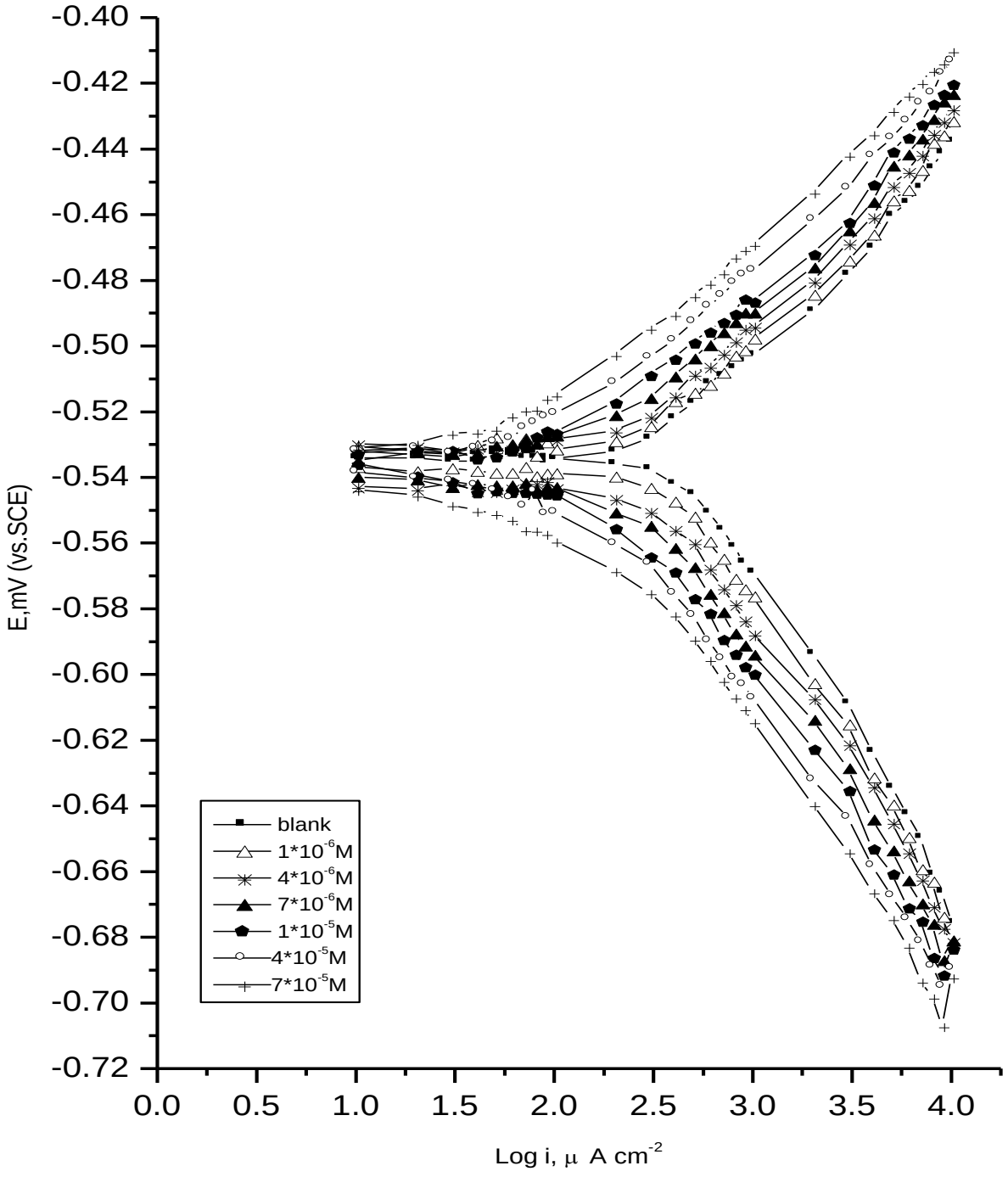

Fig.(3.48): Galvanostatic polarization curves for carbon steel in 0.5M H_2SO_4 in absence and presence of different concentrations of compound (1) at 303K.

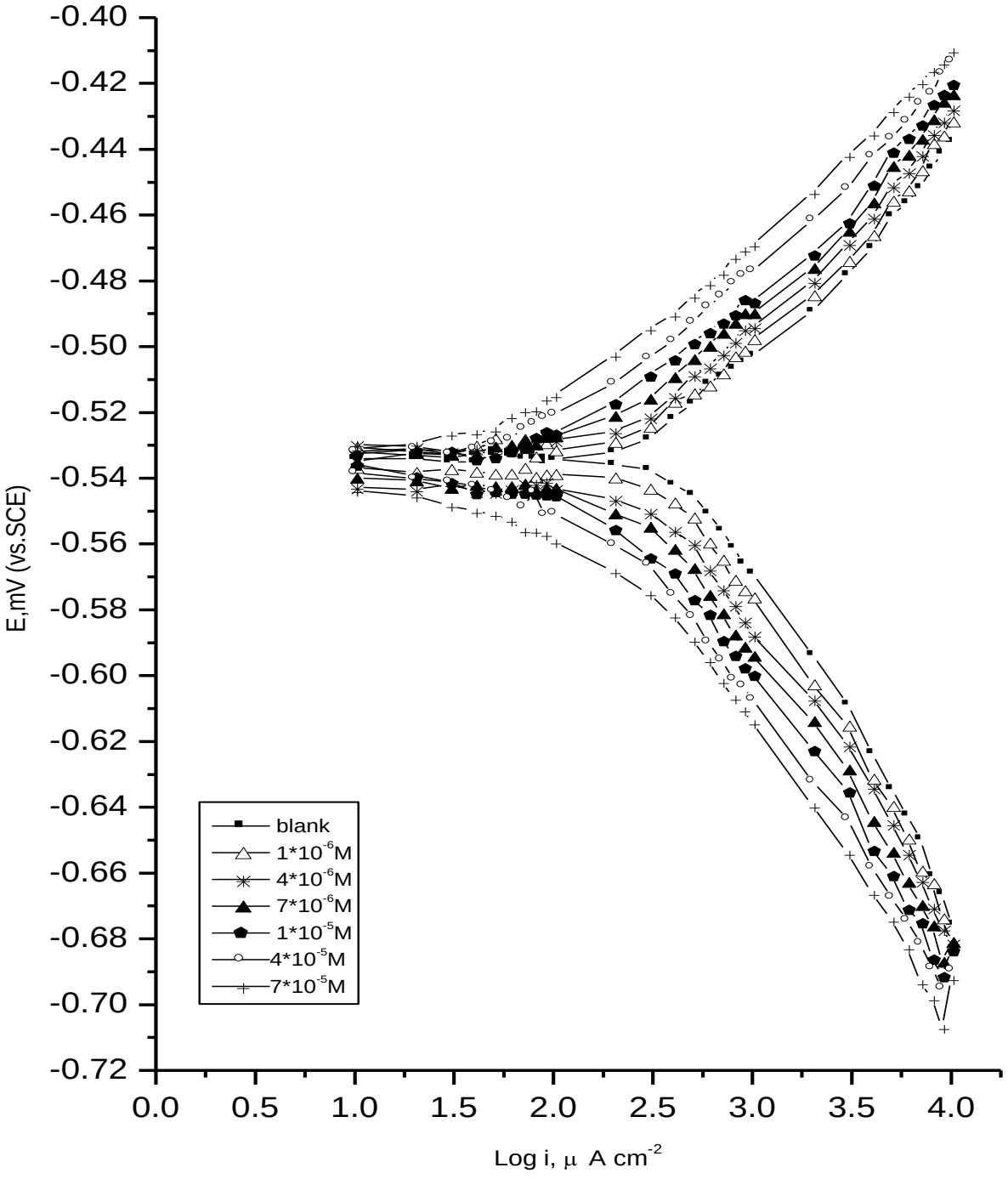

Fig.(3.48): Galvanostatic polarization curves for carbon steel in 0.5M H_2SO_4 in absence and presence of different concentrations of compound (2) at 303K.

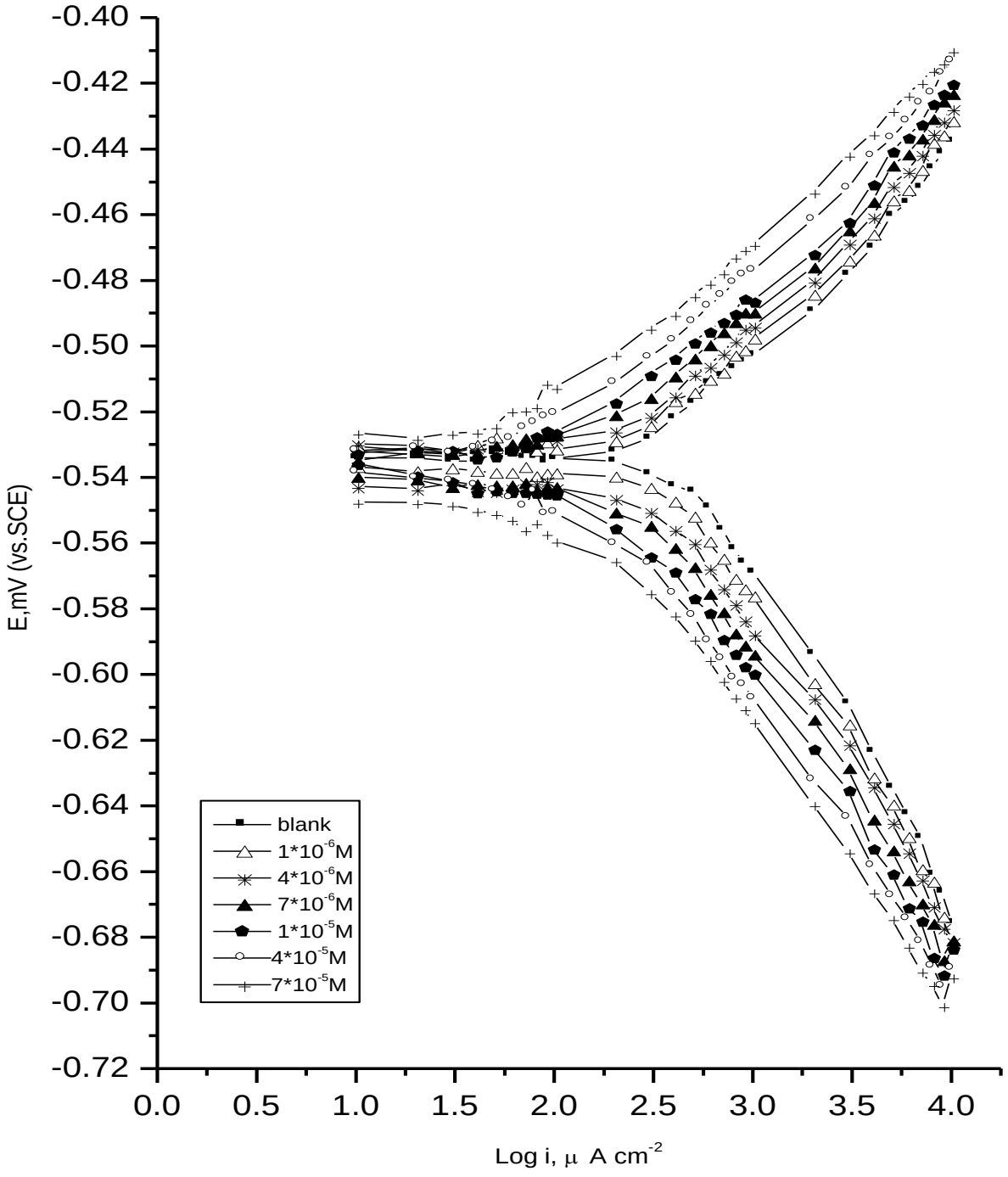

Fig.(3.48): Galvanostatic polarization curves for carbon steel in 0.5M H_2SO_4 in absence and presence of different concentrations of compound (3) at 303K.

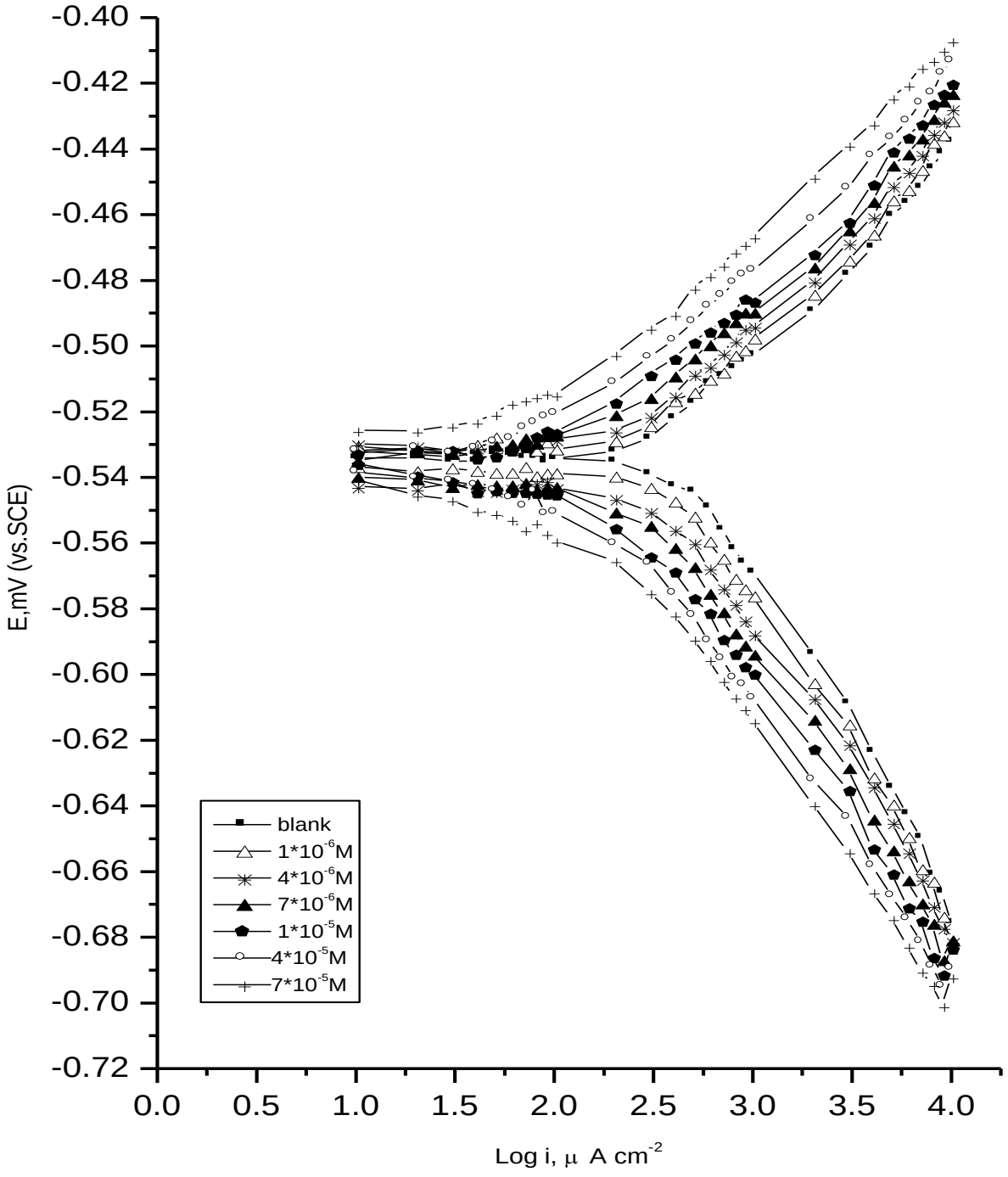

Fig.(3.48): Galvanostatic polarization curves for carbon steel in 0.5M H_2SO_4 in absence and presence of different concentrations of compound (4) at 303K.

Table (3.15): The effect of increasing concentrations of compound (1) on the free corrosion potential ($E_{corr.}$), corrosion current density (I_{corr}), Tafel slopes (β_a & β_c), percentage inhibition efficiency values (%IE) and degree of surface coverage (θ) for carbon steel dissolution in 0.5M H_2SO_4 at 303K.

Concentration M	$-E_{corr.}$ mV	$I_{corr.}$ $\mu A\ cm^{-2}$	β_a mV $dec.^{-1}$	β_c mV $dec.^{-1}$	θ	IE%
0.0	535	469.25	78	112	-	-
$1x10^{-6}$	528	316.23	65	99	0.320	32
$4x10^{-6}$	528	281.84	61	96	0.399	40
$7x10^{-6}$	527	251.19	56	94	0.464	46
$1x10^{-5}$	526	229.09	52	93	0.511	51
$4x10^{-5}$	526	208.93	51	90	0.554	55
$7x10^{-5}$	525	190.55	49	90	0.593	59

Table (3.16): The effect of increasing concentrations of compound (2) on the free corrosion potential ($E_{corr.}$), corrosion current density (I_{corr}), Tafel slopes (β_a & β_c), percentage inhibition efficiency values (%IE) and degree of surface coverage (θ) for carbon steel dissolution in 0.5M H_2SO_4 at 303K.

Concentration M	$E_{corr.}$- mV	$I_{corr.}$ $\mu A\ cm^{-2}$	β_a mV $dec.^{-1}$	β_c mV $dec.^{-1}$	θ	IE%
0.0	535	469.25	78	112	-	-
$1x10^{-6}$	529	436.74	71	103	0.260	26
$4x10^{-6}$	529	309.03	68	100	0.340	34
$7x10^{-6}$	527	275.42	63	98	0.412	41
$1x10^{-5}$	525	263.03	60	100	0.439	44
$4x10^{-5}$	526	239.88	57	96	0.488	49
$7x10^{-5}$	523	204.17	51	95	0.564	56

Table (3.17): The effect of increasing concentrations of compound (3) on the free corrosion potential ($E_{corr.}$), corrosion current density (I_{corr}), Tafel slopes (β_a & β_c), percentage inhibition efficiency values (%IE) and degree of surface coverage (θ) for carbon steel dissolution in 0.5M H_2SO_4 at 303K.

Concentration M	$E_{corr.}$- mV	$I_{corr.}$ $\mu A\ cm^{-2}$	β_a mV $dec.^{-1}$	β_c mV $dec.^{-1}$	θ	IE%
0.0	535	468.81	78	112	-	-
$1x10^{-6}$	531	363.08	74	103	0.225	23
$4x10^{-6}$	528	323.59	71	101	0.309	31
$7x10^{-6}$	525	259.12	70	98	0.370	37
$1x10^{-5}$	525	275.42	68	100	0.412	41
$4x10^{-5}$	525	251.19	63	101	0.464	46
$7x10^{-5}$	522	223.87	60	103	0.522	52

Table (3.18): The effect of increasing concentrations of compound (4) on the free corrosion potential ($E_{corr.}$), corrosion current density (I_{corr}), Tafel slopes (β_a & β_c), percentage inhibition efficiency values (%IE) and degree of surface coverage (θ) for carbon steel dissolution in 0.5M H_2SO_4 at 303K.

Concentration M	$-E_{corr.}$ mV	$I_{corr.}$ μ A cm^{-2}	β_a mV $dec.^{-1}$	β_c mV $dec.^{-1}$	θ	IE%
0.0	535	468.81	78	112	-	-
$1x10^{-6}$	532	371.54	77	101	0.200	20
$4x10^{-6}$	532	338.84	77	101	0.277	28
$7x10^{-6}$	526	309.03	74	99	0.340	34
$1x10^{-5}$	525	281.84	71	100	0.398	40
$4x10^{-5}$	522	254.04	65	100	0.451	45
$7x10^{-5}$	521	234.42	63	104	0.500	50

Table (3.19): The degree of surface coverage (θ) from electrochemical method of carbon steel dissolution in 0.5M H_2SO_4 at different concentrations of these invistigated compounds at 303K.

Concentration, M	Surface coverage (θ)			
compounds	1	2	3	4
$1X10^{-6}$	0.32	0.26	0.23	0.20
$4X10^{-6}$	0.40	0.34	0.30	0.28
$7X10^{-6}$	0.46	0.41	0.37	0.34
$1X10^{-5}$	0.51	0.44	0.41	0.40
$4X10^{-5}$	0.55	0.49	0.46	0.45
$7X10^{-5}$	0.59	0.56	0.52	0.50

Section C

Studying the Correlation Between Inhibition Action and Chemical Structure of the Inhibitors

Skeletal representation of the mode of adsorption of N-3-Hydroxyl-2-Naphthoyl Hydrazones derivatives on C-steel surface is shown in Fig (3.50). As shown from this figure, there are only two adsorption active sites in all investigated compounds (1-4).nitrogen atom of the hydrazones and oxygen atom of the hydroxyl group. Hence we can not take the adsorption active sites in my comparison in % inhibition for these derivatives. So, the molecular size is the determining factor. Compound (1) is the most efficient one in % inhibition; this is due to its larger molecular size (354) and presence of two benzene rings which provides some of their electronic density to the active sites. Compound (2) comes after Compound (1) in % inhibition. This is due to its lower molecular size (316) than compound (1) and it contain five saturated ring and benzene ring which provide no electrons to the active sites. Compound (3) comes after Compound (2) in % inhibition due to its lower molecular size (290) than Compound (1) & Compound (2) and the larger distance between the benzene ring and the active sites, so the sharing of π-electrons of the benzene ring is lesser. Compound (4) is the least one in % inhibition due to: i) its lower molecular size (282) and ii) the presence of cyclohexyl ring which does not provide charge density for the active sites. The order of decreasing inhibition efficiency is:

Compound (1) [354] > Compound (2) [316] > Compound (3) [290] > Compound (4) [282].

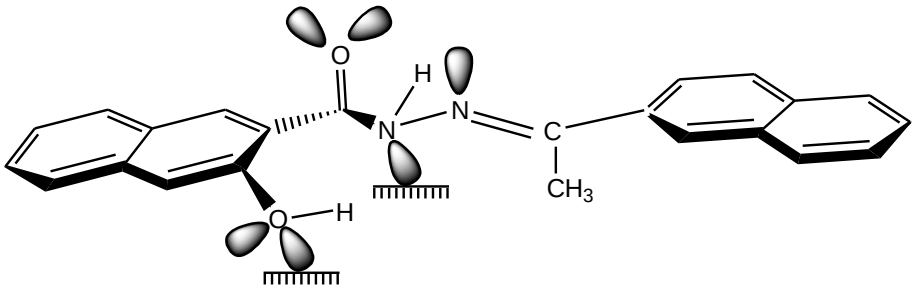

Compound(1)

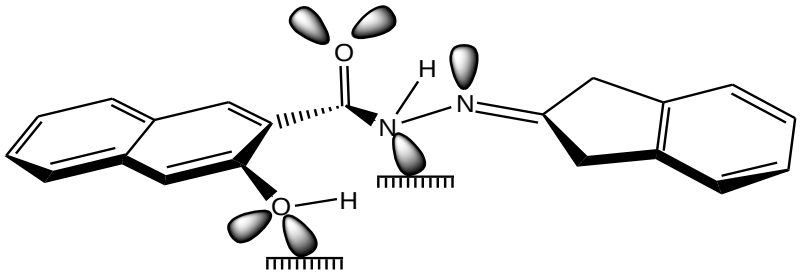

Compound(2)

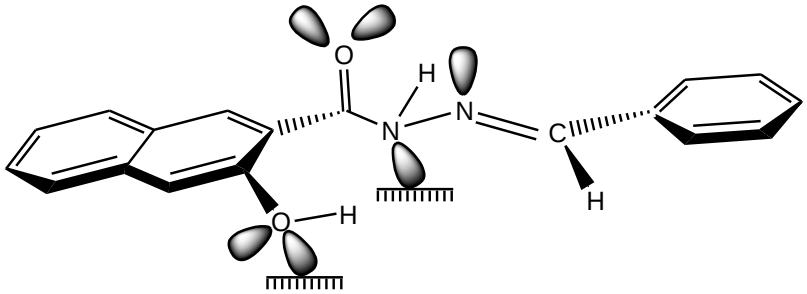

Compound(3)

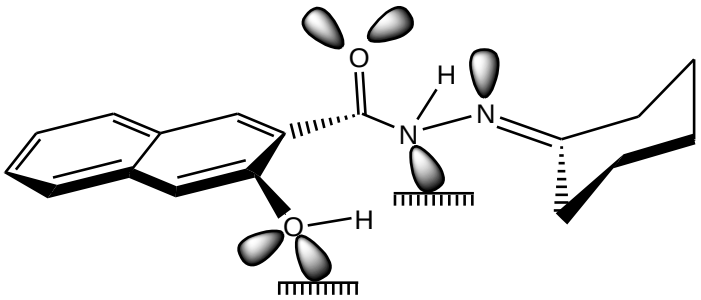

Compound(4)

Fig (3.50) : Skeletal representation of the mode of adsorption of all

N-3-Hydroxyl-2-Naphthoyl Hydrazone derivatives.